Two Micron Tm Doped ZBLAN Double Clad Fibre Laser

By
Md. Samiul Islam Sarker

Supervisors:
Prof. Tanya M. Monro
Associate Prof. David G Lancaster

A thesis submitted in fulfillment of the degree of Master of Science
In the subject of

Experimental Physics

In the Faculty of Sciences
School of Chemistry & Physics

July 2011

Declaration of Authorship

I, Md. Samiul Islam Sarker certify that this work contains no material which has been accepted for the award of any other degree or diploma in any other university or other tertiary institution and, to the best of my knowledge and belief contains no material previously published or written by another person, except where due reference has been made in the text.

I give consent to this copy of my thesis when deposited in the university library, being made available for loan and photocopying subject to the provision of the Copyright Act 1968.

I also give permission for the digital version of my thesis to be made available on the web, via the University‟s digital research repository, the Library catalogue and also through web search engines, unless permission has been granted by the University to restrict access for a period of time.

To My Parents

Abstract

Tm:ZBLAN fibre lasers have potential applications in many research areas, such as eye safe range detection, medical science and materials processing. In this thesis we investigate improving the laser performance of a thulium doped fluoride fibre (specifically ZBLAN) to generate laser output with wavelengths near 2 μm. Two approaches are demonstrated to investigate laser performance at 2 μm. One is 790 nm pumping in which the cross-relaxation mechanism is used for efficient operation by populating the upper laser level. Another is in-band pumping, where 1570 nm light is directly pumps the emitting laser level, reducing the quantum defect between the pump and lasing wavelengths, reducing the threshold and increasing the efficiency of the fibre laser. Tm:ZBLAN fibres fabricated in-house, we also characterized with the aim of processing towards the development of new classes of fibre laser.

A Tm:ZBLAN double clad fibre laser operating at 1.96 μm is demonstrated with a 1.53 W maximum output power and slope efficiency of 45% with respect to the launch pump power. Thereafter, the laser performance is analysed using cavity mirrors of various reflectivities.

A laser with an operating wavelength of 1.57 μm is demonstrated with 1 watt output power using an Er:Yb co-doped double clad fibre. The slope efficiency of this laser is measured to be 28.3% with respect to the diode pump power, with a measured beam quality (M^2) of 1.3. This 1.57 μm in-band pump source is then used to pump the 2 μm Tm:ZBLAN fibre laser.

In addition to the laser development, this thesis also analyses the pump absorption for different shaped double clad fibres numerically. Understanding of pump absorption is required to develop an efficient double clad fibre laser. The pump absorption is measured using cut-back method and compared with the modeled results.

Motivation and Thesis Outline

Thulium doped fibre lasers at 2 μm can be developed either using Tm:Silica or Tm:ZBLAN fibre. There have also been 2 μm lasers in other materials including tellurite [29]. The higher phonon energy of Tm:Silica ~1000 cm-^{1} limits the infrared transmission up to 2.2 μm. On the other hand ZBLAN is a heavy metal fluoride glass that offers a mid-infrared transparency out to 6 μm due its lower phonon energy of ~500 cm^{-1}. Singly charged fluoride ion and weaker bond strength of ZBLAN glass leads to greater mid-infrared transparency. Lower phonon energy and lower background loss around 2 μm of thulium fluoride fibre makes it is a suitable host material for an efficient operation of fibre laser at around 2 μm.

ZBLAN is therefore a promising glass material for the development of fibre lasers at 2 μm and in other infrared wavelengths. A thulium ion is chosen as a rare earth dopant due to the fact that, when using high thulium concentrations, cross-relaxation processes lead to highly efficient lasing at around 2 μm. As a result, Tm:ZBLAN fibre is considered for the development of the 2 μm laser in this research.

In band pumping approach is focused in this thesis due to the fact that laser active ions are pumped directly to the upper laser level from ground state. Using in-band pumping it is therefore possible to improve slope efficiency and threshold pump power by reducing quantum defects. To date the highest output power reported for a Tm:ZBLAN fibre laser at ~2 μm is only 53 mW [4], using in-band pumping, but had record slope efficiency of 74%. This low output power was believed to due to the unavailability of ~1.6 μm pump sources with sufficient power. It is now possible to develop a ~1.6 μm source with very good beam quality by using commercial components. Good beam quality source offers the potential to pump directly into the core of a Tm:ZBLAN double clad fibre and develop higher output powers at ~ 2 μm than before. The content of this thesis are:

Chapter 1: Chapter 1 contains a general overview of fibre lasers. The importance of thulium fibre laser operating around 2 μm and their applications. The importance of in-band pumping for the development of 2 μm Tm:ZBLAN fibre laser as well as review for the development of ~1.6 μm Er:Yb sources for in-band pumping are also summarised. In addition to the literature review, the author provides his own insights and deeper explanation of these systems.

Chapter 2: The introduction of this Chapter describes the motivation for conducting the pump absorption calculation of a double clad fibre. The result of the simulation for different outer cladding shapes of Tm:ZBLAN double clad fibre are provided along with impact of offsetting core and varying the core diameter. Apart from this a pump absorption measurement of Tm:ZBLAN double clad fibre using cut-back technique is compared to the modeled result.

Chapter 3: This chapter comprises three sections. The first section is about the experimental demonstration of ~2 μm 790 nm pumping Tm:ZBLAN fibre laser, results and discussions. It also includes the characterization of homemade Tm:ZBLAN double clad fibre. Second section is about the development of Er:Yb in-band pump source at 1.57 μm, where high reflective Fibre Bragg grating (FBG) and 4% Fresnel reflection formed the resonator cavity including a critical discussion. The third section represents the in-band pumping approach i.e. towards the development of an in-band pumped Tm:ZBLAN fibre laser.

Chapter 4: This chapter concludes the thesis with a general discussion and a description of possible promising future work.

List of Publications

Conference paper

H. Ebendorff-Heidepriem, D.G. Lancaster, K. Kuan, R.C. Moore, M.S.I. Sarker, T.M. Monro, “Extruded fluoride fiber for 2.3μm laser application”, accepted for oral presentation at CLEO PACRIM, 2011.

Acknowledgements

I would like to express gratitude from the very core of my heart to my supervisor Prof. Tanya Monro for giving opportunity to perform this research in a world class research environment. Her direction and guidance helps me to learn many things which were very essential for me. This research would not be possible to finish without her constant support and co-operation.

I also want to express my cordial gratitude to my co supervisor Associate Prof. David G. Lancaster. I discussed about many valuable things with him and got ideas to perform the experiment.

I would also like to thank to the rest of Institute for Photonics & Advanced Sensing (IPAS) people specially Heike Ebendorff-Heidepriem, Ori Henderson-Sapir, Michael Oermann, Richard White, Matt Henderson, H. Tilanka Munasinghe, Krishtopher Rowland, Sebastian Ng, and Chris Kalnins. They helped me in different ways and I am really grateful to them all.

I would like to acknowledge Dr. Ioannis Dritas, School of Engineering & Mathematical Science, City University London, who provide me the simulation code for calculation of pump absorption of a double clad fibre. I am very grateful to him for his kind cooperation.

Thanks also Dr Selim Mahbub for his support during the time I stayed in Adelaide.

Finally but most importantly, I would like to thank my wife Saki Farhana Noor for her support, encouragement and willingly offered sacrifice during the time I spent in Adelaide.

Contents

Chapter1. Literature Review

Chapter 2. Double Clad Fibre: Comparison of Predicted and Measured Pump Absorption

Chapter 3. Development of 2 µm Tm:ZBLAN Fibre Laser

3.2 Development of Er:Yb Fibre Laser at 1570 nm

Amendment of thesis

This document provides the answer on comments of referee 1 and referee 2.

Answer on comments of referee 1

Chapter 1

Section 1.3

- The near-IR spectral region, i.e. from 1.4 to 1.8 μm is called eye safe region, where optical absorption by water in the eye prevents power from reaching to the retina.
- For cross relaxation and resonant pumping process reference diagram has given. Energy level diagram for resonant pumping process has moved earlier in the chapter.

Section 1.3.1

- Suitable plot for tuning range of Tm fibre laser has been added.
- Reference has given to the 1st sentence of last paragraph.

Section 1.5

- Figure 1.4 (b) is fixed as a rectangular inner cladding.

Section 1.6

- Corrected sentence is: Single mode guidance can be done either by increasing the core diameter or by decreasing the numerical aperture (NA) at a certain V value.
- Corrected sentence is: For a multimode fibre the intensity distribution function often approximated as a top-hat function of radius a, with uniform intensity distribution along the core of the fibre.

Section 1.8

- Energy level diagrams have given to the first paragraph.
- In 1998, when diode pump power began to available, a 5.4 W output power was achieved from a double clad fibre laser at wavelength near 2 μm.
- References added to the last sentence.

Section 1.9

- Dichroic mirror act as an input coupler for pump light in Fig 1.7(a).

Section 1.11

- Corrected sentence is: The energy transfers for laser materials are mainly through radiative and nonradiative process. In case of radiative energy transfer process, the emission of photon by one ion causes the absorption of that photon by another ion.

Section 1.12

- Corrected sentence is: The short-infrared wavelength range effectively covered by Tm^{3+} doped lasers can pump directly with ~800 nm diodes.
- Moreover, it also observed from Figure 1.11 and 1.12 that the absorption wavelength range spanning from ~1550 nm to ~1850 nm, which is near to laser emitting wavelength at ~ 2 μm.
- Corrected sentence is: A smaller efficiency of the cross relaxation process has the effect of raising the laser threshold
- The $^3F_4$ lifetime is shortened through multiphonon decay. This shortening the life time of the $^3F_4$ manifold due to multiphonon decay will reduce the $^3F_4 \rightarrow {}^3H_6$ quantum efficiency. The lower quantum efficiency would reduce the slope efficiency.

Section 1.14

- Corrected sentence is: The effective absorption coefficient for pump light launched into the cladding of Er:Yb fibre as a function of pump wavelength is shown in Figure 1.18. In this case the core diameter of an Er:Yb fibre was 30 μm having numerical aperture 0.22 and the core was surrounded by a pure silica D-shaped inner-cladding of 400 μm diameter (~360 μm along the short axis) and the numerical aperture was 0.4. The doping concentration to the core of Er:Yb fibre was respectively Yb^{3+} ion ($\sim 8.7 \times 10^{20}$ cm^{-3}) and Er^{3+} ion ($\sim 5.1 \times 10^{19}$ cm^{-3}).

Chapter 2

Section 2.1

- The first paragraph has deleted as it was repetition of material in Chapter 1.
- For consistency “outer core” replaced as “inner cladding” in everywhere.
- Corrected sentence is: For small inner cladding area, fibre losses are reduced at laser wavelength due to the reduction of absorption length.
- Corrected sentence is: The core area and numerical aperture should be high enough to allow a high absorption efficiency of pump power in the single mode core as well as be able to excite single mode oscillation at laser wavelength.

Section 2.2

- Corrected sentence is: A beam propagation method (BPM) can be approximated by the effective index method to reduce a 3D problem to a 2D one, and still it suffers from the need to discretize paraxial wave equation throughout dense grids over realistic propagation distances, especially when large and complex geometries are involved.
- Corrected sentence is: They have demonstrated that the absorption is influenced by the bend radius for circular fibre, but in fibre design with offset core and rectangular inner cladding the bend effect is negligible.

Section 2.3 (model verification) now in Appendix

- Model verification has moved to appendix (as with other referee comments). In model verification 1000 container used.
- Corrected sentence is: Pump absorption for circular shape becomes saturated with increasing fibre length due to the non absorption of skew rays.
- Figure 2.1 now becomes Figure A1: the caption changed to square shape

Section 2.4 is now 2.3

- Corrected sentence is: The interface between inner and outer cladding is an ideal surface, has no reflective aberration and uniform step refractive index distribution. Under these conditions the propagated rays in model strictly follow the geometrical

optics domain. Regarding the geometrical boundary condition, it is also assumed that there are no losses when a pump ray is scattered by a dielectric interface and that during total internal reflection the refracted energy is negligible compare to the reflected energy when refraction takes place [92]. Moreover, it is assumed that all rays propagate in the fibres are independent of each other and have no mode coupling.

Section 2.4.1 now 2.4

- Corrected sentence is: The incident points i.e. the spot centre of incident pump photons are generated on to equally distant co eccentric circumferences (see Figure 2.1) which are centred on the fibre axis and cover a circular area defined by the pump delivering core.
- Corrected sentence is: The incident points are shown Figure 2.1(previously it was Figure 2.2) as blue star marks at the input end of the fibe.
- Figure 2.3 now becomes 2.2 and axes labels have fixed.
- Figure 2.3 caption also changed to become understandable.

Section 2.5

- ρ is density of ions and recalculated after each time step.
- Model verification part transferred to the Appendix section.

Section 2.6

- Concentration is fixed as 20000 ppm by weight.
- Figure 2.5 is now as 2.4 and explanation as follows:

  It is observed in Figure 2.4 (a), that the magnitude of core optical path for circular inner cladding is levelled around 0.6 mm, also shows the wider groups of bars and bigger valleys observed in the patterns of optical paths when it compared to Figure 2.4(b). This pattern supports that for circular inner cladding there is a strong overlap between core volume and meridional rays. On the other hand in figure 2.4 (b) the magnitude of core optical path in square shape cross-section is levelled at around 0.5 mm and more noisy bar groups emerging above the base line. Therefore, the propagation of skew rays contributes more strongly in parallelogram shape. Moreover, in case of circular inner cladding, it is observed in Figure 2.4(a) that longer

ray paths are recorded inside the core containers, they correspond mainly to a small population of meridional lines which become completely absorbed during the first few tens of centimetres. In case of square inner cladding Figure 2.4(b), the total ray spatial paths are generally shorter inside each container but they represent the contribution of a larger population of rays more sporadically interacting with the core volume and thus being able to transfer their energy along longer propagation lengths.

- Chaotically propagated rays changes to skew rays.
- For circular shape, the pump absorption tends to saturation along with the increasing of length. At the beginning the absorption increases with length sharply. After a certain distance the increasing becomes smaller and smaller due to the non-absorbtion of skew rays to the core of a fibre.

Section 2.6.2

- Figure 2.8(d) now as 2.7(d): The horizontal axis as well as legend has been fixed.

Section 2.7

- “In conclusion” changes to appropriate word.
- Corrected sentence is: The presence of higher order modes lead to degradation in the output beam quality, but most of the application requires diffraction limited beam quality.

Section 2.8.1 is now as A2 in Appendix

- “100 μm” is a core diameter of a fibre
- In Figure A2 the units of efficiency η corrected as W/A
- Table is deleted according to other referee comments and also standard deviation is omitted from the graph as the fluctuations are mostly due to a drift rather than normally distributed random fluctuations

Section 2.8.2 is now 2.8.1

- The pump light coupled from the patch fibre to Tm:ZBLAN fibre using the optical system in section A2.

- Corrected sentence is: The cleaving ends have been tested every time by placing fibre ends under microscope throughout the experiment to ensure the nice cleaving end.
- $P_p(Z_o)$ is defined for $A(Z_i)$ as: $P_p(Z_o)$ is pump power measured for smallest fibre length Zo, very close to the input end of the fibre.
- Corrected sentence is: In an optically active fibre the pump wave absorption rate at a certain point depends on the local population inversion and consequently on the local flurescence. However, to avoid the flurescence effect, the launched power should be kept resonably low so that the population inversion remains negligible.
- The label on vertical axis of Figure 2.12 is now 2.9 changes to 10log10(P).

Section 2.9

- Absorption efficiency is calculated as follows:
  Firstly, cutback data is fitted and extrapolated to zero length of a fibre, which gives the launch pump power at input end. Therefore, with the help of launch pump input and the transmitted output for every cutback length, absorption efficiency is calculated.
- Further explanation of model calculation differ from experimental valuesas follows:
  There might be two other possibilities to differ experimental result from model calculation. Firstly in model calculation effect of fibre bending was not considered for pump absorption calculation. Secondly for cut-back measurement we measured absorption at 10 metre and below 1 metre length only. For more accuracy of measurement it could be performed the cut back experiment repeatedly througout the whole length of fibre. But we had limited length of commercial fibre and also needed to perform fibre laser experiment.

Chapter 3

Section 3.1.2

- As it is evident from the microscopic view of the end facet of the fibre that the fibre is 5 μm offset. Considering that we used pump absorption 0.76 dB/m (measured for 10 m length of fibre) to calculate the pump absorption for 5 m fibre.

- Explanation for launch efficiency measurement: After collimating and focusing, 790 nm light has been coupled to Tm:ZBLAN fibre and optimised for maximum coupling. After optimisation output power is recorded. Therefore the launch efficiency to the fibre was calculated by measuring the difference of input power and transmitted output power with power absorbed to the fibre, which is 92%. It is noted that absorbed power is calculated by using cut-back absorption.
- Output coupler having 0% reflectivity at 2000 nm butted to the output end of fibre to examine fibre laser spectrum at ~2 μm laser. It is noted that we didn't used any index matching gel to mitigate against Fresnel reflection.

Section 3.1.3

- Figures are rearranged
- The figure 3.2 (a) for 0% reflective output coupler. The data showed in table 3.2 but all the data tables have been deleted according to other referee comments.
- Resonator layout has explained.
- In initial configuration 4% Fresnel reflection used to form the resonator. For 0% reflective output coupler, mirror butted to the output end.
- Here forward direction refers to the increment of input power from zero to maximum value used in this experiment and backward direction refers to the decrement of input power started from forward directions maximum value.
- Corrected sentence is: Further scaling the output is possible by increasing the launch pump power as well as by maintaining proper cooling system to protect from thermal damage of the fibre.

Section 3.1.5.1 is now 3.1.5.2

- Fibre fabrication section is now as 3.1.5.1
- To increase the core refractive index of ZBLAN fibre part of BaF_2 replaced with the PbF_2.

Section 3.1.5.2 is now 3.1.5.3

- The variation of NA values might be due the defect of interface between core and cladding.

- Assuming a refractive index of Tm:ZBLAN glass 1.495 at 790 nm, the core refractive index is 1.4954 ± 0.0001,
- Δn, the index difference between core and cladding is 0.0004 ± 0.0001.

Section 3.1.5.3 is now 3.1.5.1

Section 3.1.5.5

- To reduce the loss of the fibre the outer and inner surface of the tube should be etched prior to fibre drawing to achieve a pristine surface. A defect free interface between the core and cladding glass is prerequisite to achieve low fibre loss. Therefore future work will focus on further reducing the fibre loss through optimization of fibre drawing conditions and demonstration of lasing at 2.3 μm.

Section 3.2.5 is now 3.2.4

- Corrected sentence is: By pressing the fusion button fibre becomes spliced and the splicing loss was observed 0.02 dB in Ericsson splicer.
- A pump mirror which has HR (900-990 nm) >99.9% and HT (1500-1650 nm) >98% butted to the rear side of the fibre to separate the lasing signal from pump laser wavelength.

Section 3.2.6 is now 3.2.5

- Corrected sentence is: To verify the accuracy of measurement of a monochromator it was calibrated for 2nd order wavelength using HeNe source.
- Table 3.8 has deleted according to other referee comment.
- The length of the fibre was 3.85 m for 1570 nm laser output.

Section 3.2.7 is now 3.2.6

- “xx” software changes to LabVIEW software.

Section 3.2.8 is now 3.2.7

- For core pumping approach absorption coefficient is very high. Therefore relatively short length of fibre can be used to form the fibre resonator. That's why we chose double clad fibre in our case.

Section 3.3.1

- Reference has given for 2nd sentence of 2nd paragraph.
- Laser reported by [63] now becomes [2] was single mode.

Section 3.3.2

- First the absorption is calculated at 1570 nm from absorption spectra (chapter 1 Fig. 1.11) of a Tm doped ZBLAN glass. As the graph was given absorption (cm^{-1}) as a function wavelength, so the absorption (cm^{-1}) at 1570 nm was calculated by deducing the value from base line to 1570 nm. Therefore, the absorption coefficient at 1570 nm becomes 0.03 cm^{-1} and the corresponding absorption is 0.13 dB/cm. The data in Table 3.10 was calculated using Beer Lamberts law(data is deleted now).

Section 3.3.3

- Initially 1570 nm light is collimated and focused using 18.4 mm and 15.29 mm aspheric lenses to coupled the light to the core of a Tm:ZBLAN fibre . As the light was not coupled to the core, therefore 4.5 and 4.51 mm aspheric lenses used to collimate and focus the light to the core of a Tm:ZBLAN fibre.
- The length of fibre 30cm chosen and the absorption at 1570 nm is 60.84% as evident from figure 3.19.

Section 3.3.4.1

- Schematic figure is added to understand the knife edge measurement. 15.29 mm lens was the same as used in section 3.3.3
- Corrected sentence is: the beam cut into micron distance along the x direction as shown in figure 3.21
- The number of significant figures in the spot size in Figure 3.22(a) has changed.
- The explanation for overfilling the beam as follows:

The table below provides the relative picture of beam diameter for different lenses used to collimate and focus 1570 nm light. The diameter of a beam is calculated using the relation, Beam diameter=2*E.F.L*NA, where, E.F.L is the effective focal length of a lens and NA is the numerical aperture of the source

Table 3.2. Calculation of a beam diameter of a beam coming out from 6 μm core having NA 0.18 of Er:Yb fibre

Focal length (mm)	NA of lens	Acceptance angle(deg)	Diametre of a lens(mm)	Beam diameter(mm)
4.50	0.42	24.83	3.70	1.62
4.51	0.54	32.68	4.95	1.62
15.29	0.16	18.41	5.0	5.50
18.4	0.15	17.25	5.5	6.62

It is clear from above calculation that the beam is overfilling for longer focal length lens. Therefore the next step was to use shorter aspherics to collimate and focus the light into the core and to measure the core absorption using cut-back method.

- Due to the shortage of time knife edge spot size measurement for shorter aspherics did not perform.
- As Er:Yb fibre laser output offers very good beam quality, which is suitable for core pumping. Moreover for high absorption coefficient shorter length of fibre needed for fibre laser experiment. Therefore, we chose core pumping approach although the fibre is double clad.

Section 3.3.4.2

- Careful adjustment was required to couple the pump light to the core.
- To measure the core absorption of pump light, initially output power was recorded when light was not coupled to the core. Then, light into the core has been ascertained through optimisation and by observing the fluorescence through IR viewer. After observing the light coupled into the core, it has been optimised and input end of the fibre kept unchanged. A power metre head was fixed in position and the transmitted output was recorded for every cut-back measurement. As the transmitted output is composed of core and cladding light, therefore the core absorption for every cutback

is considered here as the difference between the output power when pump light coupled only to the cladding and when coupled both to the core and cladding. Symbolically one can write core absorption = $P_{\text{inner cladding}} - P_{\text{core \& innercladding}}$. Where, $P_{\text{inner cladding}}$ is the output power for pump light passing through cladding and $P_{\text{core \& innercladding}}$ is the output power passing through both the core and inner cladding.

- Figure 3.23 vertical axis change to 10log10(P)
- α value calculated from 0.05 dB/cm.
- We assumed the data in Figure 3.23 for core absorption, but there might be error in measurement as the light from cladding was not possible to remove.
- From Figure 3.23 the output extrapolated to zero length is 10log10(P)=17.68, i.e. 58.6 mW and the input power was 185 mW. Therefore, it is assumed that the coupling efficiency to the core of a fibre was estimated at 31.6%.
- Text has re written for logical argument. For explanation of suitabality of 30 cm fibre than 56 cm Please see the explanation in page 105.
- Most of the pump light should couple to the core. As Er:Yb fibre laser output offers very good beam quality, which is suitable for core pumping. Moreover for high absorption coefficient shorter length of fibre needed for fibre laser experiment. Therefore, we chose core pumping approach although the fibre is double clad

Answer on comments of reffere report 2

- Page 20, 2nd paragraph: repititive part of second paragraph has been deleted.
- Page 20, Fig 1.2 has deleted.
- Page 22, 2nd paragraph corrected the word from confirm to confined
- Page 24, 1st paragraph: Figure 1.4(b) is corrected as a representative of a offset fibre.
- Page 25: V number has linked linked to normalised frequency as well as weak guiding regime. Please see page 25. Core refractive index n_c used ingeneral. Poulain's unexpected discovery of fluorozirconate glasses.
- Page 31: K changed to k for Boltzman constant. The value for K also followed by standard SI table.
- Page 34: Figure becomes visible.
- Page 38: In band ZBLAN results are plotted with a muliplier factor.
- Page 45: 1st paragraph has deleted as it was contained repetition material of chapter 1.
- Page 46: Double clad fibre consists of three different layer having step index refractive index profile from core to outer cladding. The detail has been discussed in previous chapter.

  Explanation for second sentence as follows:

  For non circular shape of DCFs, the symmetry of light rays is broken and the absorption efficiency is improved by blending of the pumping waves [76, 82]. This is because for non circular shape of inner cladding the symmetry of pumping wave is broken as well.

  Although various cross-sectional shapes have been employed, in practice, only a few researchers have focused on the influence of cross-sectional shape on the absorption characteristics of DCF lasers. The reason can be explained as follows.

  In order to calculate the absorption characteristics by solving the wave propagation equation in DCFs it is necessary to calculate the eigen modes. Generally typical double clad fibre having NA 0.5 and 100 μm inner cladding will support more than 10^4 eigen modes. It will require a very large amount of computing time and cumbersome to include all these modes in the calculation.
- Page 47: Model verification moved to Appendix.

For circular shape, the pump absorption tends to saturation along with the increasing of length. At the beginning the absorption increases with length sharply. After a certain distance the increasing becomes smaller and smaller due to the non-absorbtion of skew rays to the core of a fibre.

- Page 50: Labels become visible now.
- Page 52: This sentence moved to the result section.
- Page 52: Fig 2.3 Labels have been modified
- Page 53: Fig 2.4 labels have been modified
- Page 55: ppm by volume changes to ppm by weight. Also explained more explicitly the reason for only meridional rays contribution for circular shape and logical flow is maintained.
- Page 58: The sentence is corrected. Please see page 58.
- Page 61: Horizontal axis label is corrected. Also the pump absorption explanation is changed according to comment.
- Page 62: Corrcted as advised.
- Page 63: Table 64,65 as well as other tables have been deleted where the graph represents the data.
- Page 64,65: Pump laser scaling and fluctuation has moved to Appendix.
- Page 66: Extra value of 10 in the equation has been deleted.
- Page 69 now page 66: Fig 2.13 becomes 2.10, label has changed.
- Page 70 becomes page 67: Further explanation of model values differe from experimental values as follows:

  There might be two other possibilities to differ experimental result from model calculation. Firstly in model calculation effect of fibre bending was not considered for pump absorption calculation. Secondly for cut-back measurement we measured absorption at 10 metre and below 1 metre length only. For more accuracy of measurement it could be performed the cut back experiment repeatedly througout the whole length of fibre. But we had limited length of commercial fibre and was needed to perform fibre laser experiment.
- Page 72: Repetitions contains in indroduction and motivation section has deleted.
- Page 73: V number of 1.88 at 2 μm wavelength.
- Page 74: Figures are rearranged accordingly. Also Fig 3.3 (a), (b), (c) plotted seperately. Please see section 3.1.3, page 71.

- Page 76: Modified accordingly as comments. For 0% output coupler we did not use index matching gel.
  Upward direction changes to forward direction.
  Increasing the output coupler reflectivity's causes the decrease of slope efficiency of Tm:ZBLAN fibre laser.
- Page 79: Labels are modified
- Page 80: Modified according to comments.
- Page 82: The trerm dag is replaced to to unabsorptive surface coating every where.
- Page 83: Refractive index of Tm:ZBLAN 1.495 used as supplied by commercial Tm:ZBLAN fibre data sheet. In the future, we will measure the refractive index of our core and cladding glasses to provide insight into the predicted NA.
- Page 89: The calculation is for only the cladding absorption. Please see page 85 for detail
- Page 92 now page 87: Fig 3.13 is now 3.12, axis label has been fixed.
- Page 93: It has been confirmed from the transmission measurement graph (Figure 3.12) that the reflectivity of FBG is around 1570 nm.
  Second sentence is corrected as: By pressing the fusion button fibre becomes spliced and the splicing loss was observed 0.02 dB in Ericsson splicer.
- Page 96: Additional explanation added for the purpose of transmission measurement.
- Page 97: horizontal axis fixed to match with other figures.
- Page 100: xx softaware changes to LabVIEW software .
- Page 106: M2 value changes to 1.3
- Page 107: Initially 100% output is recorded. Therefore data is recorded from above 90% to below 10%. The label of of 90% and 10% indicated in graph.
- Page 109: Number of significant figure has modified.
- Page 108: Convention for molar weight has chnged to MW
- Page 116: Journal for ref 29 now ref 28 has been added.

List of Figures

List of Tables

Chapter 1

Literature Review

1.1 Introduction

LASER stands for light amplification through stimulated emission of radiation and many types of lasers have been demonstrated. Fibre lasers at around 2 μm play a key role as a high intensity source in a diverse area such as telecommunication, laser radar, materials processing as well as medicine. Many researchers have been involved in the development of 2 μm lasers using bulk crystals as well fibres. The thulium ion has been used rigorously to develop these 2 μm lasers. The maximum Tm:Silica fibre laser reported 1 KW using 790 nm source [1] and 415 W using 1.567 μm pumping in all fibre format [2]. The slope efficiency of these fibre lasers are respectively 53% and 60%. While in the case of Tm:ZBLAN, 2 μm fibre lasers have reported a maximum output of 20 W [3] using 790 nm pumping, and when using in-band pumping only 53 mW [4] with high slope efficiency. In in-band pump the absorption is around 1.6 μm, near to lasing emission. Therefore, it is also possible to pump directly to the emitting level using this wavelength as a pump source. Thus in-band pumping approach excites directly the thulium ions into the upper laser level ($^3F_4$) increasing the maximum stokes efficiency providing an attractive means to scale the output power of Tm:ZBLAN fibre lasers at 2 μm. Presently watt level commercial lasers are achievable at around 1.6 μm using commercial components. These diodes can be used to exploit in-band pumping of Tm:ZBLAN fibre lasers.

This thesis is devoted to the development of a Tm:ZBLAN fibre laser at ~2 μm through 790 nm pumping as well as ~1.6μm in-band pumping. The in-band pumping approach is based on a hybrid fibre laser scheme, where a cladding-pumped Er,Yb fibre laser operating at 1.57 μm would be used to pump the Tm:ZBLAN fibre laser. The goal is to demonstrate an efficient operation of Tm:ZBLAN fibre laser at ~2 μm.

This chapter is therefore describe the need for fibre laser, the state of the art for fibre laser at 2 μm and also the literature review and scope to develop 2 μm fibre laser.

1.2 Fibre Lasers

Lasers can make in various forms from nano-lasers to compact semiconductor based lasers, which are common in CD and DVD player, barcode scanner as well as to building sized systems like the National Ignition Facility. Because of lasers high average power, compact and portable size, high reliability and the ability to propagate a beam over long distances, its application is rapidly increasing in different areas, such as, medical, material processing, defence and sensing.

The fiber laser has emerged as a laser design that is an excellent fit for the needs of such highly demanding applications due to the invention of large mode area (LMA) fibres and the availability of high brightness semiconductor diode pumps. Normally the fibre is consisted of the high index core and lower index cladding. The active core is doped with rare earth ions chosen based on the desired emission wavelength. The cladding is designed in such a way so that light can be able to propagate through the core and excite the laser ions. Extensive research has been carried out to fabricate rare-earth ion doped crystals and glasses after the first lasing demonstration using a ruby crystal [5]. These rare-earth doped glasses and crystals have been used to demonstrate solid state lasers for coherent emission of different wavelengths. In comparison to crystals, glasses have broader laser transitions, which is an essential feature for wavelength tuning and ultra short pulse generation. Moreover, it also has wider absorption spectra, relieving the wavelength tolerance for pump sources. Apart from this single mode optical fibres, which are drawn from glasses exhibit a flexible and compact gain media for efficient and excellent beam quality laser generation. To date, single mode fibres can be drawn from silicate, phosphate, fluoride, tellurite, germinate and chalcogenide glasses etc. The spectral range of glass fibre lasers can cover from the ultraviolet (UV) to mid-infrared and the output power of a single-element fibre laser can be up to kilo-watts [6]. The emergence of fibre lasers are even more important as they are practical to use. Fibre lasers can be made monolithic and compact while at the same time being highly efficient. They are more straightforward to assemble compared to the complex and highly skilled assembly processes essential for the production of conventional laser cavities. The appropriate fibre laser design which is compact, efficient and flexible, is likely to replace most conventional solid state lasers in

applications where peak power is not required. Nonlinearity and mode field diameter are the main factor that limits the power to further scale for fibre laser.

The fibre laser cavity can be formed by either butt-coupled mirrors or fibre-integrated mirrors such as Bragg-gratings or loop mirrors. Fibre-based laser systems have the reputation of being immune to many thermo-optical problems due to their geometry. Moreover, the beam quality of the guided mode is power independent, as it is determined by the fibre core design. Their excellent heat dissipation is due to the fact that heat can be dissipated over the longer length of the fibre and the gain medium is only a short distance from the outer surface of the fibre. The gain of the laser medium is determined by the product of population inversion, and interaction length with the laser radiation in the gain medium and emission cross-section. This can be orders of magnitude higher in fibres than in other bulk solid state lasers. This results in a very efficient operation of fibre laser systems exhibiting very high gain and low pump threshold values.

1.3 2 μm Lasers

Laser sources around two microns have many potential applications in the field of medicine, communication and eye safe laser radar or lidar. For many of these applications the wavelength, pulse energy and pulse duration are of primary interest [7]. The near-IR spectral region, i.e. from 1.4 to 1.8 μm is called eye safe region, where optical absorption by water in the eye prevents power from reaching to the retina [9]. From here on the term “eye safe wavelength” will be used for wavelength range from 1.4 μm to ~2.2 μm. The favourable absorption in water also makes such lasers useful for medical applications. A spectrum of the optical absorption in water is shown in Figure 1.1, measured by Hale and Querry [8].

It is observed from the graph that there is strong absorption around 2 μm in human tissue, which results in a penetration for this particular wavelength of a few hundreds of microns [9]. The strong absorption by the water in living cells allows for very precise cutting of biological tissue. The coagulation effect helps to reduce the bleeding during the laser cutting. 2 μm lasers are therefore ideally suited for many surgical procedures [9].

Figure 1.1. Optical absorption in water [8].

Extensive research has been carried out on different crystals as well as silica fibre for the development of 2 μm laser sources. A thulium doped fibre laser, operating in a broadly tunable region around 2000 nm, can be operated efficiently when the fibre core is heavily doped. In that case, due to a cross relaxation process between pairs of thulium ions one pump photon at 790 nm can generate two laser photons. See Figure 1.13 (section 1.12) for cross relaxation process.

In the case of Tm:Silica fibre both 790 nm pump source and resonant pump source at ~1600 nm (see Figure 1.6) have been rigorously studied and it has become a mature technology. Studying the performance of Tm:ZBLAN fibres is significantly less mature particularly in-band pumping.

1.3.1 Applications of Thulium Fibre Lasers

Many applications for fibre lasers, including most materials processing applications, call for raw power and do not require specific wavelengths or have spectral constraints to be effective. These applications use the most efficient, robust and cheapest technology, which, in the current market are ytterbium fibre lasers [10]. This preference is mainly due to the low cost of the 915-976 nm pump diodes required for pumping and the low quantum defect of the ytterbium laser scheme [10]. It is understandable that

thulium lasers cannot compete with ytterbium systems in terms of costs. However, in many cases where the application requires a specific spectral region, thulium doped fibre lasers are suitably efficient. In order to better understand the needs of the more advanced thulium fibre lasers systems it is important to understand the applications that will benefit from their implementation. The following section will discuss this in detail.

There is a great market potentiality for lasers operating in the "eye safe" wavelength range, especially in free space applications where eye safety is very important. Because of the tuning range of thulium laser transmission it provides differential studies of absorption or optimisation of laser signal based on selecting the optimal transmission wavelengths [11, 12]. Figure 1.2 shows the tuning range of thulium fibre laser.

Figure 1.2. Tuning range of Tm fibre laser [14]

In addition to applications which generally fall into the eye-safe regime, there are also applications which specifically call for wavelengths around 2 μm. Medical applications where particular biological absorption resonances must be hit (or avoided) to optimize a

particular procedure are one large area requiring spectrally controlled thulium fibre lasers. Studies are being conducted to prove the usefulness of the thulium fibre lasers and allow their use in clinical trials. As thulium lasers prove themselves for medical applications over conventional surgical alternatives [13], numerous new medical applications requiring power scaled thulium lasers in the hundreds of watt range will continue to rise. Such applications will have steep demands on spectral control to target particular molecules within the thulium bandwidth such as haemoglobin, melanin or water.

The 2 μm wavelength range is also very attractive for material processing especially for plastics [9]. Using the absorbed energy of a 2 μm laser; cutting, welding, and marking are easily possible. Apart from the above described applications, 2 μm laser systems are also interesting for military and security applications, free space optical (FSO) communication as well as for the pumping of laser sources for the mid infra-red region. Thulium lasers have a use in almost every field that a laser might find an application, as its uniquely broad tuning range enables it to be used for applications where absorption features must be missed or hit and for applications requiring broad spectra.

1.4 Limitation of Core Pumping Scheme for Fibre Laser Development

Fibre laser research has accelerated since the first demonstration of a core pumped Nd-doped silica fibre by a laser diode in 1985 due to great effort by Payne and his co-workers [15]. The lasing achieved had a low threshold and the output power was extremely low due to the poor coupling efficiency of 1.5 mW diode into the core. In a core pumped system, the optical pump beam is injected to the core of the active fibre. For an efficient coupling efficiency a single mode diode is required. Such pump sources are low power and costly. When power scaling end pumped laser system, desired a high input power can only be provided by multimode pump sources. This limitation is overcome through cladding pumping [16, 17]. The next section will describe the advent of cladding pumping fibre laser.

1.5 Cladding Pumping Fibre Laser

A fibre laser based on ordinary doped single mode fibre can generate a diffraction-limited output, but it is restricted to pump sources with diffraction limited beam quality and thus normally to those with low power. However, multimode fibres are optical fibres which support multiple transverse guided modes for a given optical frequency and polarization. To increase the coupling efficiency, it is necessary to use a larger fibre diameter that is matched to the area of high power diode laser. However, an increased fibre diameter leads to multimode operation and reduced beam quality.

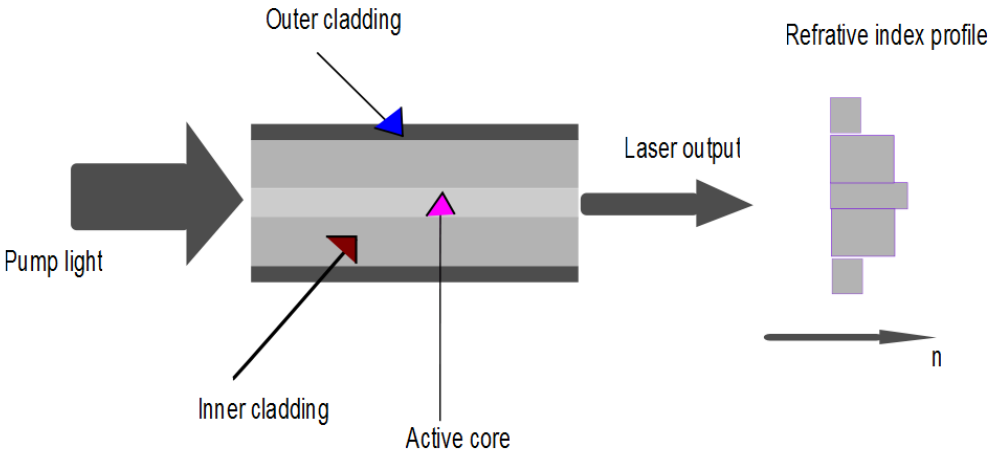

Figure 1.3. Double clad fibre concept.

This dilemma has been resolved with the invention of double-clad fibres [18], which consists of three different refractive index layers $n_{core} > n_{inner\ clad} > n_{outer\ clad}$ as shown in Figure 1.3. In a double clad fibre the pump light is confined to the inner cladding by the outer cladding. Low-brightness high-power diode laser radiation can therefore be launched into the fibre. This pump light is gradually absorbed over the entire fibre length (or more precisely, the pump light that overlaps with the central doped core region is absorbed) and is converted into high-brightness, high power laser radiation in the core. Due to the low NA of the core, the beam quality of the output can be diffraction-limited despite the use of multimode pump. The brightness of the laser or amplifier output can therefore be much higher than that of the pump source.

Thus, double-clad rare-earth-doped fibres can provide a highly efficient brightness improvement by pump to laser radiation conversion by the laser. In cladding pumping, however, the core‟s effective absorption coefficient is smaller than true absorption coefficient by a factor roughly equal to the overlap between the pump area and the core area. For a given doped core the length of the fibre must be increased in order to achieve sufficient pump absorption.

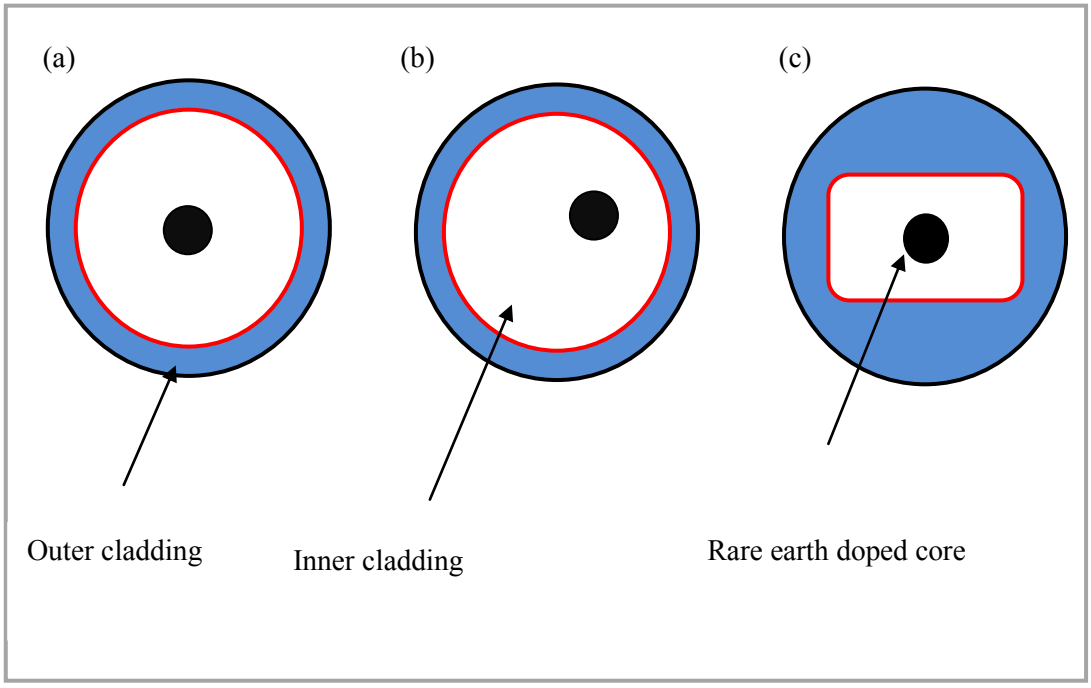

Figure 1.4. Various forms of cladding pumped fibre laser. In each case the black circle represents the fibre core.

This length increasement depends on the core/cladding area ratio as well as the design of the fibre profile. Thus when cladding pumping, efficient brightness conversion from a multimode pump to a single mode output can be achieved, if propagation losses are not significant despite increasing the fibre length.

For higher laser efficiency it is therefore important to optimize the coupling of pump radiation from cladding to core. This can be achieved by altering the geometry of the inner and outer cladding. e.g. Figure 1.4. In the inner cladding of a cylindrically symmetric double clad fibre Figure 1.4 (a), intensity distribution can exist which have no overlap with the doped core. This leads to a degradation of the laser efficiency. Because a portion of the launched light is skew to the fibre axis which will never

crosses the central region of the pump cladding. The pump light absorption can be significantly improved by breaking the cylindrical symmetry of the inner cladding. Geometries such as offset core Figure 1.4 (b) or rectangular inner claddings Figure 1.4 (c) have been suggested to minimize the pump absorption [19, 20].

1.6 Fibre Laser Characteristics

The fibre considered here has the central core in which light is guided. The core has a refractive index denoted by n_{core} and it is imbedded in an outer cladding with a lower refractive index, $n_{clad,}$ as shown Figure 1.5. The fibre is assumed to have a step index profile and a core diameter D.

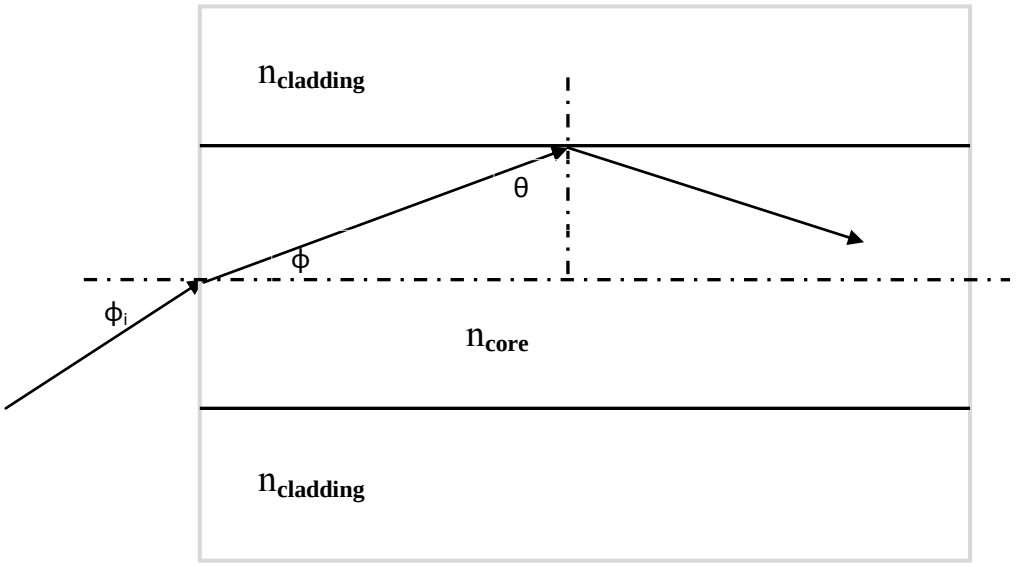

Figure 1.5. Schematic diagram for ray propagation through fibre.

The numerical aperture (NA) which determines the maximum angle of incidence ϕ_{max} for rays to be coupled into the fibre can be expressed interms of the refreative indices of the core cladding glasses by

$$NA = n_0 \sin\phi_{max} = n_{core}\sqrt{1-\left(\frac{n_{clad}}{n_{core}}\right)^2}$$

$$= \sqrt{n_{core}^2 - n_{clad}^2} \quad (1.1)$$

The number of modes supported by a fibre is defined by the normalised frequency or V number. The normalised frequency can be written as

$$V = \frac{2\pi}{\lambda} aNA = \frac{2\pi}{\lambda} a\sqrt{n_{core}^2 - n_{clad}^2} \quad (1.2)$$

where, λ is the wavelength of light in vacuum, and n_{core} and n_{clad} is the refractive indices of core and cladding of the fibre with a core radius a.

The single mode guidance of a fibre occurs when V number is less than 2.405. In this case only fundamental mode would be propagated through the gain media [21, 22]. Therefore single mode guidance can be done either by increasing the core diameter or by decreasing the numerical aperture (NA) at a certain V value. For single mode guidance the index contrast between core and cladding is typically small, so that fibers are weakly guiding, but in general the guidance is sufficient to negotiate bend with radii of tens of centimeters. A low V number makes a fiber sensitive to bend losses in the cladding. However, a high V number may increase scattering losses at the core-cladding interface.

For a multimode fibre the intensity distribution function often approximated as a top-hat function of radius a, with uniform intensity distribution along the core of the fibre [23]. However, for a single mode operation the intensity distribution approximates the Gaussian distribution and is given by [24]

$$I(r) = \frac{2}{\pi w^2} exp\left(\frac{-2r^2}{w^2}\right) \quad (1.3)$$

where, w is beam spot size.

1.7 Laser Host Material

ZBLAN is a heavy metal fluoride glass with a molar composition of 53% ZrF_4, 20% BaF_2, 4% LaF_3, 3% AlF_3, and 20% NaF, suitably stable glass for optical fibre fabrication which was first reported by Ohsawa et al. [25]. Low loss, high strength and high tunability of silica glass makes it suitable to construct fibre lasers. Fluoride glasses are

an attractive host for visible and mid-infrared lasers due to its low phonon energy and wide mid-infrared transparency [26].

Since Poulain‟s unexpected discovery of fluorozirconate glasses, ZBLAN glasses have drawn much attention because of its broad transmission window, low optical dispersion, low refractive index, ease of machining and polishing, and small thermal dependence of the optical properties [27]. The table 1.1, below describes the properties of ZBLAN glass compared to those of silica glass. In ZBLAN glass the singly charged fluoride ion has lower bond strength than in silica glass, which leads to its greater infrared transparency. The ZBLAN glasses stability and hardness are lower than silica glass. When light propagates through an optical glass it starts to attenuate because of intrinsic and extrinsic processes. Band-gap absorption, Rayleigh scattering, and multiphonon absorption are included in intrinsic processes. Lower intrinsic loss can obtain by shifting infrared edge of multiphonon absorption to longer wavelengths because band-gap absorption and Rayleigh scattering are only significant at short wavelengths. The materials which have lower bond strength and the higher reduced mass are expected to have lower fundamental absorptions at longer wavelength. This is the case in ZBLAN glass which has an average cation mass of typically 90 [28]. The minimum loss coefficient for ZBLAN glass is predicted to be as low as 0.01 dB/km at 2.5 μm [29], which is much less than silica‟s 0.2 dB/km at 1.5 μm.

Table 1.1. Properties for ZBLAN and Silica glass [30].

ZBLAN fibres have grown a lot of interest as an alternative fibre for long-haul optical communications since 1980s. ZBLAN fibres fabricated in labs have demonstrated attenuation coefficients of less than 1 dB/km [30]. Commercial silica fibres still have a lower background loss 0.2 dB/Km. Aalthough the lower losses have been achieved, the typical background loss of commercial ZBLAN fibres is in the range of 10–100 dB/km due to the extrinsic scattering and absorption losses that are relatively difficult to control in the fabrication process [28]. As a result of the higher loss of ZBLAN glass, output levels of ZBLAN fibre lasers would be lower than those of silica fibre lasers. Due to the vast applications of fibre lasers at 2 μm, more research would be needed into ZBLAN fibre lasers, to further develop the technology.

1.8 Two Micron Tm Doped Fibre Lasers

The development of thulium fibre lasers roots back into the early history of lasers. The use of thulium as a laser ion was first reported in thulium doped crystal lasers (CaWO4 and YAG) which occurred in the early 1960"s. During this time numerous crystal hosts and dopants were being rigorously investigated [31-34]. After being proved as a potential laser ion, further research continued in thulium"s emission wavelength in the 1.9 - 2.1 μm range. The development of first fibre lasers begun in the mid 1980s, with included the production of high quality fibres as well as the development of pump diodes. The first thulium fibre laser was reported in 1988, and was pumped with a dye laser at 790 nm. It achieved a few 10"s of mW of power [35]. Research on thulium fibre lasers accelerated due to the growing interest in fibre lasers for applications requiring compact, high power sources at flexible wavelengths. The two main attractive pump absorption bands of Tm:ZBLAN and Tm:Silica are at ~780-800 nm and at ~1550-1750 nm (see Figure 1.6) will discussed later in section 1.12. The latter absorption bands coincide with the emission wavelengths of pump erbium fibre laser sources. The detail of this will discuss in the development of the Er:Yb pump source for in-band pumping

in section 1.14. The attractive emission of thulium doped ZBLAN as well as silica lasers is very broad emission from the $^3F_4$-$^3H_6$ transition which ranges from ~1700 to ~ 2100 nm [36]. Taking advantage of this large tuning range of rare earth ion, the first tunable thulium fibre laser was reported in [37] which had a tuning range of 1780 nm to 2056 nm.

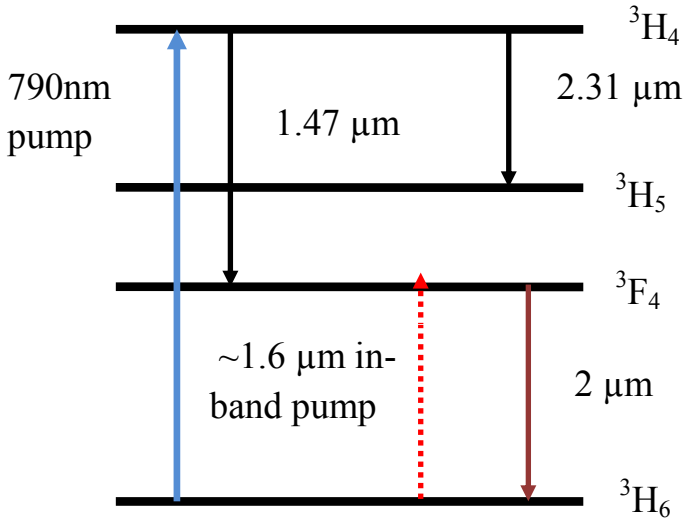

Figure 1.6. Energy level diagram of a Tm doped ZBLAN fibre laser.

The first ZBLAN fibre laser at 2 µm demonstrated around 0.2 mW of output power with slope efficiency of only 0.3% [38]. At the same time Tm:ZBLAN fibre lasers were studied for range of emission wavelengths but at 2 µm the output as well as efficiency were not improved [39]. Tm:ZBLAN fibre lasers have been pumped with semiconductor lasers as well as color centre laser. The slope efficiencies of these lasers are very high, from70 to 84% [4, 40,41], however the maximum power achieved was only 53 mW [4]. Then for a give years research on thulium fluoride fibre lasers saw little improvement in laser performance. Research therefore returned to the development of high power silica fibre laser at this wavelength. The first watt level thulium laser was give year soon after the development of the first thulium fibre laser [42], by simply scaling up pump power of the readily available Nd:YAG pump sources of 1064 nm. This laser used a single clad fibre, and was core pumped. In 1998, when diode pump power began to available, a 5.4 W output power was achieved from a double clad fibre laser at wavelength near 2 µm [43]. The slope efficiency of this laser was in the range of 30-35%. An increase in the laser efficiency was accomplished throughout the implementation of high doping concentrations and the use of the cross

relaxation process. Cross relaxation in thulium is a long understood process, as it was demonstrated in thulium doped crystals [44], the basic idea is that two laser photons can be produced from a single pump photon. The slope efficiency could therefore be double the quantum defect. This effect was first observed in thulium fibres in Ref [45] where slope efficiency 46% was achieved. This laser generated 12 W of output power. The ability to dope thulium in high concentrations was realized by the inclusion of aluminium oxide in the glass doping formula which reduced clustering and enhanced the desirable cross relaxation process. This process was further studied by Jackson in Ref [46, 47]. The realisation of this process and the increase in available diode power lead to the rapid advance in output power in thulium silica fibre lasers from 12 W in the year 2000 to the near kilowatt levels currently achievable [48].

The research contained within this thesis aims to develop ZBLAN fibre lasers using the same technology as is used in silica fibre lasers through the use of high doping concentrations and the cross relaxation process. In 2004, B.M. Walsh et al. [36] reported the comparative study on Tm:ZBLAN and Tm:Silica fibre lasers. The spectroscopy of these materials indicated that Tm:ZBLAN posseses advantages over Tm:Silica glass due to its lower phonon energies. The result of tunable 790 nm pumped fibre laser operating from 1.85 to 2.1 μm has been demonstrated that Tm:ZBLAN can be achieved a factor of 2 higher in slope efficiency and a factor of 3 lower in threshold than in Tm:Silica fibre lasers [36]. In 2005, M. Eichhorn [49] reported a high average output of a CW thulium doped fluoride fibre laser at 2 μm using a double end pumping scheme, of 6 W. The slope efficiency of 32.6% was reported for this fibre laser. A 2.4 m long fluoride double clad fibre was used by Le Verre Fluoré. The fibre was doped with 25000 ppm thulium. The fibre had a core diameter of 30 μm and an NA=0.08. The D-shaped outer cladding had an NA=0.47 with a circular diameter of 300 μm, from which 30 μm was truncated to enhance the pump absorption. Because of the core a fibre has low NA this fibre would have high bending losses which have been reduced by introducing an undoped annular ring of higher index concentrically oriented around the core of a fibre. Following this work, in the year 2008, M. Eichhorn et al. [3] reported the highest output of a Tm:ZBLAN fibre laser at 2 μm, at 20 W. They used same fibre geometry. A slope efficiency of 49% was reported, which is still lower than the reported value of Tm:Silica. There is still room to increase the slope efficiency and output power of Tm:ZBLAN fibre lasers. The increased interest in thulium fibre lasers since the mid

2000s has lead to the development of higher power pump diodes and improvements in the fibre composition to better enable cross relaxation [1, 45, 46, 48].

1.9 Laser Resonator Types of Tm^{3+} Doped Fibre

In order to develop a fibre laser it is necessary to understand the resonator cavity configuration. Commonly there are three kinds of fibre laser resonators as shown in Figure 1.7

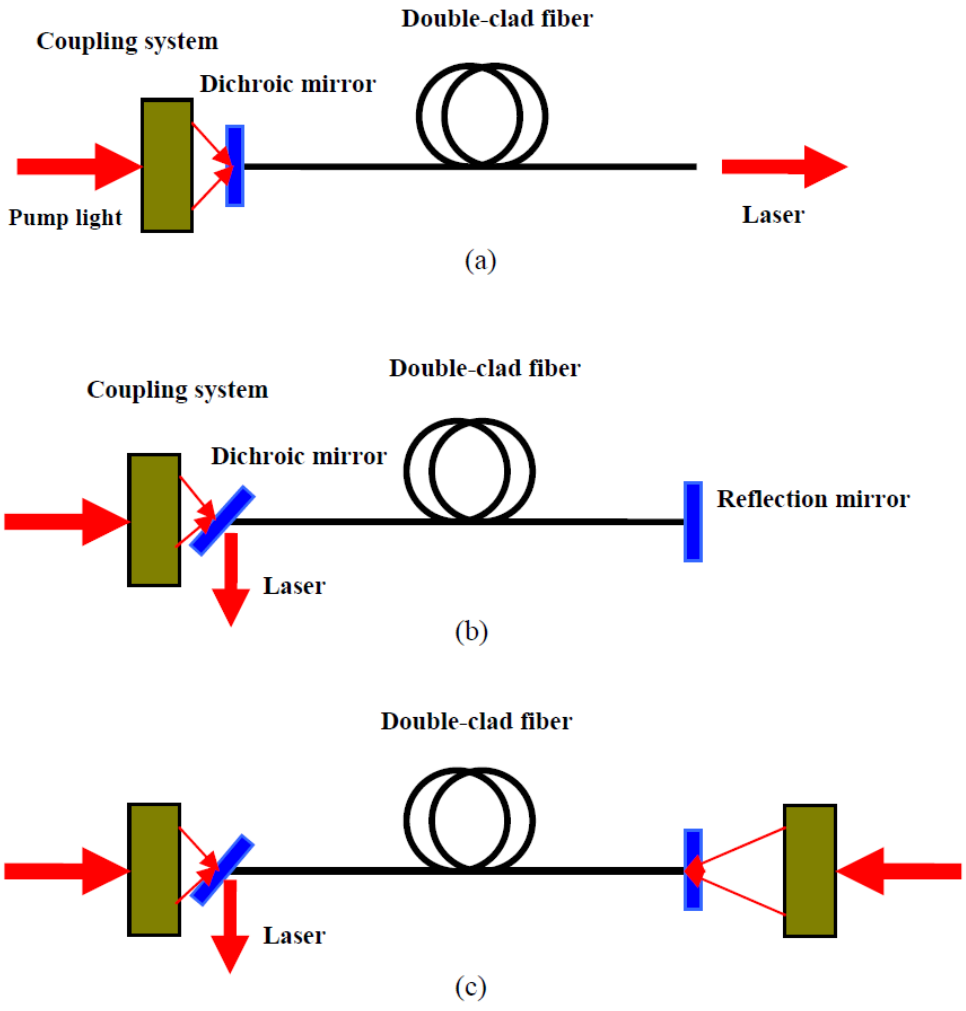

Figure 1.7 Schematic diagram of resonator, with (a) single end pumping (b) a single counter propagating end pumping and (c) double end pumping configuration [50].

Figure 1.7(a) is the simplest cavity configuration, in which the pump light is launched into the fibre through a highly reflective dichroic mirror act as an input coupler for pump light. Laser oscillation forms between the dichroic mirror and the Fresnel

reflection (depends on the index of host material) of the cleaved output end facet of the fibre. In this cavity configuration, addition of output coupler can improve the optical efficiency of the fibre laser. In Figure 1.7(b), the pump light is launched into the fibre from the output end, and the dichroic mirror is set at 45 degree with respect to the fibre axis for extracting laser output. At the end facet of the fibre, a broadband high reflection mirror is placed to form the laser resonator. For power scaling both ends of the fibre can be pumped, see Figure 1.7(c).

Fibre laser resonator can also be formed using Fibre Bragg Grating (FBG). Figure 1.8 shows the formation of resonator using FBG.

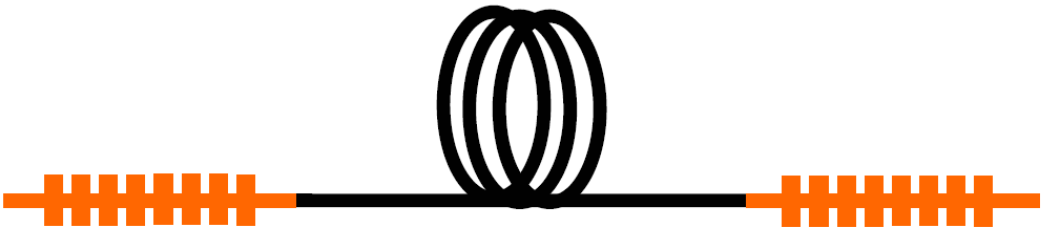

Figure 1.8 Schematic of complete-fibre resonator with fibre Bragg grating [50].

Wavelength tuning as well as narrow width laser spectra can be obtained using a bulk grating in the cavity as an output coupler. However, wavelength-tuning with a bulk grating is inconvenient, and brings laser instability [50], so the commonly used wavelength tuning in fibre lasers constructed by using fibre Bragg gratings as the feedback device and output coupler, as shown in Figure 1.8. Therefore, the FBG laser resonator can provide wavelength tuning as well as narrow spectral width and high stability. The next section will describe the quasi four level nature of the thulium fibre laser.

1.10 Quasi Four Level Lasers

The thermally distributed population of the lower laser level of quasi three level lasers can cause the laser transition to behave as a quasi four level system. As the lower laser level is only few hundred wave numbers (cm^{-1}) above ground state, it is populated at thermal equilibrium at room temperature, since kT is 207 cm^{-1} at 300K (where T is the

temperature of the host material in Kelvin and k is the Boltzmann constant 1.3806488×10^{-23} J/K). Thulium laser operation across the $3F_4 \rightarrow 3H_6$ transition (~1.9 μm) is known as quasi four level laser. The analysis of laser gain begins with the small signal gain coefficient which is given by [51];

$$g_0 = \sigma_e\,[\gamma N_2 - (\gamma - 1)C_A N_s] \qquad (1.4)$$

Where g_o and σ_e are the small signal gain coefficient and the effective stimulated emission cross section and N_2 is the upper laser manifold population. $C_A N_S$ is the product of the concentration of active atoms and number density of the sites where the active atoms can reside.

The term $\gamma=1 + f_l / f_u$, Where f_l and f_u are respectively the thermal Boltzmann factors in the lower and upper laser levels. The factor $\gamma = 1$ is for a true four level lasers and $\gamma = 2$ is for a true three level laser. A quasi-four level laser has a value of γ that is closer to 1 [36]. Figure 1.9 shows the energy level schematic for three and four level lasers. As can be seen from this figure, the lower laser level in a three level laser is the ground state and it has some thermal distribution.

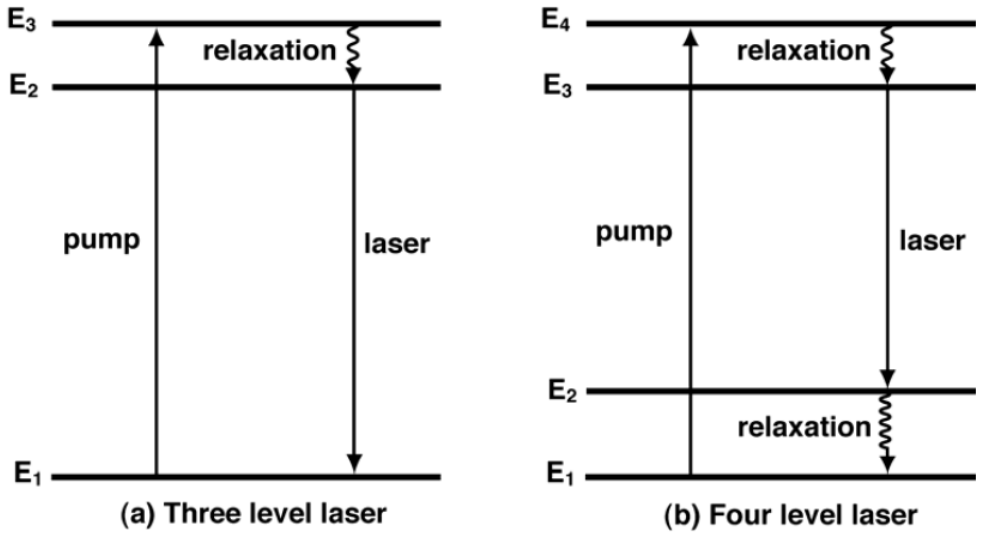

Figure 1.9.Schematic of (a) three level and (b) four level lasers [52].

In a four level laser the lower laser level is an excited state with no thermal population. Since $\gamma = 1 + f_l / f_u$ then γ must be 1 when $f_l = 0$ for a four level laser and 2 when $f_l = f_u$ for a three level laser. Although a quasi-four level laser resembles the three level laser in structure, it behaves like a four level system because f_l is small. As f_l is not zero the laser transition is referred to as quasi-four level. A transition is said to be quasi four

level if $\gamma < 1.5$, and for $\gamma > 1.5$ it is quasi-three level. The effect of the phonon energy regarding energy transfer processes is an important consideration as well. This is true for thulium lasers and the two-for-one self-quenching process will be discussed later. Energy transfer processes in thulium will be discussed in the following section.

1.11 Tm-Tm Energy Transfer Process

This section will be discussed the energy transfer process between thulium ions which are advantageous for 2 μm laser. When an optically active rare earth substance mixed with solid sate material and exposed to a radiation source, the electronic states can be excited by absorbing some of photons from the radiation field. The de-excitation of excited energy levels can be in the form of photons or phonons. The emission of phonons adds heat to the glass lattice. The energy transfers for laser materials are mainly through radiative and nonradiative process. In case of radiative energy transfer process, the emission of photon by one ion causes the absorption of that photon by another ion. The non-exponential decay of thulium ions from $^3H_4$ manifold is strongly reduced due to increasing thulium concentration, as a result of the cross relaxation process, measured in Tm:YAG [53] and Tm:YLF [54] and denoted by P_{41} in Figure 1.10.

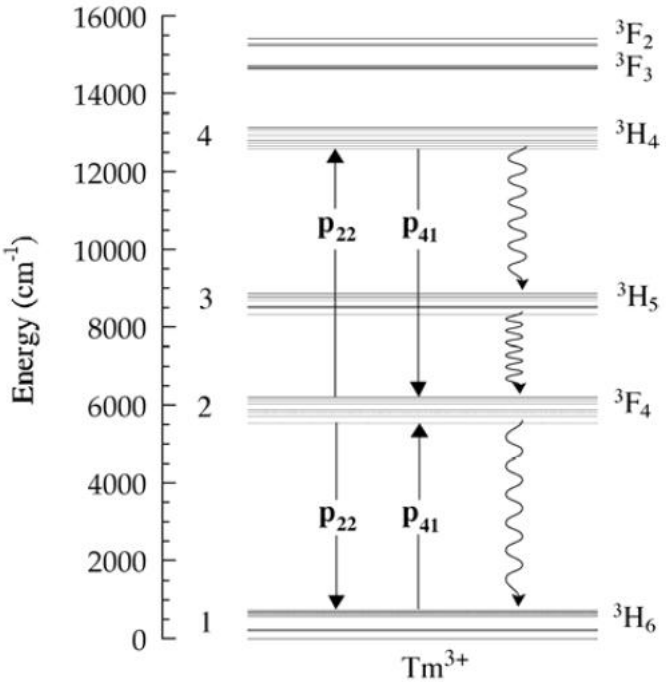

Figure 1.10. Energy level schematic of Tm-Tm energy transfer process [52].

In this process an excited ion in $^3H_4$ manifold transfers part of its energy to another ion in the ground $^3H_6$ state manifold, so that both end up in the intermediate upper laser level $^3F_4$. The cross relaxation in thulium is represented by ($^3H_4 \rightarrow {}^3F_4$); ($^3H_6 \rightarrow {}^3F_4$). The reverse process is shown in Figure 1.10 as P_{22}. Non radiative decay from the $^3H_4$ energy level competes with the cross relaxation process in thulium doped materials. Therefore, lower phonon materials are more advantageous when trying to enhance this process making ZBLAN glass a suitable host. Thulium lasers can be excited to $^3H_4$ manifold using commercially available 790 nm diodes. If each pump photon produced only one laser photon, then the ratio of pump to laser emission is limited to ~0.4.

With the enhancement of the laser efficiency through the cross relaxation process two laser photons are generated from the one pump photon, therefore increases the quantum efficiency to ~0.8 [52]. This is highly advantageous situation for 1.9 μm laser.

1.12 Tm:ZBLAN and Tm:Silica Fibre Laser at ~2 μm

Thulium doped fibre offers an alternative route compared to more conventional thulium doped bulk lasers. Despite the low emission cross section of a thulium doped fibre, it can provide high gain due to the long length of the fibre. An additional advantage of thulium doped fibre lasers is that they can be pumped directly using commercially available laser diodes. Thulium possesses strong absorption in the wavelength range 780-800 nm [55, 56]. Therefore, the short-infrared wavelength range effectively covered by Tm^{3+} doped lasers can pump directly with ~800 nm diodes.

The absorption spectrum of Tm^{3+}-doped ZBLAN glass and Tm:Silica fibre is shown in Figure 1.11 and 1.12 respectively. From this absorption spectra the strong absorption near 790 nm, is quite evident. This absorption band also aligns well with the emission band of commercial diode lasers. The pumping of Tm^{3+}-doped fibre lasers is comparatively easier and less expensive using the above mentioned source, and offers an exciting avenue for lasing in the 2 μm wavelength range. Moreover, it also observed from Figure 1.11 and 1.12 that the absorption wavelength range spanning from ~1550 nm to ~1850 nm, which is near to laser emitting wavelength at ~ 2 μm. Therefore, it is

also possible to pump directly to the emitting level using this wavelength as a pump source. The more detail will discuss in the next few pages and in later section.

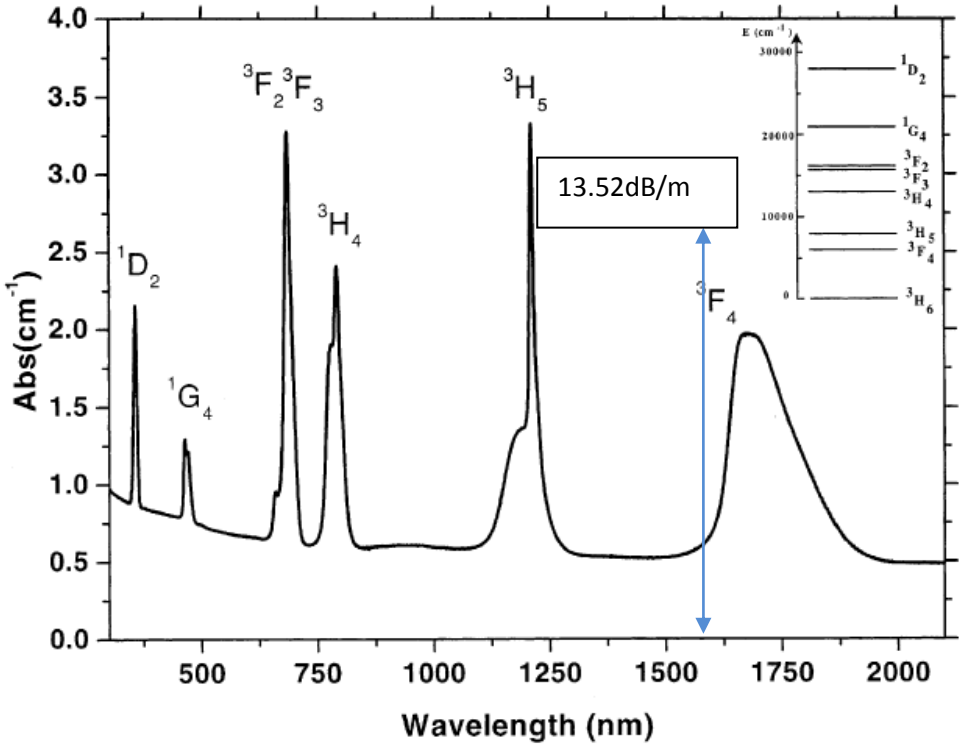

Figure 1.11.Room temperature absorption spectrum of a Tm doped ZBLAN glass for different wavelength region ranging from 300 nm to 2100 nm. [55].

NOTE:
This figure is included on page 35 of the print copy of the thesis held in the University of Adelaide Library.

Figure 1.12. Absorption spectrum for Tm-doped silica [56].

The simplified energy-level diagram of Tm^{3+} ions as well as cross relaxation process is shown in Figure 1.13. The pump light at ~790 nm excites Tm^{3+} ions from $^3H_6$ to $^3H_4$, which then generally nonradiatively decays to the upper laser level of $^3F_4$. The transition from $^3F_4 \rightarrow ^3H_6$ will radiate photons at wavelength of ~2 μm. Due to large Stark splitting of the lower laser level (the ground state level), the Tm^{3+}-doped fibre laser is a quasi-four-level system

Using cross relaxation process, higher quantum efficiencies >100% [57, 58] can be achieved in Tm^{3+}-doped fibre lasers by improving appropriately the ion doping concentration. In experiment, slope efficiency larger than 60% have been achieved (quantum efficiency >150%) in Tm^{3+}-doped fibre lasers [59, 60].

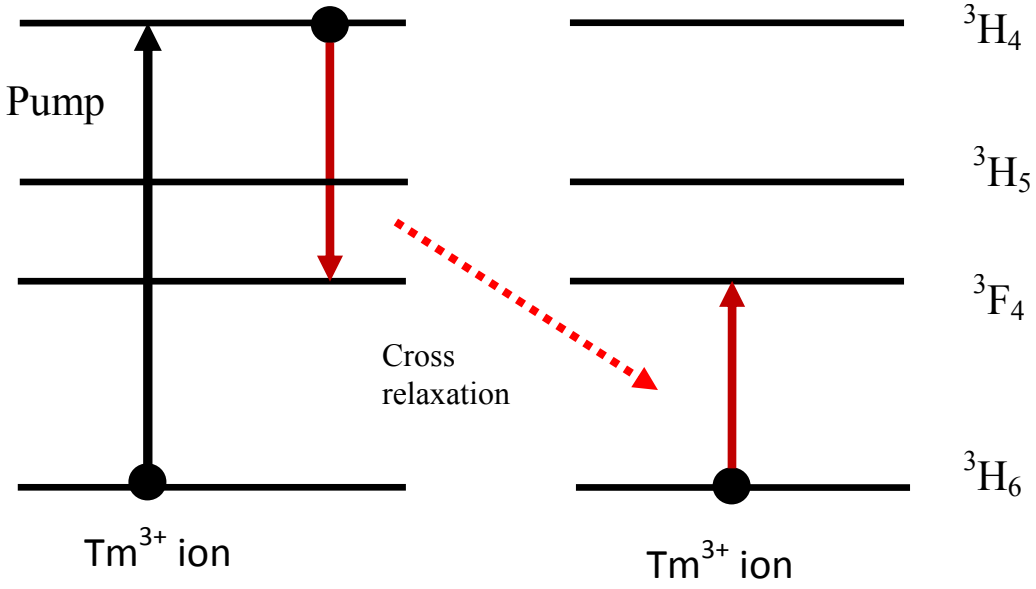

Figure 1.13.Cross relaxation between Tm^{3+} ions.

Both the Tm:ZBLAN and Tm:Silica show the broad absorption and emission characteristics due to amorphous glass host. However, these two different glass host have very different phonon energies due to their different composition. The maximum phonon energy of ZBLAN glass is around 500 $cm^{-1,}$ while the phonon energy of silica glass is around 1100 cm^{-1} [61]. The multiphonon relaxation rates from all the thulium energy levels greatly affect by large phonon energy difference. The higher maximum phonon energy in silica is responsible for an increased decay rate from the $^3H_4$ pumped energy level and hence shorter life time of the energy level.

Phonon energies in thulium affect the laser play an important role in laser performance in two major ways. Firstly, the “two-for-one” thulium-thulium cross-

relaxation process between thulium ions is highly dependent on the life time of pump energy level. Cross relaxation and multiphonon relaxation are competitive process. Due to larger phonon energies multiphonon relaxation dominates, as a result cross relaxation process will be diminished [36]. Laser threshold also depends on the efficiency of the cross-relaxation process. A smaller efficiency of the cross relaxation process has the effect of raising the laser threshold [36]. The $^3F_4$ lifetime is shortened through multiphonon decay. This shortening the life time of the $^3F_4$ manifold due to multiphonon decay will reduce the $^3F_4 \rightarrow {}^3H_6$ quantum efficiency. The lower quantum efficiency would reduce the slope efficiency.

Secondly, due to higher phonon energy, the increased emission of phonons adds to the heat load, which has a negative impact on lasers by increasing the population of lower laser level. Thus the threshold of laser will be increased [36]. Therefore, maximum phonon energies of these two materials play a major role to populate $^3F_4$ energy level for laser actions.

From the absorption and emission spectra reproduced in Figure 1.14 and 1.15, measured by Walsh et al. [36], it was observed that the absorption and emission cross section of Tm:ZBLAN is lower than Tm:Silica. Despite the lower phonon energies of the Tm:ZBLAN which increases the radiative transition rate [36], laser performance is therefore greatly influenced by the nonradiative quenching.

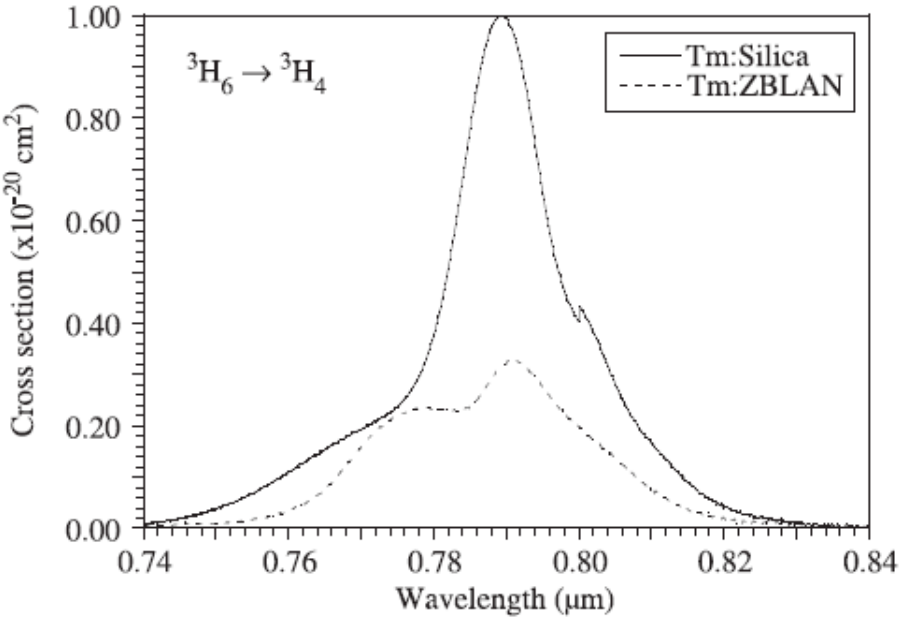

Figure 1.14. Absorption cross-section of Tm:ZBLAN and Tm: Silica [36].

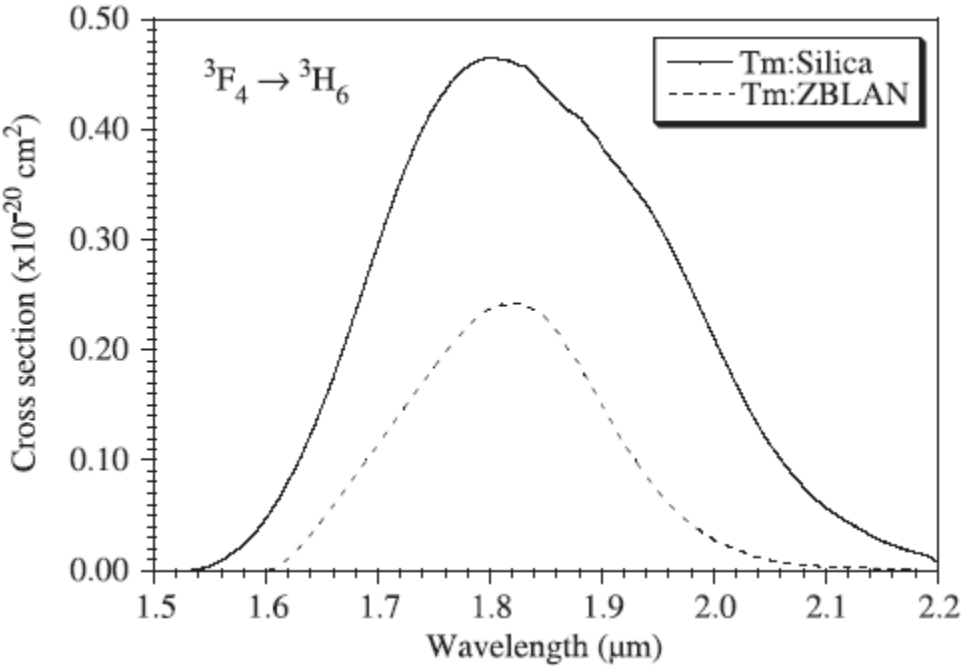

Figure 1.15.The emission spectrum of the $^3F_4 \rightarrow {}^3H_6$ transition in Tm^{3+}-doped silica and ZBLAN fibre [36].

Figure 1.16 illustrates the highest ever reported output of Tm:ZBLAN and Tm:Silica glasses.

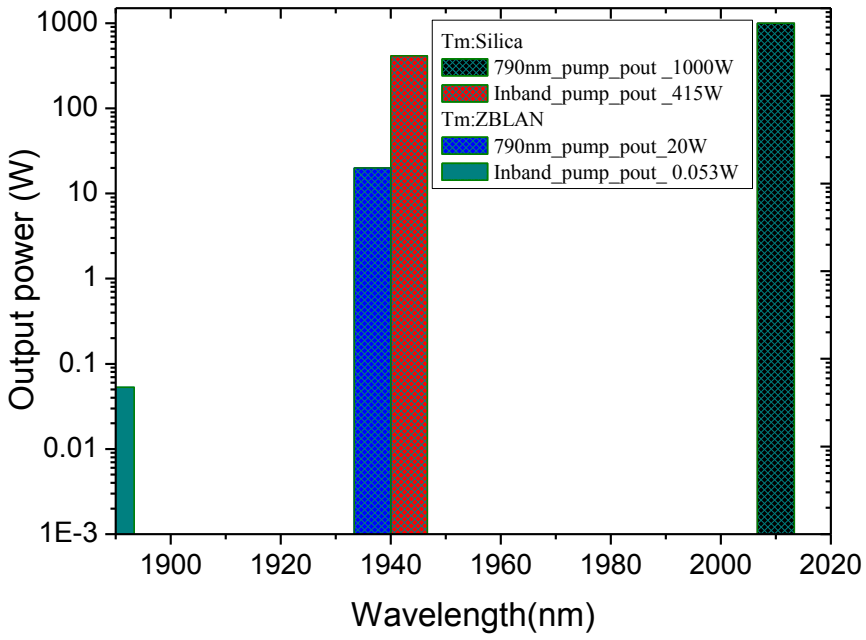

Figure 1.16. Schematic of comparative output of Tm:ZBLAN and Tm:Silica at ~2 μm through 790 nm pumping as well as in-band pumping [1-4]

It is clear from the Figure 1.16 that Tm:Silica is the most mature technology in efficient lasing at ~2 μm, using 790 nm pumping and ~1.6 μm in-band pumping. Output powers from Tm:ZBLAN fibre lasers at ~2 μm is still comparatively low when compared to Tm:Silica fibre lasers.

1.13 In-Band Pumping Tm:ZBLAN Fibre Laser

As previously mentioned thulium doped fibre lasers operate in eye safe ~ 2 μm spectral regions and as such has attracted an enormous interest due to its potential application in medicine, remote sensing and LIDAR. Also discussed previously there are two main host glasses used for thulium doped fibre lasers around ~2 μm, namely the thulium doped silica and thulium doped ZBLAN. Various parameters of laser operation, e.g. threshold pump power, slope efficiency or overall optical to-optical efficiency can be improved by reducing the quantum defect between the pump wavelength and the laser wavelength. A method to reduce the quantum defect is in-band pumping directly into the emitting laser level. It has already shown in Figure 1.6 section 1.8 that the possible pumping routes are 790 nm and ~1600 nm to develop ~2 μm Tm fibre laser.

For 2 μm lasers using 790 nm pumping, most of the problem associated to the larger quantum defect ((λ_p/λ_l)) and low branching ratio to the $^3H_4$ level in thulium [62, 63]. This problem can be solved to the similar way of pumping to the erbium 1.53 μm transition at 1.48 μm [64], i.e. by pumping to the short wavelength wing of the ground state absorption.

The development of a thulium doped fibre lasers at 2 μm by in-band pumping at ~1.6 μm offer the advantages of high Stokes limit of up to 84%. Several authors have reported on Tm:Silica as well as Tm:ZBLAN fibre lasers at ~2 μm using in-band pumping approaches. A 14% slope efficiency was achieved in a Tm:Silica fibre laser operating at ~2 μm has been achieved by in-band pumping at 1.61 μm [65]. In 2006, D.Y. Shen et al. [66] reported an a high power and widely tunable core pumped and cladding pumped Tm:Silica fibre laser at ~2 μm. It has pumped by a 1565 nm Er:Yb fibre laser. They used a 3 m double clad fibre with a 30 μm (0.22NA) Er:Yb phospo-silicate core surrounded by a 400 μm diameter D shaped pure silica inner clad with a

NA of 0.49. The reported output at 1.565 nm was 58 W. Using this Er:Yb 1.565 nm laser as a pump source and using a free running cavity configuration a maximum 17.4 W at 1941 nm was reported. The fibre had a length of 5 m Tm:Silica and had a ~72% slope efficiency with respect to absorbed pump power. The fibre used is a thulium doped alumino-silicate core having a diameter of 20 μm and 0.12 NA, surrounded by a D-shaped pure silica inner cladding with a 200 μm diameter and a 0.49 NA. The thulium concentration used was ~1.48 wt.% [66]. The effective absorption coefficient for cladding pumping at 1.565 nm has been reported at ~1.5dB/m. For core pumping a much shorter length of the fibre (24 cm) was used due to high absorption efficiency (~150 dB/m). A maximum output of 12.1 W at 1861nm reported with slope efficiency of 59% with respect to absorb power for the core pumping configuration. A multimode Tm:Silica fibre laser at 2μm has also been reported through 1.61μm in-band pumping [67]. They demonstrated the maximum output 370 mW with a 42% slope efficiency. Moreover using an all fibre format a maximum of 415 W power with a slope efficiency 60% [2] was reported at ~2 μm using 1567 nm pumping. The Tm:ZBLAN fibre has been pumped with a semiconductor laser at 1.57 μm (FWHM~12 nm) [40], 1.58 μm [4] and a 1.64 μm pump source generated from a color centre laser (FWHM~0.1 nm) [41]. The slope efficiencies of these Tm-fluoride fibre lasers are generally high (70% to 84%) and a maximum 2 μm output power achieved so far from an in-band pumped Tm:ZBLAN fibre is only 53 mW [4]. Therefore, there is great potential to increase the output power as well as efficiency of Tm:ZBLAN fibre lasers through in-band pumping scheme.

Figure 1.17 shows the variation of absorption and emission cross section for $^3F_4$-$^3H_6$ transition. The graph is reproduced from R. M. Percival et al. [41], where the fluorescence spectrum has recorded for a short length (≈1 m), of doped fibre by 30 mw of 790 nm pumping. The Tm^{3+} concentration was used for this fibre is 1000 ppmw. As is observed from Figure 1.17, the absorption for $^3F_4$ level starts at 1550 nm and is very wide. Several authors have used different pump wavelength from 1550 nm to 1660 nm [4, 40, 41]. Moreover, from Figure 1.17, it also shows that this pump wavelength has both absorption as well as emission. Choice of the pump wavelength for this band of pump wavelength is tricky because of the absorption as well as emission [41]. Although the absorption peak at 1.67 μm in a thulium doped fluoride fibre, it is typically pumped in the 1.55-1.65 μm wavelength range.

Figure 1.17. Absorption and emission cross section as function of wavelength of a Tm doped ZBLAN glass for the $^3F_4$-$^3H_6$ transition [41].

Summarizing the above discussions, for in-band pumping of Tm:ZBLAN lasers, the output remains low, this was due to the unavailability of high power in-band pump sources with a good beam quality at ~ 1.6 μm. There is therefore an opportunity to improve on this through the use of a commercial, high beam quality in-band pump source. By using such a source there is a prospect to get higher output than previous reported results at ~2 μm. The following section will review the development of the pump sources at around 1.6 μm.

1.14 Review for the Development of ~1.6 μm Pump Source for In-Band Pumping

Er^{3+} doped fibre lasers between 1.5 and 1.6 μm offer high output power with good beam quality. In contrast to bulk lasers, fibre lasers have the benefit that due to its geometry, heat extraction can occur close to the heat source. Cladding pumped fibre lasers based on erbium have been demonstrated at multi watt power levels with wavelength tunable operation covering the wavelength range from 1.53 μm to 1.62 μm [68]. The absorption peak in thulium doped ZBLAN for the $^3H_6$ to $^3F_4$ is ~1670 nm, however it is very broad, allowing for efficient pumping of Tm:ZBLAN fibre laser by

an Er:Yb fibre laser. The good beam quality available from the high power an erbium fibre laser allows for directly pumping of the core of a thulium doped fibre laser. This cause pumping also allows for the use of a much shorter length of a fibre. This approach has an advantage over pumping of of a thulium fibre laser with 790 nm diodes. Erbium fibre lasers are an excellent pump sources for bulk erbium lasers and thulium fibre lasers due to the combination of wavelength flexibility, high efficiency and good beam quality [69]. There are currently two approaches of cladding pumping erbium fibre lasers emitting at 1.5 μm. One is singly doped with erbium doping and the other is with Er:Yb co-doping. The main issue of purely erbium doped fibres is the relatively low achievable doping concentrations due to the detrimental effects of the onset of ion clustering and simultaneously relatively low values of erbium absorption cross sections [14]. An alternative approach to overcome the described limitations is the utilization of Er:Yb co-doped fibres, which are most commonly pumped in the ytterbium absorption band between 915 nm and 980 nm with diode sources. The effective absorption coefficient for pump light launched into the cladding of Er:Yb fibre as a function of pump wavelength is shown in Figure 1.18. In this case the core diameter of an Er:Yb fibre was 30 μm having numerical aperture 0.22 and the core was surrounded by a pure silica D-shaped inner-cladding of 400 μm diameter (~360 μm along the short axis) and the numerical aperture was 0.4. The doping concentration to the core of Er:Yb fibre was respectively Yb^{3+} ion (~$8.7x10^{20}$ cm^{-3}) and Er^{3+} ion (~$5.1x10^{19}$ cm^{-3}). It can be seen from Figure 1.18 that the absorption coefficient for pump wavelengths in 974-978 nm regime is >6dB/m indicating that relatively short fibre lengths (< 3m) would be sufficient for efficient pump absorption. For efficient operation of a cladding pumped Er-doped fibre device it is necessary to co-doped with Yb^{3+} ions to increase the pump absorption coefficient and to broaden the absorption band to better match the emission wavelengths available from high power diode pump sources. In the pumping scheme of an Er:Yb co-doped fibre as shown in Figure 1.19, the Yb^{3+} ions are excited to the $^2F_{5/2}$ level and the Er^{3+} ions are then excited via nonradiative energy transfer from the Yb3+ ion [70, 71]. In addition, to achieve reasonable efficiency values, strong codoping with Phosphorus is needed to suppress the back-transfer of energy to the Yb^{3+} ions, thus allowing for an efficient amplification of radiation around 1550 nm by using pump light around 976 nm [72]. The maximum CW power reported to date for a cladding-pumped Er,Yb co-doped fibre laser is 297 W at 1567 nm [73].

Figure 1.18. Effective absorption co-efficient versus pump wavelength [14]

This laser employed a simple resonator configuration with a 6 m long Er,Yb co-doped double-clad fibre and a 30 μm core diameter with a numerical aperture of 0.21. The diameter of the D-shaped silica inner cladding was 600 μm. Feedback for lasing was provided by a perpendicularly cleaved fibre facet and by a butted high reflectivity mirror. The fibre was pumped by a diode-stack at 975 nm and yielded 297 W of output at 1567 nm in a beam with M^2 parameter of 3.9 for 1.3 kW of pump. 100 W class single-mode linearly polarized all-fibre sources [74] and wavelength-tunable erbium fibre sources [75] have also been reported.

It is clear from the above references that the development of ~1.6 μm pump sources with efficient operation higher outputs have been achieved to use Er:Yb co-doping fibre rather than erbium doping.

Figure 1.19. Energy level diagram of Er:Yb co doped silica [14]

1.15 Summary

As the Tm:ZBLAN has a low phonon energy as well transparency from the visible to the mid-infrared region, it would be the good choice to pursue Tm:ZBLAN fibre laser at 2 μm. In-band pumping directly into the emitting laser level is a potential candidate to increase the efficiency of fibre laser. This can be achieved through currently available commercial components and the development of a ~1.6 μm source using an Er:Yb co-doped fibre. The use of a Er:Yb co-doped fibre offers laser outputs at ~1.6 μm with very good beam quality. With the help of the developed ~1.6 μm source is to the aim of this research, pump directly into the core of a Tm:ZBLAN fibre. This chapter has discussed the need for the development of Tm:ZBLAN fibre lasers emitting at 2 μm. It also discussed the importance of 2 μm fibre lasers in the wide variety of potential applications in the different field of sensing, medical and material processing. This thesis is devoted to development of a 2 μm Tm:ZBLAN fibre laser through 790 nm pumping. Following the development of 1.57 μm in-band pump source and it was used to pump a Tm:ZBLAN fibre laser.

Chapter 2

Double Clad Fibre: Comparison of Predicted and Measured Pump Absorption

2.1 Introduction and Aim

It has already mentioned in Chapter 1, that power scaling in conventional rare-earth-doped single mode fibres is limited because of poor coupling efficiency from multimode diode laser arrays to the single mode core of the fibre. To overcome these problems, double-clad fibres have been developed. A few simple considerations are needed for an optimum design of a fibre. The pump absorption coefficient in a single mode core is determined by the absorption cross-section of the dopant in the host glass, by dopant concentration, and by a reduction factor that in current literature is roughly approximated by the ratio of inner core area to multimode core area [76]. A large inner cladding area and high numerical aperture are the prerequisites to ensure high diode power launch efficiency. On the other hand, a small inner cladding area giving rise the possibility of increased pump absorption coefficient in the core, as well as reduced absorption length. As a result, for small inner cladding area, fibre losses are reduced at laser wavelength due to the reduction of absorption length. Thus, considering the above two requirements the outer cladding area should be the compromise between these two for an optimum operation. For the same reason, the core area and numerical aperture should be high enough to allow a high absorption efficiency of pump power in the single mode core as well as be able to excite single mode oscillation at laser wavelength, [77]. Moreover, to increase the pump absorption it is necessary to use a high doping concentration.

As for the efficient operation of a double clad fibre laser, it is necessary to understand the pump absorption behaviour for different shapes of a double clad fibre. So the aim of this chapter is to calculate the pump absorption for different shapes of Tm:ZBLAN double clad fibre. Further the simulation results would be compared with the experimental pump absorption measurement of a Tm:ZBLAN double clad fibre.

2.2 Review of Pump Absorption Calculation for Double Clad Fibre

Double clad fibre consists of three different layer having step index refractive index profile from core to outer cladding. The detail has been discussed in previous chapter. The inner cladding of a double clad fibre act as a power reservoir for pumping waves and enhances the launching efficiency. On the contrary, it degrades the absorption efficiency because significant absorption occurs only in the doped core region of a double clad fibre. To improve the absorption efficiency in double-clad fibres, many schemes, such as fibre bending [78], multi core fibres [79] etc., have been suggested in the past years. Among these schemes, DCFs with noncircular inner claddings have been widely applied [79-81], due to their simplicity and high efficiency. In these DCFs, the symmetry of light rays is broken and the absorption efficiency is improved by blending of the pumping waves [76, 82]. This is because; in case of non circular shape of inner cladding the symmetry of pumping wave is broken as well. Although various cross-sectional shapes have been employed, in practice, only a few researchers have focused on the influence of cross-sectional shape on the absorption characteristics of DCF lasers. The reason can be explained as follows. To calculate the pump absorption characteristics by solving the wave propagation equation in DCFs it is necessary to calculate the eigen modes. Generally typical double clad fibre having NA 0.5 and 100 μm inner cladding will support more than 10^4 eigen modes. Therefore, it will require a very large amount of computing time and cumbersome to include all these modes in the calculation. In order to understand the pump absorption of a double clad fibre, different modelling approaches have been demonstrated [77]. The direct solution of a Maxwell‟s equation offered by finite difference time domain (FTDT) method [83, 84], is computationally expensive in restricted spatial dimensions. A beam propagation method (BPM) can be approximated by the effective index method to reduce a 3D problem to a 2D one, and still it suffers from the need to discretize paraxial wave equation throughout dense grids [85] over realistic propagation distances, especially when large and complex geometries are involved [86]. In spite of this, a 3D fast Fourier Transform (FFT) BPM conducted by Leproux and Fevrier for pump absorption of a double clad fibre [87]. Liu et al. [88] reported an analytical ray tracing technique to calculate the pump absorption of circular, offset and rectangular fibre cross-section. They have demonstrated that the absorption is influenced by the bend radius for circular fibre, but

in fibre design with offset core and rectangular inner cladding the bend effect is negligible. Kouznetsov et al. [89] reported a model for pump absorption in a circular symmetry double-clad optical fiber amplifier with the paraxial propagation of spatially random monochromatic light in a fiber with an absorbing core. They reported that pump absorption is increased due to the mode coupling caused by the fluctuation of refractive index. They also used the extension of above mentioned technique to calculate absorption for non-circular cross-sections [86]. Moreover, using an analogy with quantum mechanics their work has been conducted on double clad fibres with arbitrary geometries [90]. Furthermore, Mortensen [91] used finite element method (COMSOL multi physics software) to calculate the fully vectorial eigenmodes for pump absorption calculation. According to these authors, the calculation of the several hundred modes is cumbersome.

Recently, I. Dritsas et al. [92] reported a computationally inexpensive method written in MATLAB to calculate the pump absorption efficiency of a double clad fibre. They have used a 3D ray tracing technique to record the ray spatial paths occurring inside the core finite volume elements. This technique is very simple and is validate to experiment. Therefore in this research ray tracing approach will be used to calculate the pump absorption for Tm:ZBLAN double clad fibre, to understand the impact of choice of inner cladding geometry.

2.3 Boundary Condition for Pump Absorption Calculation

MATLAB code written by I. Dritsas et al. [92] has been used for pump absorption calculation of different cross-section types of a double clad fibre. The motivation is to understand the pump absorption behavior of different shaped double clad fibres, which is essential for fibre laser development. Moreover the simulation result would be compared with measured pump absorption, which will be discussed in later.

Here the pump wavelength λ_p = 790 nm is used to calculate the pump absorption of a Tm:ZBLAN double clad fibre having 8 μm core (0.15NA) and 125 μm inner cladding (0.50NA) and the doping concentration of 20000 ppm by weight. The refractive index of core is 1.5075. The inner and outer cladding refractive indices are 1.50 and 1.4142, respectively. In case of outer cladding, the model considered the refractive index of outer cladding in order to determine the reflection properties back

into the inner cladding. For instance for total internal reflection only the refractive index of the outer cladding is required, as rays are propagated only within the inner cladding. In this investigation higher numerical aperture of inner cladding has been chosen to ensure high diode power launch efficiency.

The pump radiation wavelength is transmitted through the various shapes of a double clad fibre, having the inner cladding diameter of 125 μm. In model [94], it is assumed that the materials are homogeneous, isotropic and lossless dielectric media. Moreover further assumption considered in model as follows, the inner cladding diameter is much larger than the pump wavelength and is suitable for geometrical optics domain. The interface between inner and outer cladding is an ideal surface, has no reflective aberration and uniform step refractive index distribution. Under these conditions the propagated rays in model strictly follow the geometrical optics domain. Regarding the geometrical boundary condition, it is also assumed that there are no losses when a pump ray is scattered by a dielectric interface and that during total internal reflection the refracted energy is negligible compare to the reflected energy when refraction takes place [92]. Moreover, it is assumed that all rays propagate in the fibres are independent of each other and have no mode coupling.

2.4 Launched Pump Initial Condition

The pumping scheme considered herein is free space coupling single end pumping, as it is widely used in the laboratory experiment. All the parameters used for the simulation is stated in section 2.3. The ray propagation through the fibre is shown in Figure 2.1. This is accomplished by MATLAB code [92]. The light delivered through a 125 μm core with a 0.22 numerical aperture. In free space pumping, it is assumed that the perfectly collimated light is focused into the input facet of a double clad fibre and the spot size is slightly smaller that the area of a double clad fibre [92]. By assigning a set of points in the input facet of a double clad fibre, pump photon density distribution is described in the model. These points represented the spot centre of the incidence pump photons in the inner cladding. The incident points i.e. the spot centre of incident pump photons are generated on to equally distant co eccentric circumferences (see Figure 2.1) which are centred on the fibre axis and cover a circular area defined by the pump delivering core [92]. Figure 2.1 describes the ray propagation path for different shapes

of a double clad fibre. The incident points are shown Figure 2.1 as blue star marks at the input end of the fibe, while the red line represents the ray propagation path through the fibre.

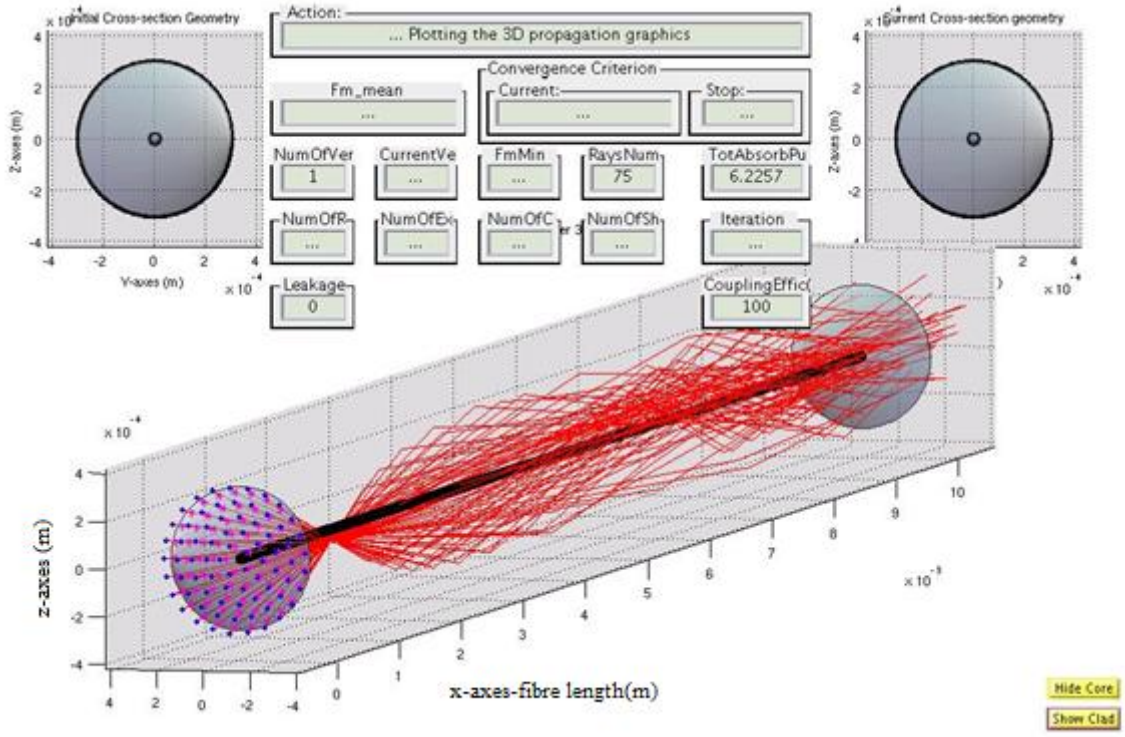

(a)

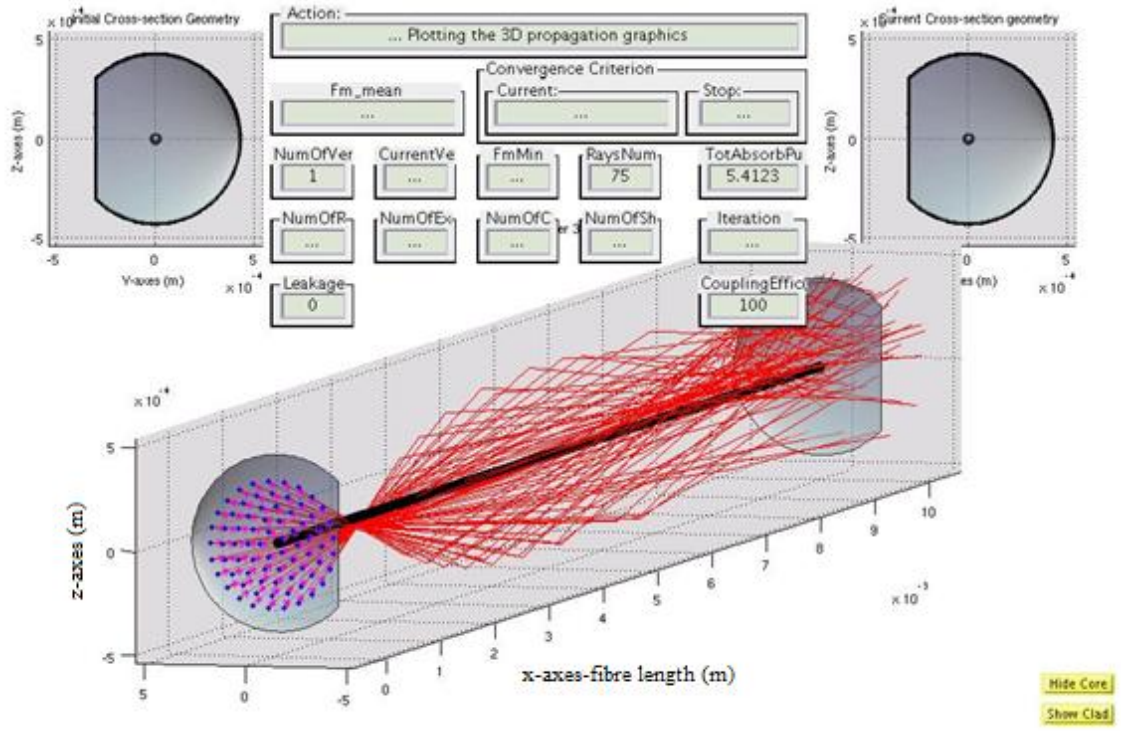

(b)

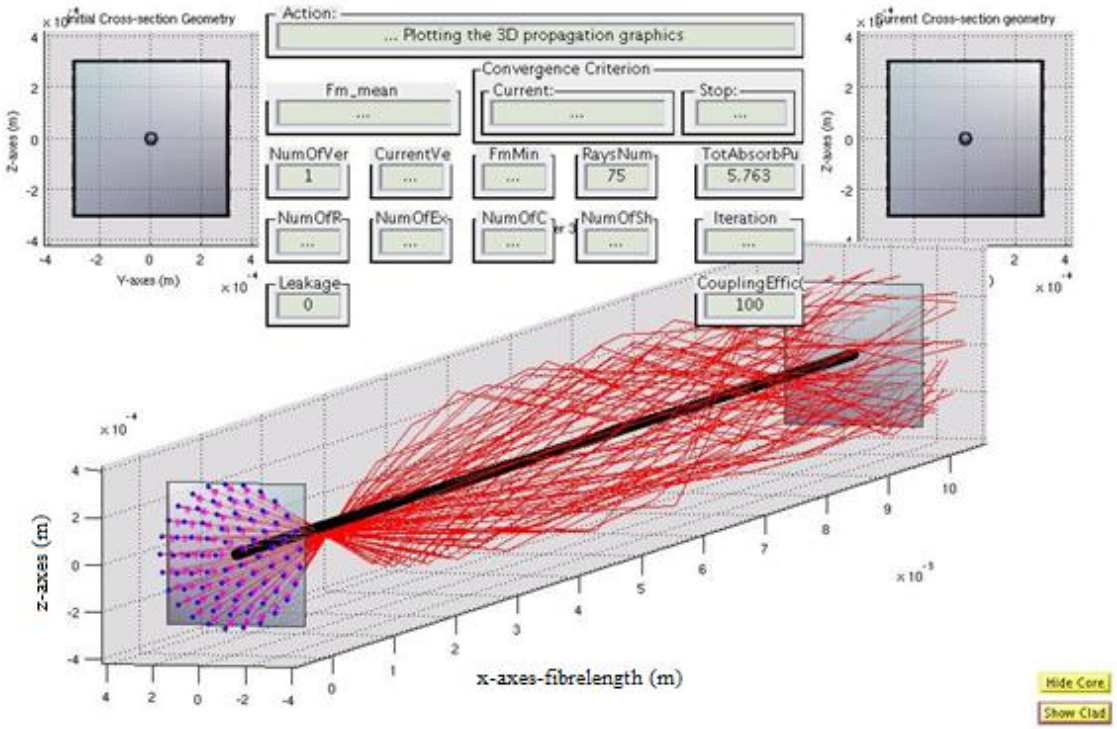

(c)

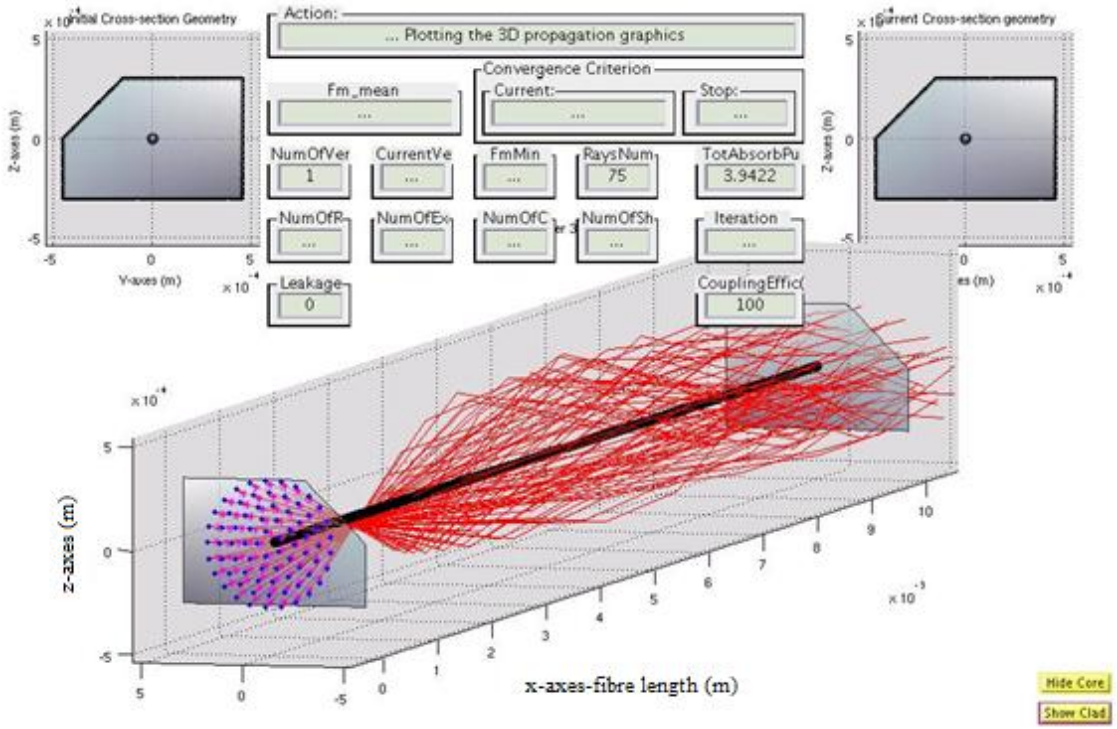

(d)

Figure 2.1. The propagation of 75 rays of a (a) circular (b) D-shape (c) square (d) broken-parallelogram of a double clad fibre for free space pumping.

The energy density distribution of a pump field has also been tested for free space coupling system. Figure 2.2 shows the pump density distribution for free space coupling scheme of a double clad Tm:ZBLAN fibre.

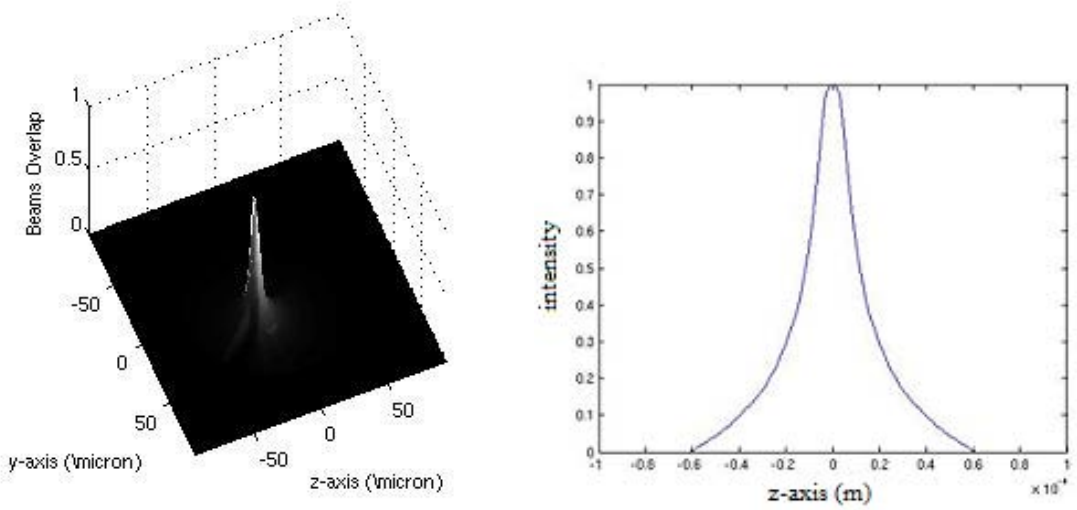

(a) (b)

Figure 2.2. Normalized overlap image of 936 rays propagated along 0.1 mm length of a fibre without an absorbing core (a) axially focused free space coupled system and (b) corresponding cross view in two dimensions.

It is observed from Figure 2.2 that the distribution exhibits the Gaussian shape. After confirming that the pump density distribution exhibits Gaussian shape, the next step is to perform a convergence test for the optimum container number for optimum pump absorption of a double clad fibre.

2.4.1 Optimum Container Number Convergence Test

Container number is a virtual container that segments the core volume of a fibre. When a ray is passed through the fibre it intersects the core container and transfer its photon energy to the ion population of a core container and the container records the locally absorbed power. For optimum absorption of pump wavelength for 1 meter Tm doped ZBLAN double clad fibre, different container number has been used (see Figure 2.3). In Figure 2.3 (a), for 8 μm core and 125 μm inner clad, it is observed that for 1000

container the pump absorption is 40.88 % (model assumption). It is observed from Figure 2.3 (a), (b) that the pump absorption converges at 1600 container number. Physically this converges means the saturation of inversion of ions in the core volume.

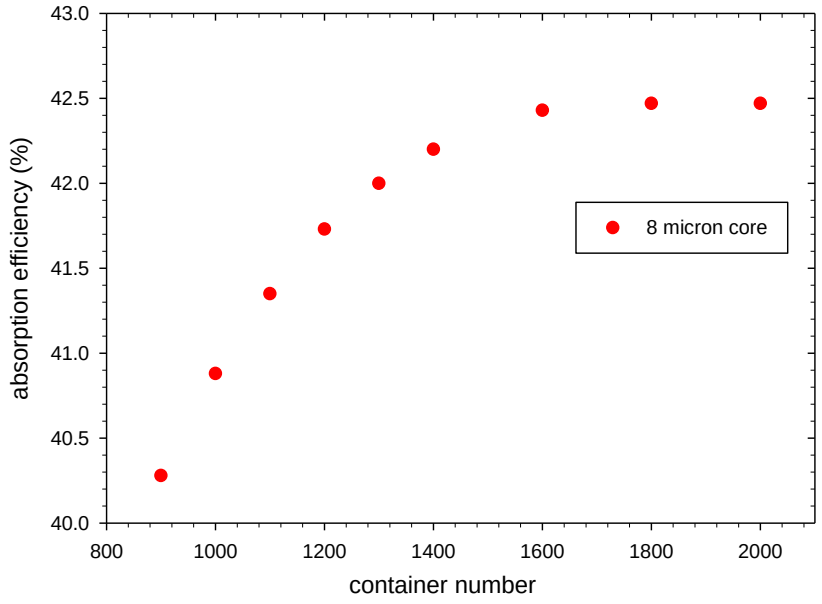

(a)

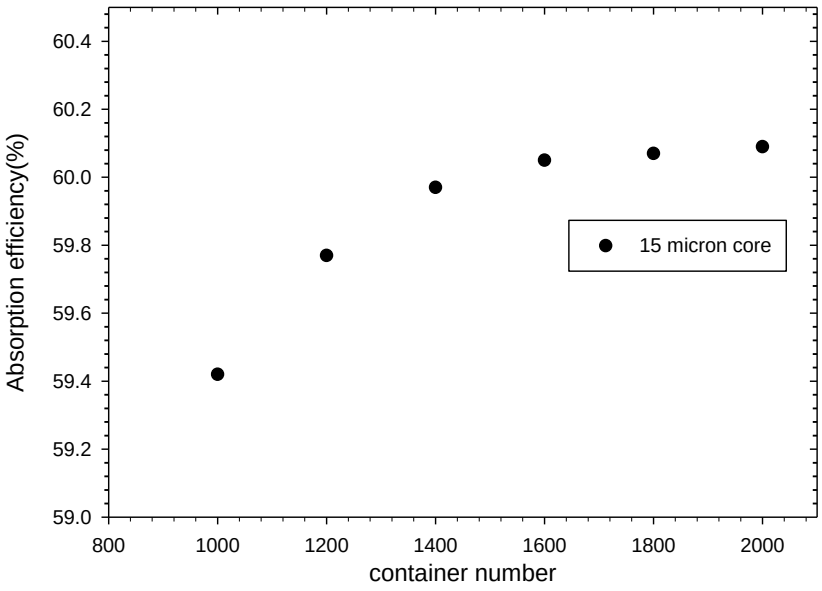

(b)

Figure 2.3. Verification of pump absorption for 1 meter Tm:ZBLAN double clad fibre with core NA 0.15 and inner cladding NA 0.50. (a) 8 µm core diameter and (b) 15 µm core diameter.

From Figure 2.3 (b) it is observed that the pump absorption is increases due to the increase of core diameter, but the container number converges to same value, i.e, 1600 as it is observed in Figure 2.3 (a). Thus it can be concluded that for any geometry the optimum container number remains the same.

2.5 Theory of Pump Absorption

To calculate the pump absorption in this model, each ray considered as coherent stream of a parallel photons. The flight path of each ray conveyed the propagation of energy by the photons beam it represents [92]. The core of a fibre segmented into small containers in order to be able to perform this numerical calculation. When a ray intersects the core, the path of each ray inside the container is recorded and stored to calculate the pump absorption. Thulium ion is considered as an active rare earth dopant in ZBLAN glass. To focus on the influence of pump absorption for different geometries, in model the absorption starts from when all the ions in the ground state, and finish when it is inverted. When a ray is passed through the fibre it intersects the core container and transfer its photon energy to the ion population. This depends on the inversion status of given containers. The optimum container number for 1 m fibre has chosen 1600, as discussed detail in container number convergence test, section 2.4.1.

Each ray carries an equal fraction of the photon population launched into double clad fibre during each time steps (Δt). The number of transmitted photon can be calculated using the relation $N_{trn} = N_{inc} \exp(-\sigma\rho L)$ and the number of locally absorbed ion is determined by using$N_{abs} = N_{inc}[1 - \exp(-\sigma\rho L)]$. Where, N_{inc} is the number of incident photons, N_{abs} is the number of absorbed photon, σ is the absorption cross section and ρ is the density of unexcited ion inside the container [92]. The measure of the reduction of the population of unexcited ions inside the container also gives through the result of absorption. This reduction of population is always compared against the unexcited ion population left in the container. Therefore the absorption of photons stopped when all ions have been inverted, indicating a saturated container [92]. The thulium absorption cross section $\sigma = 0.25 \times 10^{-20} cm^2$ at pump wavelength $\lambda_p = 790$ nm [35] used in the simulation. The thulium concentration, which is 20000 ppm by weight has also been used as supplied by FiberLabs, Japan for Tm:ZBLAN data sheet. The ground state thulium ion of each container before launching the pump light is

given by $\rho = C_{T_m} N_A / V_{T_m}$ [92], which is equal to the number of thulium ions per cubic meter of core material, where, C_{T_m} is the concentration of thulium in ppm by weight, N_A is the Avogadro‟s constant, V_{Tm} is the thulium atomic volume, in $cm^{3.}$ mol^{-1}. After propagating light through the container the pump absorption for the kth container can be calculated through the following [92].

$$N_{abs,tot,k} = \sum_{j=1}^{T} \sum_{i=1}^{R} N^{inc}{}_{(i,k)} \left[1 - \exp(\sigma \rho_{j,i,k} L_{i,k})\right]$$

where, R is the number of rays and T is the time steps, $N^{inc}{}_{(i,k)}$ is the population of the ith beam after passing through the k-1containers, $\rho_{j,i,k}$ is the ion density of the container after traversed by all beams that intersects its volume during all j-1 time steps and a maximum of i-1 beams during the jth time step and $L_{i,k}$ is the spatial path length of the ith beam inside the container. Therefore the absorbed pump power is given by [92]

$$P_{abs,k} = N_{abs,tot,k} h \left(c/\lambda_p\right) \left(\sum_{j=1}^{T} T\Delta t\right)^{-1}.$$

Moreover, the cumulative absorption efficiency for the entire (k-1) containers is given by $P_{tot,k}\% = \sum_{m=1}^{k} P_{abs,m} \left(P_p\right)^{-1} \times 100\%$.

2.6 Simulation Results

The results reported here for pump absorption calculation of different shapes of a Tm:ZBLAN double clad fibre using 790 nm pumping. It is noted that the model has been verified before starting pump absorption calculation. See Appendix for the detail of model verification.

Tm:ZBLAN double clad fibre having 8 µm core (0.15NA) and 125 µm inner cladding (0.50NA) and the doping concentration of Tm ion is 20000 ppm by weight. The refractive index of core is 1.5075. The inner and outer cladding refractive indices are 1.50 and 1.4142, respectively. These parameters here used as in the commercial double clad fibre supplied by FiberLabs, Horiba, Japan. A 8 µm core Tm:ZBLAN fibre considered here for pump absorption calculation. According to V parameter, fibre laser at 2 µm will follow the single mode guidance. As the larger core would lead to the propagation of higher order transverse modes and the bending loss is significantly higher for higher order modes compared to the LP_{01} mode.

The doping density used here is 20000 ppm-by-weight, the launched pump power is 90 W and 936 rays are considered for simulation. The energy is propagated through 16000 core containers and 100 times step used for 10 m fibre. Figure 2.4 (a), (b) plotted the core optical path as a function of fibre length of all rays inside each of the 16000 containers.

It is observed in Figure 2.4 (a), that the magnitude of core optical path for circular inner cladding is levelled around 0.6 mm, also shows the wider groups of bars and bigger valleys observed in the patterns of optical paths when it compared to Figure 2.4(b). This pattern supports that for circular inner cladding there is a strong overlap between core volume and meridional rays. On the other hand in figure 2.4 (b) the magnitude of core optical path in square shape cross-section is leveled at around 0.5 mm and more noisy bar groups emerging above the base line. Therefore, the propagation of skew rays contributes more strongly in parallelogram shape. Moreover, in case of circular inner cladding, it is observed in Figure 2.4(a) that longer ray paths are recorded inside the core containers, they correspond mainly to a small population of meridional lines which become completely absorbed during the first few tens of centimetres. In case of square inner cladding Figure 2.4(b), the total ray spatial paths are generally shorter inside each container but they represent the contribution of a larger population of rays more sporadically interacting with the core volume and thus being able to transfer their energy along longer propagation lengths.

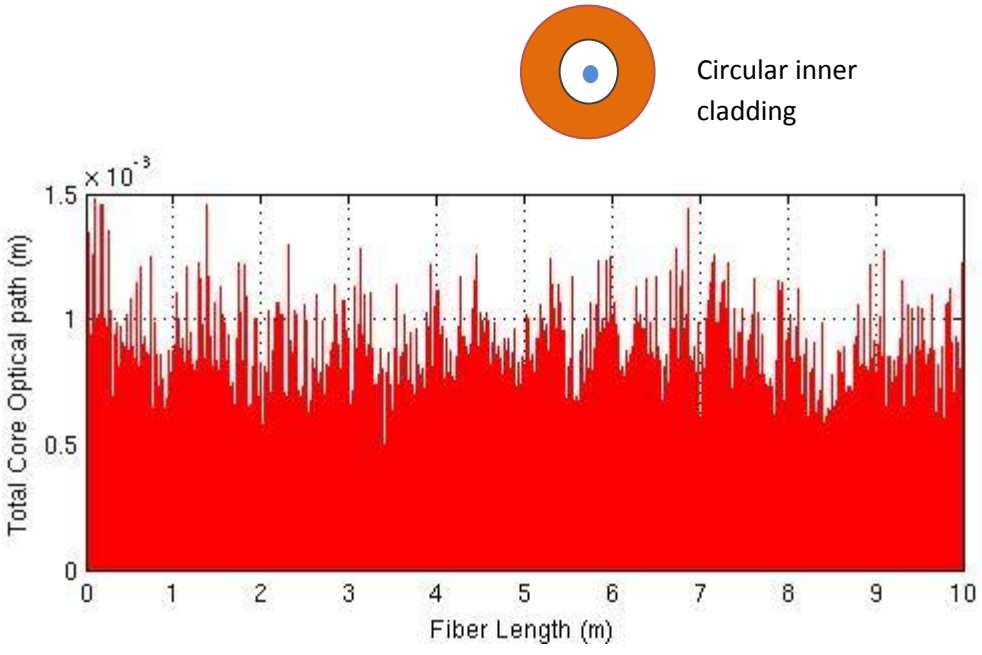

(a)

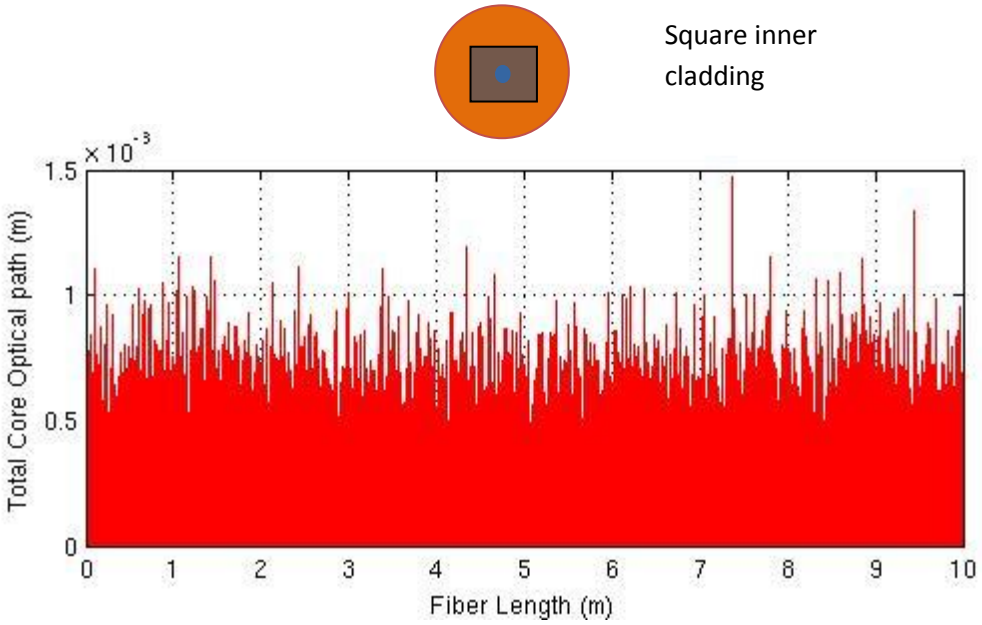

(b)

Figure 2.4. Image of the core optical path of (a) circular and (b) square inner cladding shape of a Tm:ZBLAN double clad fibre.

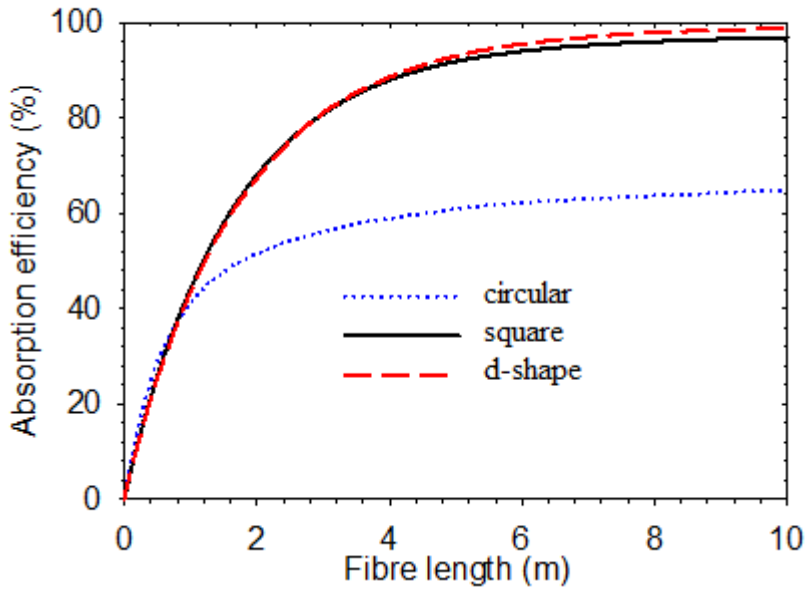

Figure 2.5. Result for pump absorption of a circular, square and d-shape geometry of a double clad fibre.

Figure 2.5 plotted the absorption efficiency as a function of length of a fibre. In Figure 2.5, the dotted line shows the absorption for a 125µm straight circular inner

cladding with centered core, while the dash line represents the result for d-shape inner cladding and the line represents the results for parallelogram shape. For circular shape, the pump absorption tends to saturation along with the increasing of length. At the beginning the absorption increases with length sharply. After a certain distance the increasing becomes smaller and smaller due to the non-absorbtion of skew rays to the core of a fibre. For square and d-shape it is observed that the pump absorption increases for an increase of fibre length up to 5 m and most of the pump light absorbed at 5 m length.

It is also observed from the Figure 2.5 that the lowest absorption is for circular shape this is because of that only meriodional but skew rays intersect to the core of a double clad fibre. On the contrary, the absorption for square and d-shape observed much higher than circular shape. Because for breaking the symmetry of a double clad fibre the skew rays contribute more strongly.

2.6.1 Quantification of a Pump Absorption by Offsetting the Core

Pump absorption of a double clad fibre can be improved by breaking the symmetry of an inner cladding or by offsetting the core of a double clad fibre. The simplest kind of design is a circular pump cladding with a centered core. This is relatively easy to make and use. But in this kind of fibres there are some skew rays of the inner cladding which have hardly any overlap with the core, so that some significant part of the pump light exhibits incomplete absorption. As a result, the gain and power efficiency are compromised.

As it is known that the pump absorption can be improved by offsetting the core [18], as a result gain and efficiency can be improved. Therefore, this section is devoted to calculations of the pump absorption by offsetting the core for better understanding the pump absorption in the offset case. The aim is to implement this offset geometry to make a double clad fibre. The ultimate goal is to produce fibre laser with optimum gain and efficiency.

To quantify the pump absorption, Tm:ZBLAN double clad fibre has been chosen, with the same fibre parameters as stated earlier in the boundary condition section. Length of the fibre is 5 metre. Core container number has been chosen to be

1600, for 1 metre fibre according to convergence test for optimum container number. A free space pumped configuration has been used in model to quantify the pump absorption of a double clad fibre by offsetting the core. The Figures 2.6 (a) and (b) give the pump absorption quantification.

In Figure 2.6 (a), the absorption efficiency is plotted against fibre length for different core offset for 5 metre length of a fibre. In Figure 2.6 (b), absorption efficiency plotted against different core offset values. It has been observed from Figure 2.6 (a) that the maximum absorption is 92% for 30 μm core offset.

In Figure 2.6 (b), it is also noticeable that for a small change in offset distance there is a significant change in pump absorption that can be achieved for offset distance up to 15 μm. Moreover, very similar absorption is achieved as long as the offset is > 15 microns. In case of centered core, the pump absorption is 60.5% provided that a sufficiently long length of fibre is used (5 m). While for off centered core, maximum pump absorption is 92% for 30 μm offset from the centre. The pump absorption is increased in case of offset core because of energy propagated by skew rays strongly interact with offset core.

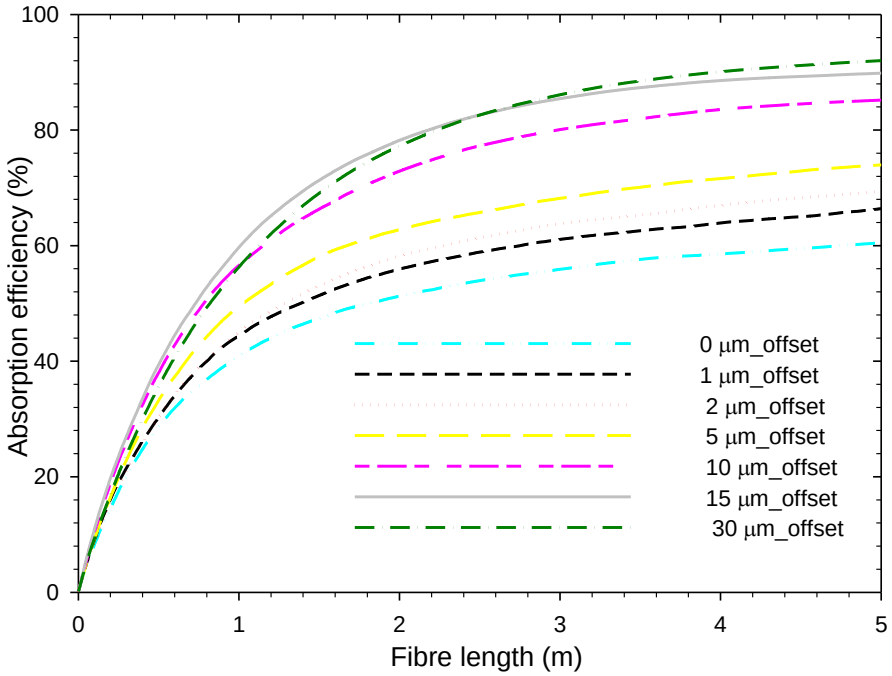

(a)

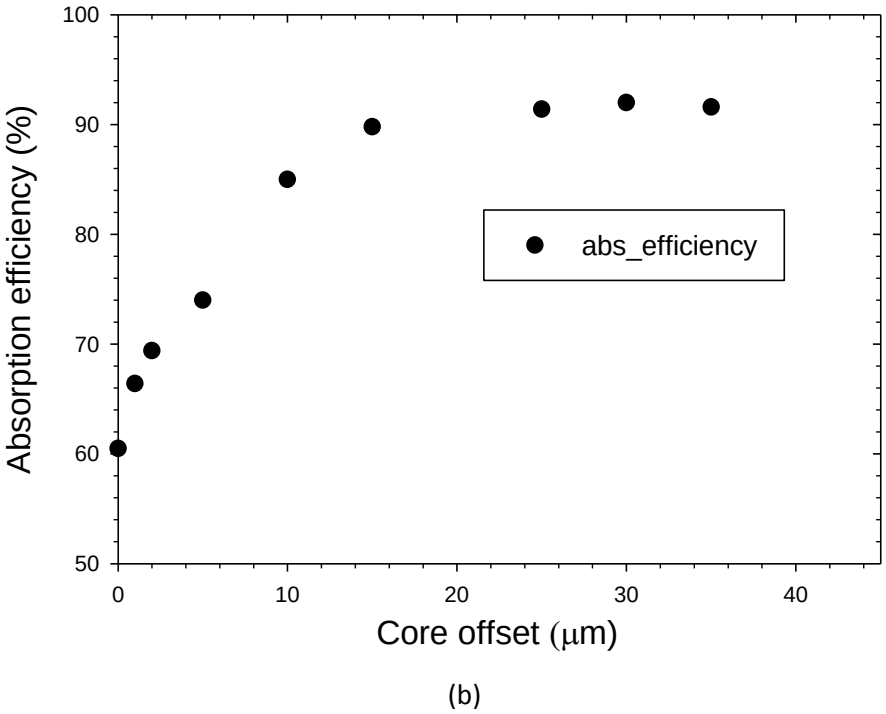

Figure 2.6. Pump absorption quantification for 8/125 μm Tm:ZBLAN double clad fibre (a) using the different offset values of 8 μm core (b) total absorption efficiency versus core offset of 8 μm core and length of fibre of 5 m.

2.6.2 Quantification of Pump Absorption for Increasing the Core Diameter

Figure 2.7 (a), (b) and (c) measures the pump absorption quantification for different values of offset distance by varying the core diameter. Here the numerical aperture kept fixed for both the core and inner cladding, but have varied diameter of core by keeping the fixed inner clad diameter. The length of the fibre was set 1 m for the simulation. In Figure 2.7 (a), (b) and (c) all the parameter are same except the core diameter, which is 10, 15 and 20 μm.

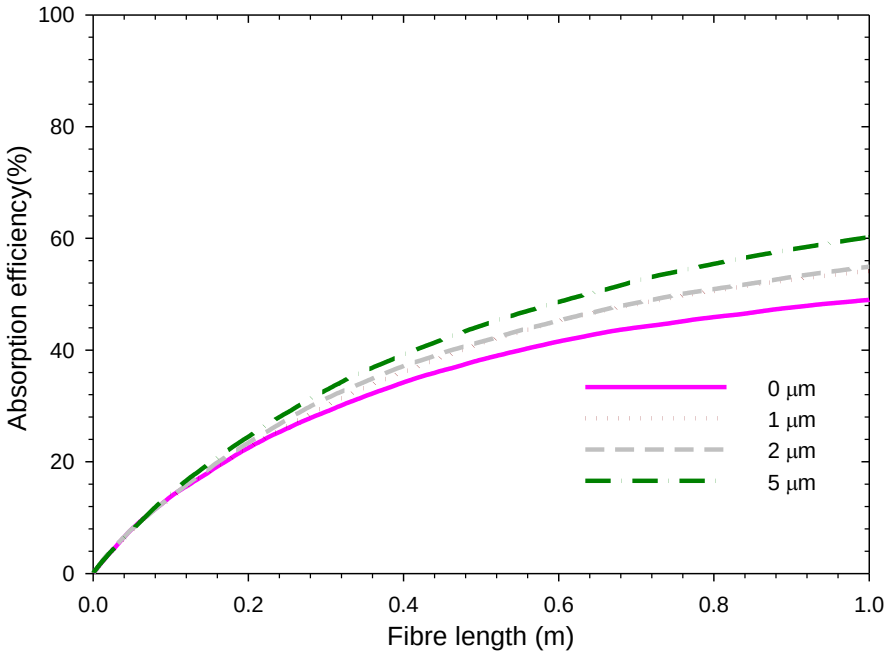
Absorption efficiency(%)
Fibre length (m)
0 μm
1 μm
2 μm
5 μm

(a)

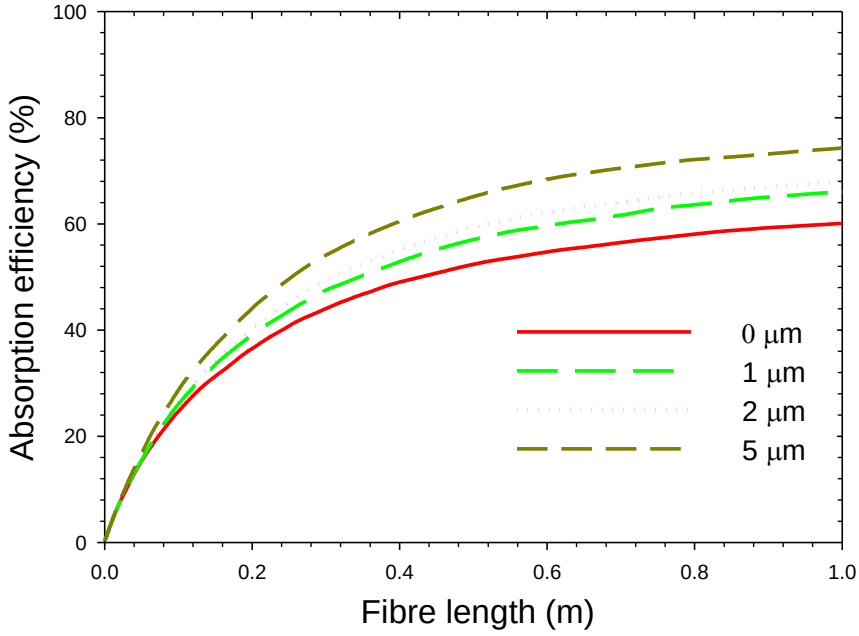
Absorption efficiency (%)
Fibre length (m)
0 μm
1 μm
2 μm
5 μm

(b)

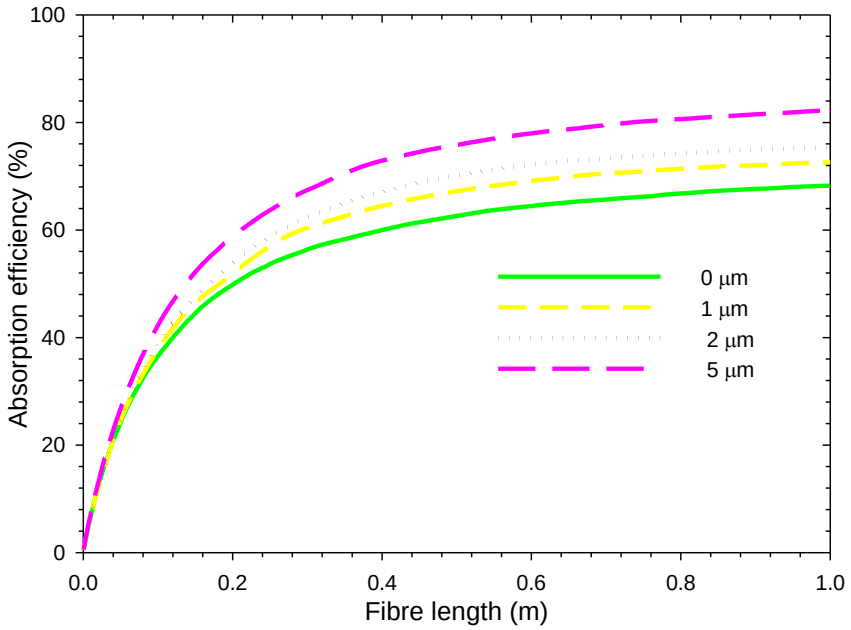

(c)

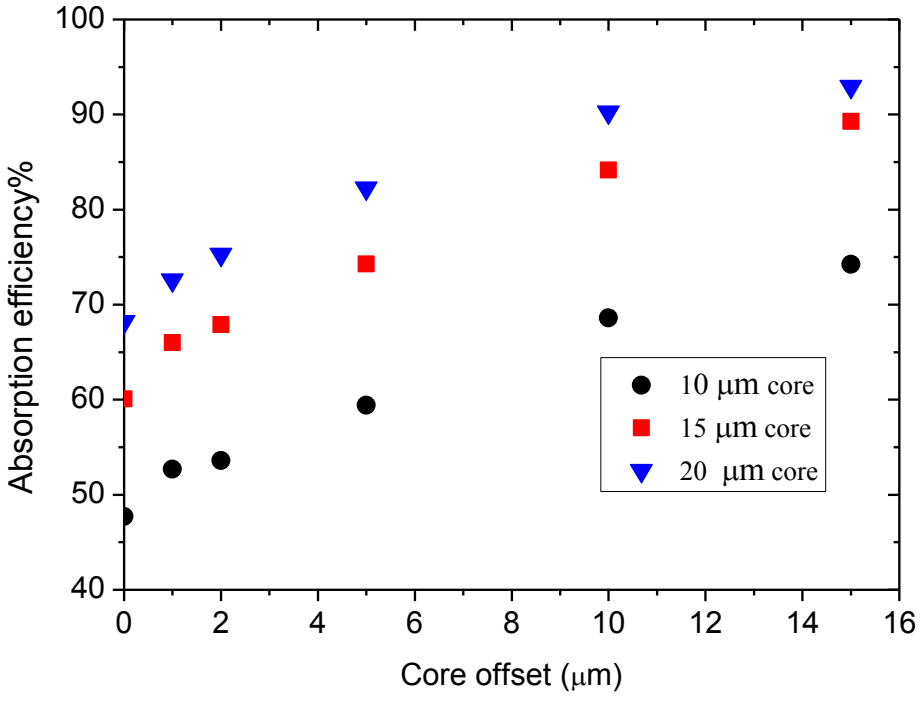

(d)

Figure 2.7. Pump absorption quantification for different offset values of (a) 10 μm core (b) 15 μm core (c) 20 μm core and (d) is the comparison of absorption efficiency for different offset values of 10 μm, 15 μm and 20 μm core.

As it is observed in Figure 2.7 (a) that for 10 μm core, at 0 μm offset values the pump absorption is 47.7% and it increases as the offset distance increases. An increase of the offset distance by 1 μm increases the pump absorption to 52.7%, i.e. an improvement of 5% absorption. For an offset 2 μm, the pump absorption increases, but not in the same rate as 1 μm offset, because the skew rays interaction mostly happen just for offsetting the core. In Figure 2.7 (b) pump absorption is also increases with the increase of offset distance. Here for 15 micron core at 0 μm offset values, the pump absorption is 60%, whereas, for 1μm offset distance this value reaches to 66%, i.e. 6% pump absorption increases. The maximum absorption at 5 μm offset is 74.3%. In Figure 2.7(c) maximum absorption at 5 μm offset is 82.2%. Figure 2.7 (d) shows the relative picture of offset distance versus absorption efficiency for 1metre length of a fibre. In Figure 2.7 (d), the circle represents the pump absorption for 10 μm core, the square represents for 15 μm core and the lower triangle in the legend but upper curve in the Figure represents the 20 μm core diameter of a fibre. Here it is observed that for increasing the core diameter as well as increasing the offset distances the pump absorption also increases. The maximum pump absorption for 10 micron core at 15 μm offset distance is 74%, for 15 μm core it is 89% and for 20 μm core it is 93%.

2.7 Summary

Pump absorption calculation of a double clad fibre presented above in this chapter demonstrates that the pump absorption increases by breaking the symmetry of a double clad fibre. Moreover, pump absorption can also be increased by increasing the core diameter, as well as offset distance. This means that, a short length of fibre can be used to absorb the pump power for fibre laser operation. Non absorptive losses also reduced because of a reduction of length of fibre. However, increasing the core size creates core waveguides that are no longer single mode. The presence of higher order modes lead to degradation in the output beam quality, but most of the application requires diffraction limited beam quality. Therefore, it is required to choose a fibre design such that it has small core diameter with non circular symmetry as well as core offset. Within this approach one can maintain the single mode guidance, as well as high gain and efficiency for fibre laser operation.

2.8 Experimental Measurement of Pump Absorption of a Tm:ZBLAN Double Clad Fibre

To compare with model results it is necessary to measure the pump absorption experimentally. Therefore, the pump absorption is measured through the cut-back experiment. Before starting cut-back measurement, a 35 W 790 nm limo diode has been characterised. The efficiency of a diode was 0.9 W/A. Apart from this; diode fluctuation has also been measured to check the stability of a diode power. The detail of diode characterisation and fluctuation measurement has given later in appendix section.

2.8.1 Cut-back Experiment

In this section, the experimental pump absorption measurement through cut-back method is discussed. The aim is to compare the measured absorption with numerical results. A destructive cut-back technique [93] has been employed in a commercial Tm doped ZBLAN double clad fibre to calculate the pump absorption. A 790 nm light coming through a 100 μm patch fibre used an input source for the experiment. The schematic diagram and experimental setup for cut-back absorption measurement is shown in figure 2.8. After collimating 790 nm pump source, a 4% Fresnel reflection power has been used as an input and focused with appropriate optics to couple the pump light to the Tm:ZBLAN fibre (see diode characterization in appendix section for detail). A 10.34 m Tm:ZBLAN double clad fibre has been chosen for the experiment. In order to remove the polymer coating from the fibre, the fibre ends were put in a dichloromethane (DCM) for about 3 minutes and then stripe the fibre using cleaning tissue. It is noted that the commercial Tm:ZBLAN double clad fibre has two layers of coating and it is very fragile. Therefore the fibre handled very carefully and the second coating removed from the fibre by using Acetone in the cleaning tissue, and stripe until the second coating is completely removed. After removing the polymer coating from the fibre ends, it has been cleaved using YORK clever. After cleaving, both ends of the fibre are placed on V groove upon nano stages. The collimated light is properly coupled into the inner cladding of a Tm:ZBLAN double fibre. After launching the pump light into the input end of the fibre, the launching condition kept unchanges. The cleaving

ends have been tested every time by placing fibre ends under microscope throughout the experiment to ensure the nice cleaving end. The fibre under test is successively cut at different point of M_i at a distance Z_i from the input end and the corresponding output power P(Zi) is measured at each point of fibre (Figure 2.8). Finally, the pump absorption is measured in dB using the expression

$$A(z_i) = 10\log_{10}\frac{P_p(Z_o)}{P_p(Z_i)}\,dB$$

where, $P_p(Z_o)$ is pump power measured for smallest fibre length Zo, very close to the input end of the fibre. The slope of the curve A (Z_i) gives the absorption per unit length in dB.

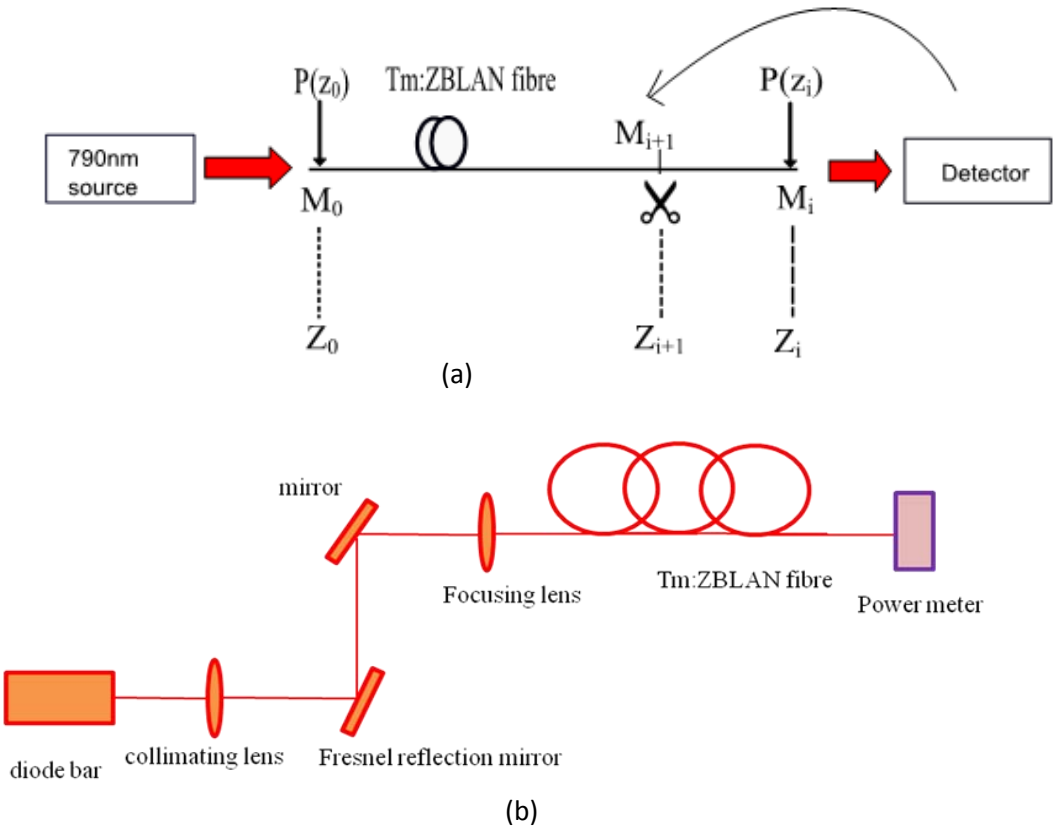

Figure 2.8. (a) Schematic diagram for cut back measurement and (b) experimental setup

It is noted that, in an optically active fibre the pump wave absorption rate at a certain point depends on the local population inversion and consequently on the local flurescence. However, to avoid the flurescence effect, the launched power should be kept resonably low so that the population inversion remains negligible. It is mentioned

in appendix section that, the diode power fluctuates at low input. In order to satisfy the experimental condition diode has been operated in high power and a Fresnel reflection of 4% reflective power has been used as an input power (Figure 2.8(b)), wich is launched to an input facet of fibre.

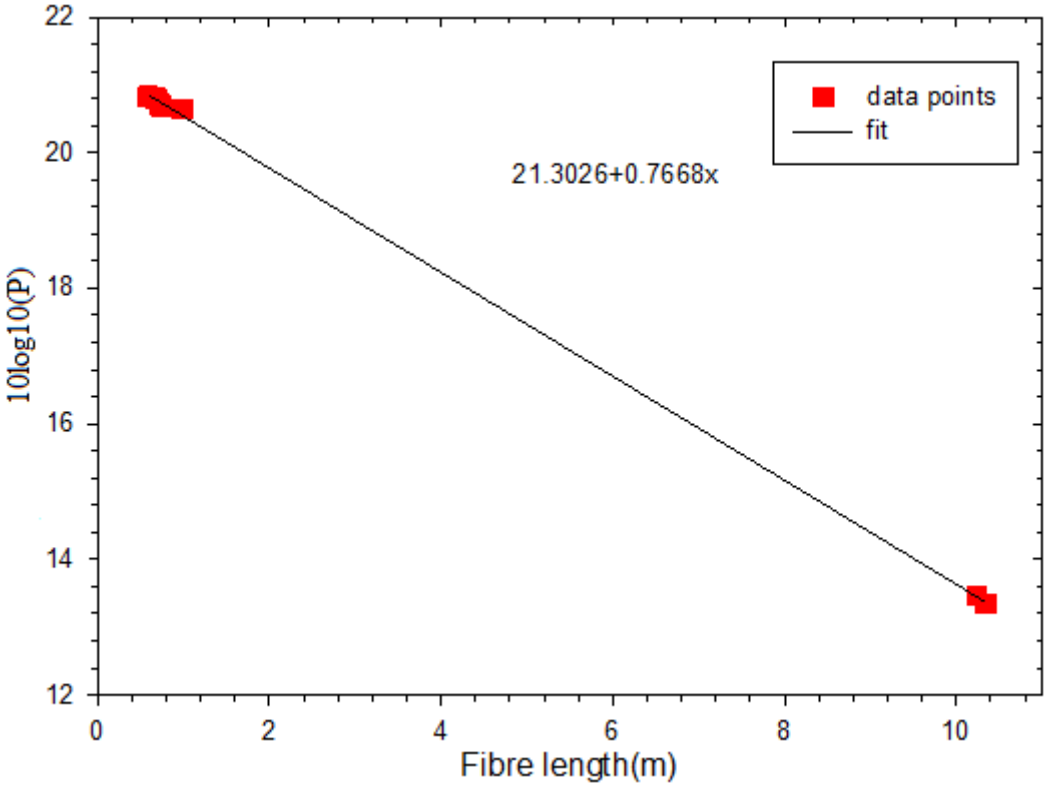

Figure 2.9. Pump absorption measurement of a Tm:ZBLAN double clad fibre.

Figure 2.9 shows the pump absorption measurement using cut-back technique. It is observed from figure that the pump absorption of Tm:ZBLAN double clad fibre is 0.77 dB/m. Using this measured absorption, the next step is to compare the model absorption of Tm:ZBLAN double clad fibre.

2.9 Comparison of Pump Absorption Between Model and Experiment

The Tm:ZBLAN double clad fibre was supplied by FiberLabs. The fibre data sheet did not provide any information regarding the fibre core, in particular no information was provided about whether it is centred or off centred within the cladding, therefore a microscope image of the end face of Tm:ZBLAN fibre as shown in Figure 2.10, was taken. After post processing and careful observation of this picture reveals that the core

is off centred by about 5 µm. After confirmation of the fact that the core is off centred, a MATLAB code is used to calculate the absorption for a fibre of 10 m length, with cntred core as wll as off centred. The analysis is performed as follows.

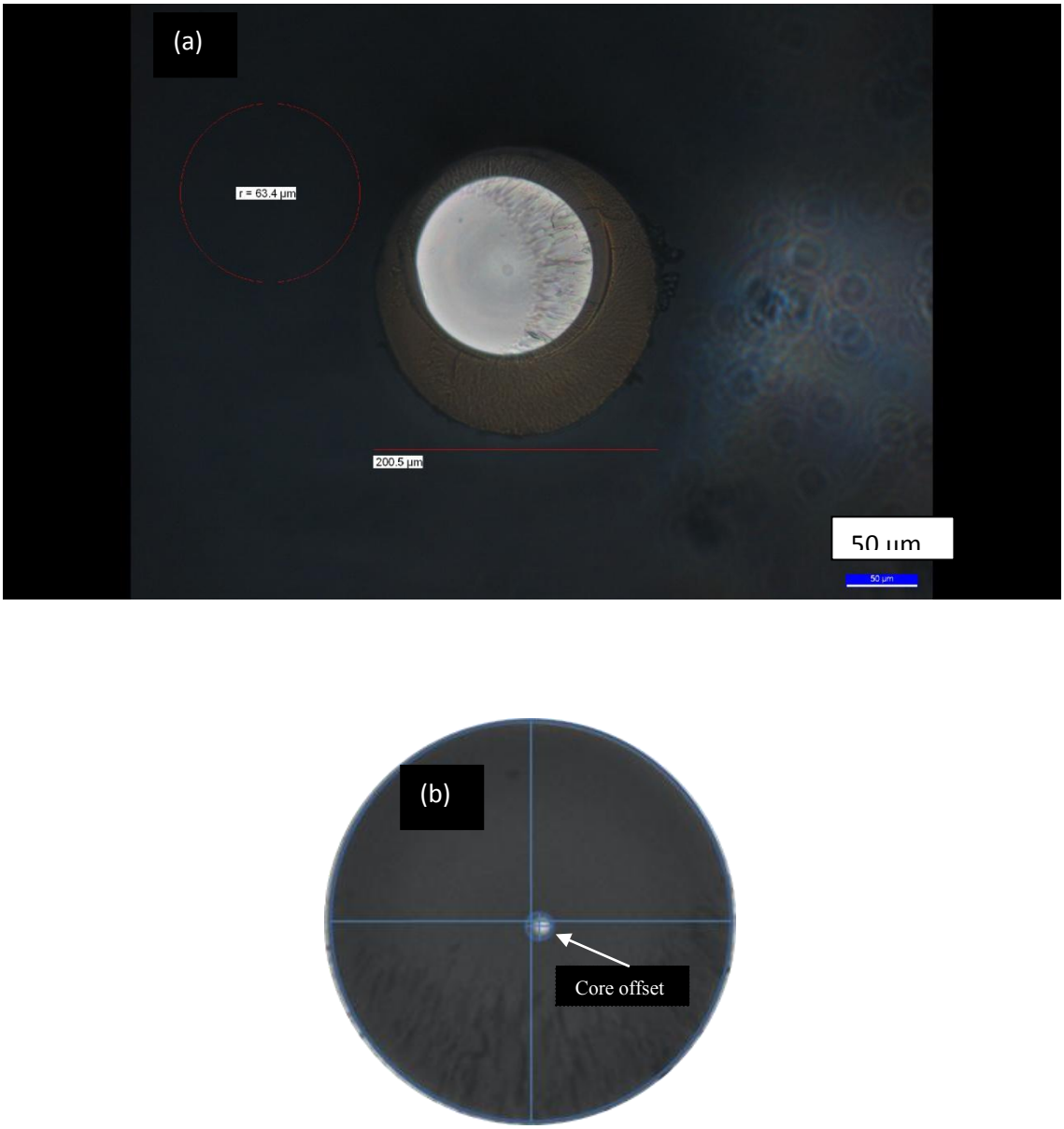

Figure 2.10. Microscopic image of a (a) Tm:ZBLAN double clad fibre and (b) coreresponding postprocessing image

Initially it has been consider the same unit length of a fibre of cut back method and then reduced the simulation length gradually and the corresponding pump absorption is

noted. For off centred core the absorption is calcualted for a length of 10.34 m fibre, same length as used in the cut-back experinment. Moreover, cut-back absorption efficiency is calculated as follows. Firstly, cutback data is fitted and extrapolated to zero length of a fibre, which gives the launch pump power at input end. Therefore, with the help of launch pump input and the transmitted output for every cutback length, absorption efficiency is calculated.

Figure 2.11 shows a comparison between the model calculation and cut back experiment. The traingle denotes the measured absoorption from cut-back experiment, while circles represents model calculations for a centred core and line represents absoprtion for an off-centred core.

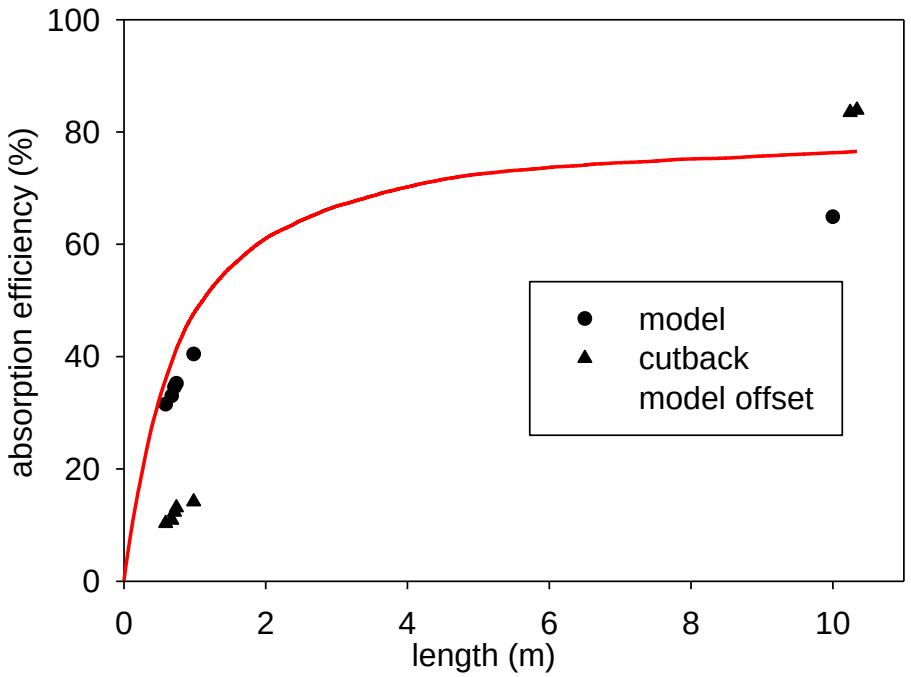

Figure 2.11. Comparison of pump absorption between model and experiment, for circular geometry of the double clad fibre.

It has been observed from figure that the pump absorption is comparable at longer length for model offset, while at shorter length model calculation reveals high values for the absorption efficiency than the experimental mesurement. Energy losses could occur during the scattering mechanism such as material impurities as well geomtric perturbation in a fibre. Moreover model neglects the reflection loss. Therefore, losses

can be taken into model, and thus the absorption efficiency are expected to shift towards lower level at a shorter length of a fibre. There might be two other possibilities to differ experimental result from model calculation. Firstly in model calculation effect of fibre bending was not considered for pump absorption calculation. Secondly for cut-back measurement we measured absorption at 10 metre and below 1 metre length only. For more accuracy of measurement it could be performed the cut back experiment repeatedly througout the whole length of fibre. But we had limited length of commercial fibre and was needed to perform fibre laser experiment.

2.10 Conclusion

It can be concluded from above simulation as well as experimental analysis that, the pump absorption is favourable when the symmetry of a double clad fibre is broken. This is due to the fact that in circular fibres the skew rays never interact to the core. Pump absorption can be improved by increasing the inner clad diameter as well as off centred core. Therefore, for appropriate design of a double clad fibre, it is necessary to understand the pump absorption behaviour, which is essential to develop the fibre laser in an efficient way.

Chapter 3

Development of 2 μm Tm:ZBLAN Double Clad Fibre Laser

3.1.1 Introduction

In Chapter 1 it has been discussed that fibre lasers offer an attractive alternative to conventional bulk lasers. It has also discussed the detail of lasers operating ~ 2 μm spectral region have a wide variety of potential application such as free space communication, remote sensing and medicine are of primary interest. Moreover it has also discussed about the potentiality of developing Tm:ZBLAN fibre laser at ~ 2 μm. Therefore this chapter will describe studies and experiments aimed at the development of efficient Tm:ZBLAN fibre lasers operating at 2 μm. Moreover, in-house Tm:ZBLAN fibre characterisation will also be investigated.

3.1.2 Experimental Setup

The experimental set up for the development of ~ 2 μm fibre laser is shown in Figure 3.1. Tm:ZBLAN double cald fibre has been used for this experiment, which is supplied by FiberLabs Inc. Japan. The core diameter of a Tm:ZBLAN fibre is 8 μm (NA 0.15), and inner clad diameter 125 μm (NA 0.50) with a thulium doping concentration of 20000 ppm by weight. The circular inner-cladding diameter was surrounded by low refractive index polymer as outer cladding. The V number of Tm:ZBLAN fibre is 1.88 at 2 μm. The length of a Tm:ZBLAN double clad fibre used for this experiment was 5.45 m. The fibre was coiled around a 10 cm diameter aluminium cylinder for cooling to avoid the heating of a fibre. The main body of the fibre was cooled through a cooling fan. The absorption of the fibre was measured using the cut-back technique [93], to be 0.76 dB/m. Therefore, for a 5.45 m fibre pump absorption efficiency was 62%. As it is evident from the microscopic image of Tm:ZBLAN double clad fibre that the core is 5 μm offset from the centre (see Figure 2.10, chapter 2), therefore we followed the

cutback absorption as explained in chapter 2, to measure the absorption of a 5.45 m fibre.

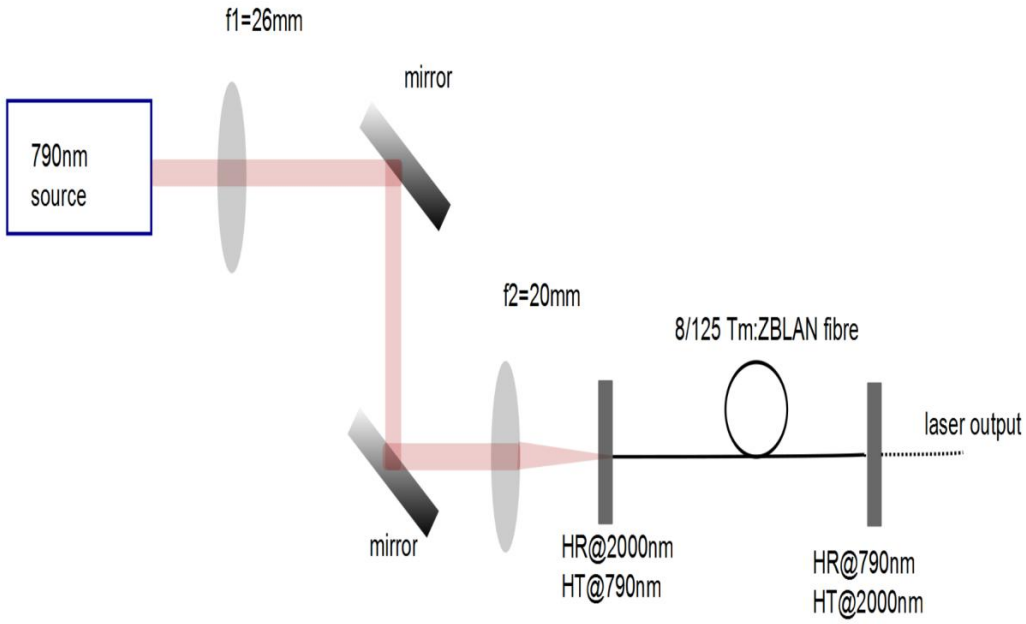

Figure 3.1. Cladding pumping Tm:ZBLAN fibre laser.

The pump source was a 790 nm laser diode with a 100 µm patch fibre (made in Germany by LIMO GmbH). For collimating and focusing lenses with foci f=26 mm and f=20 mm have been used. After collimating and focusing, 790 nm light has been coupled to Tm:ZBLAN fibre and optimised for maximum coupling. After optimisation output power is recorded. Therefore the launch efficiency to the fibre was calculated by measuring the difference of input power and transmitted output power along with power absorbed to the fibre, which is 92%. It is noted that absorbed power is calculated by using cut-back absorption.

The resonator cavity was formed by butting a dichroic mirror to the input facet of the fibre, which has high transmission at 790 nm and has high reflectivity at 2000 nm, along with a 4% Fresnel reflection of the rear end of the fibre. Moreover a dichroic mirror having high reflectivity of a 0%, 20% and 30% at 2000 nm has also been butted to the output end to measure the performance of fibre laser at ~2 µm. Here 0% reflectivity at 2000 nm output coupler butted to the output end of fibre to examine fibre

laser spectrum at ~2 μm laser. It is noted that index matching gel was not used to mitigate against Fresnel reflection.

3.1.3 Results and Discussions

A maximum 1.53 W output Tm:ZBLAN fibre laser at 1960 nm has been demonstrated. The threshold value for this laser was 0.0138 W and the slope efficiency was 45% with respect to launch pump power, as shown in Figure 3.2 (b).

The performance of laser output has been analysed for single end forward pumping resonator system using a different reflective output coupler as follows. Initially the resonator cavity was formed by butting the dichroic mirror which has high reflectivity at 2000 nm and high transmitivity at 790 nm to the input end of the fibre and the output fibre end ~4% Fresnel reflectivity act as an output coupler. An uncoated Si slice has been used to separate the lasing signal from the pump light. Laser output was collimated and focused to the monochromator. After confirmation of laser spectrum at ~ 2 μm, the output power was recorded using a power metre. The output power is plotted against the launched power which is shown in Figure 3.2. It is observed from Figure 3.2(a) the slope efficiency of laser output at ~ 2 μm is 19.5%.

Moreover, resonator cavity was also formed by keeping input coupler mirror fixed (HR at 2000 nm), a 20% and 30% reflectivity dichroic mirror butted to the output end of the fibre as an output coupler to measure the output at ~ 2 μm. The maximum recorded output is 1.53 W and the slope efficiency is 45% shown in Figure 3.2(b) for an output coupler mirror of high reflectivity at 790 nm and 20% reflectivity at 2000 nm. For a mirror of output coupler, high reflectivity at 790 nm and 30% reflectivity at 2000 nm, the slope efficiency becomes 42% with output 1.41 W as shown in figure 3.2(c). It also observed that laser performance depended on the reflectivity of the output coupler mirror. It is observed from Figure 3.2 that the maximum output is observed at 20% reflectivity of output coupler mirror at 2000 nm. Figure 3.2, also shows that increasing the output coupler reflectivity‟s causes the decrease of slope efficiency of Tm:ZBLAN fibre laser.

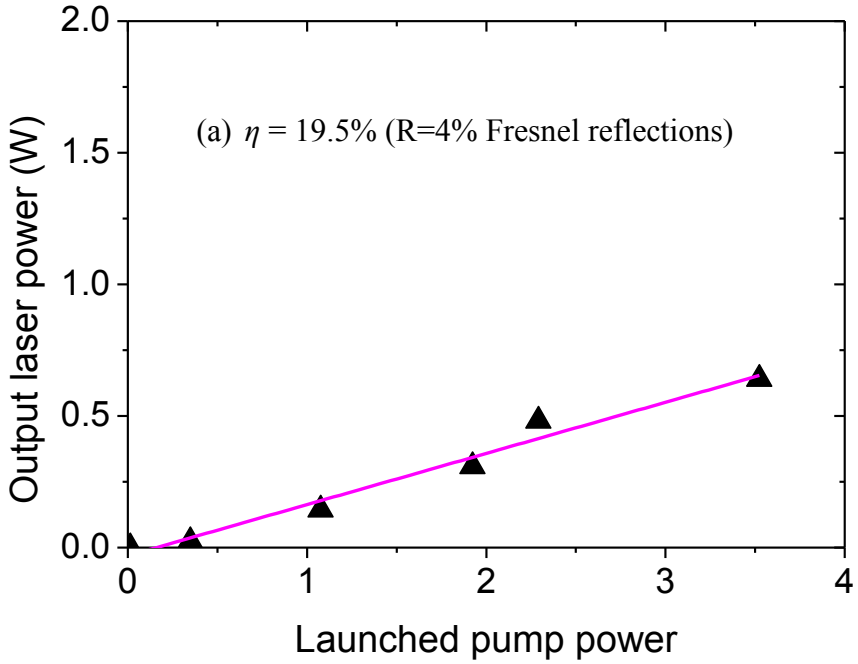
(a) η = 19.5% (R=4% Fresnel reflections)
Output laser power (W)
Launched pump power
0.0
0.5
1.0
1.5
2.0
0
1
2
3
4

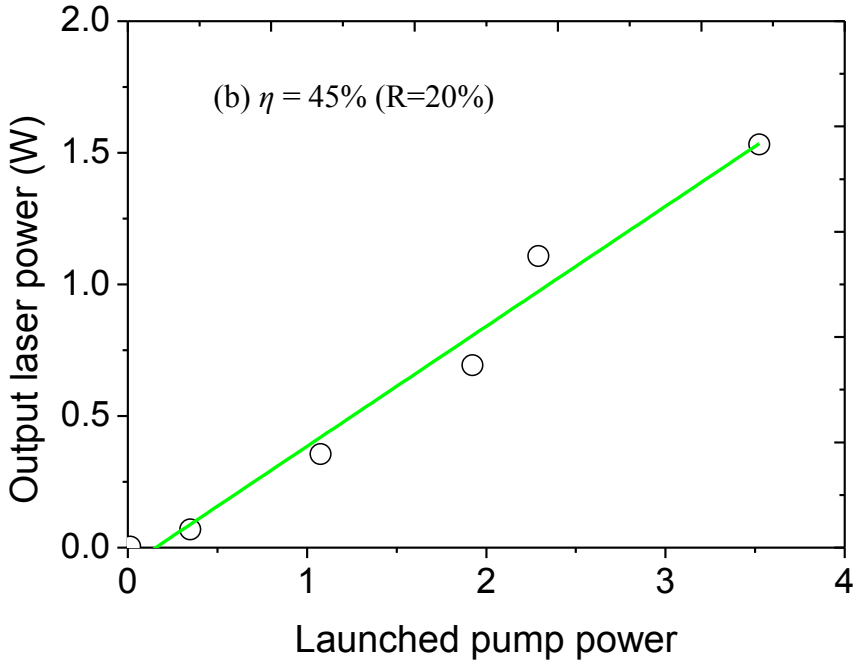
(b) η = 45% (R=20%)
Output laser power (W)
Launched pump power
0.0
0.5
1.0
1.5
2.0
0
1
2
3
4

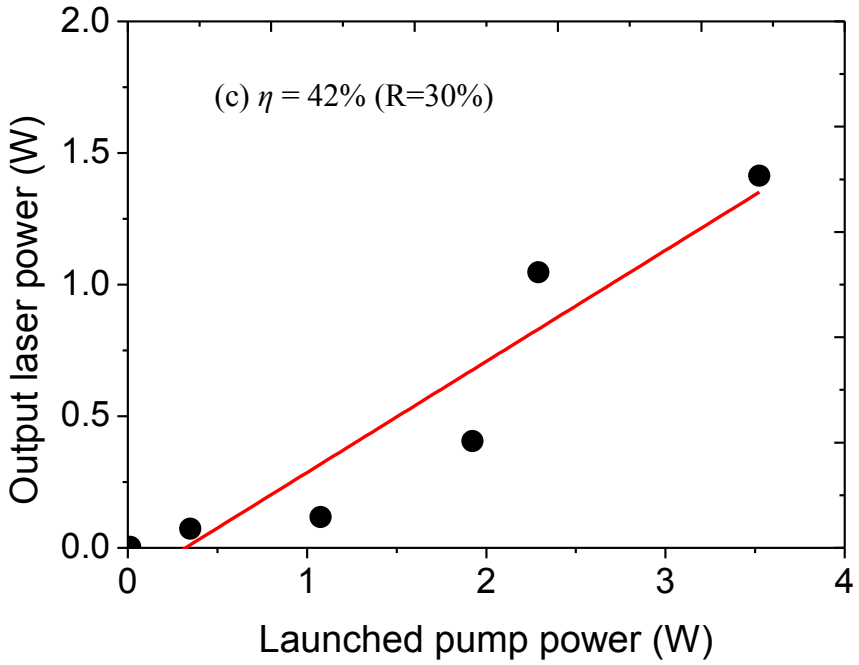

Figure 3.2. Laser output for (a) 4% Fresnel reflections and Si filter (b) 20% and (c) 30% reflectivity output coupler.

The output spectrum was measured by monochromator for different output coupler reflectivities. Figure 3.3 shows the out spectrum for different cavity reflectivity of a single end pumping system.

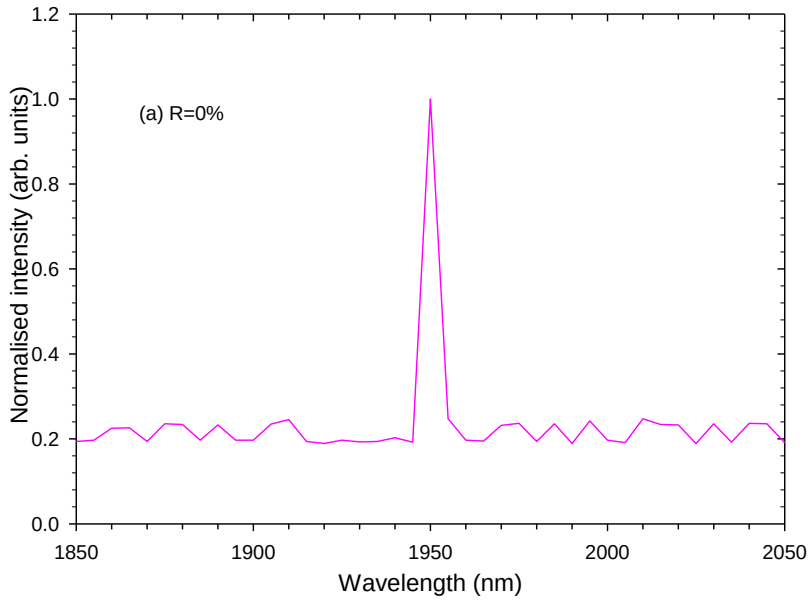

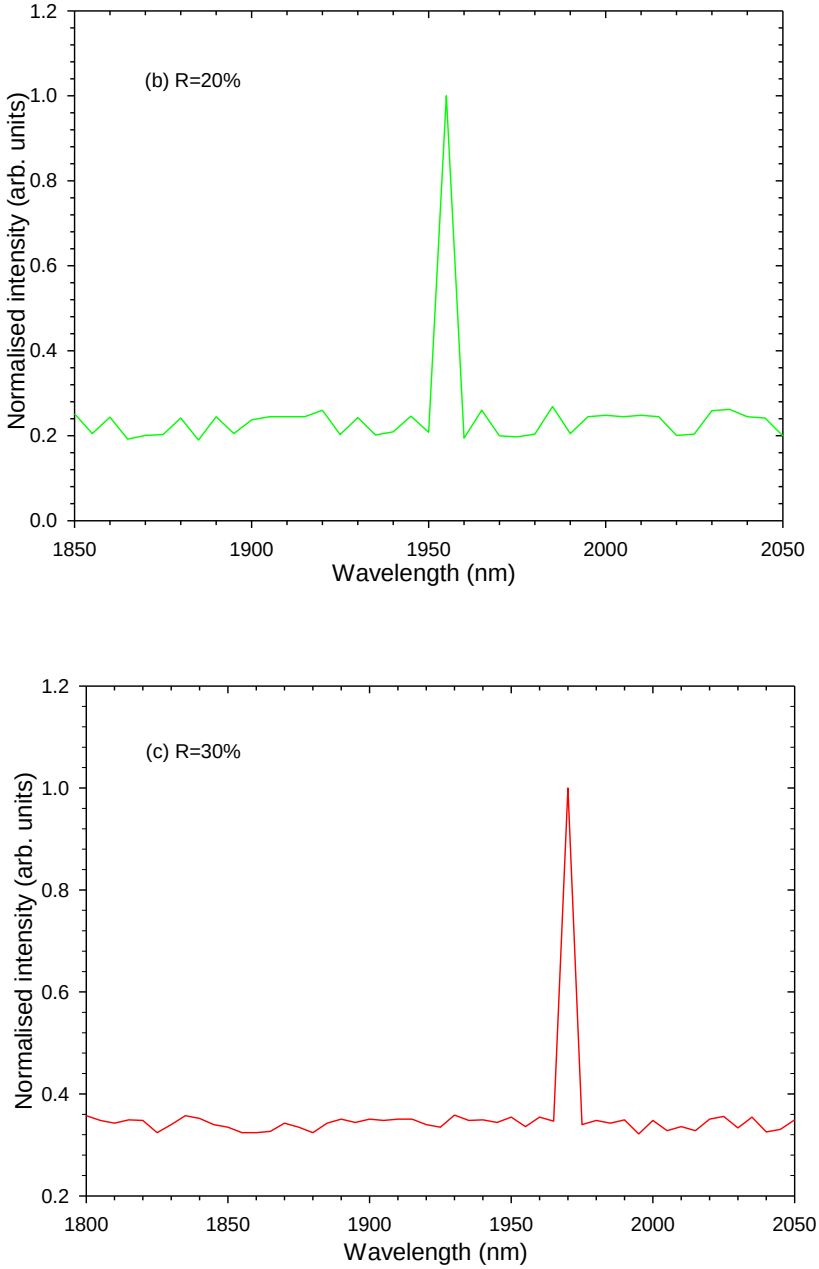

Figure 3.3. Output spectrum at ~1.95 µm for (a) R=0%, (b) R=20%, (c) R=30% mirror at 2 µm as an output coupler.

It is observed from figure 3.3 (a), (b) and (c) that the output varies from 1950 nm to 1970 nm. The lasing wavelength is between 1.95 µm to 1.97 µm depending on the cavity reflectivities. Apart from this, the output was also observed for both the forward and backward direction successively by using 0%, 20% and 30% reflective output coupler mirror at 2000 nm. The output is shown in Figure 3.4 (a), (b) and (c). For 0%

reflective output coupler resonator cavity was formed by keeping the input coupler fixed to the input end of the fibre and the output coupler was a mirror which has high reflectivity at 790 nm and high transmitivity at 2000 nm butted to the output end of the fibre.

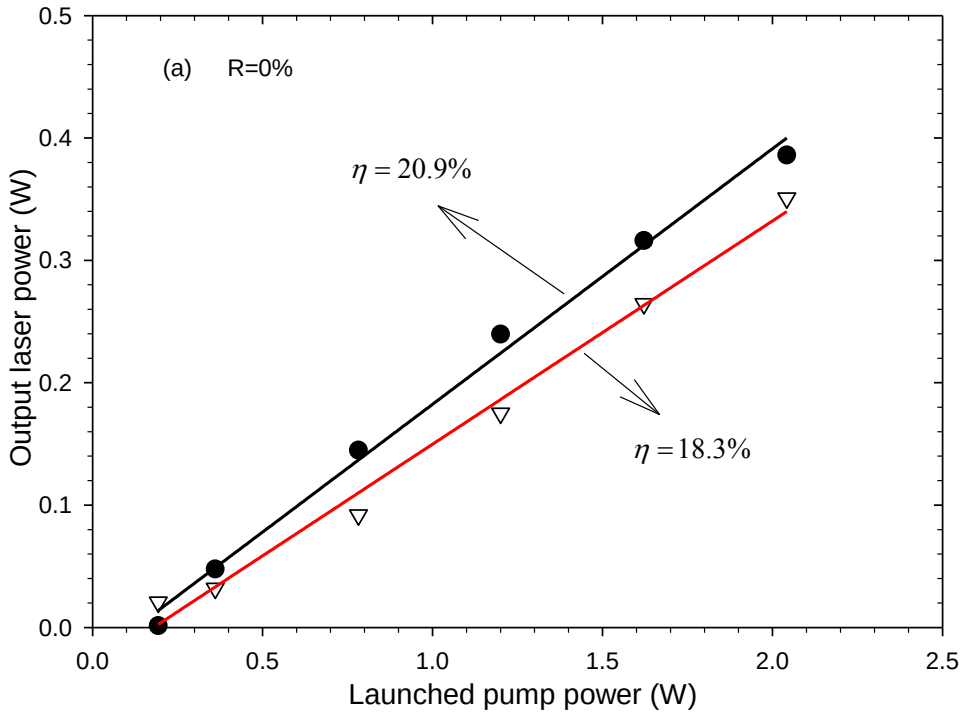

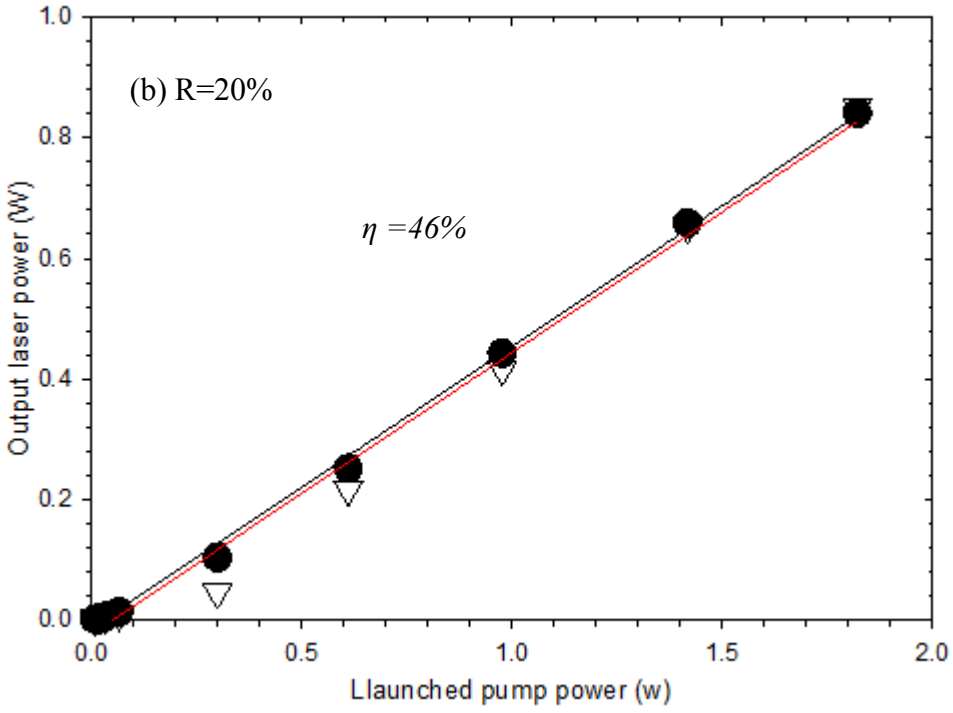

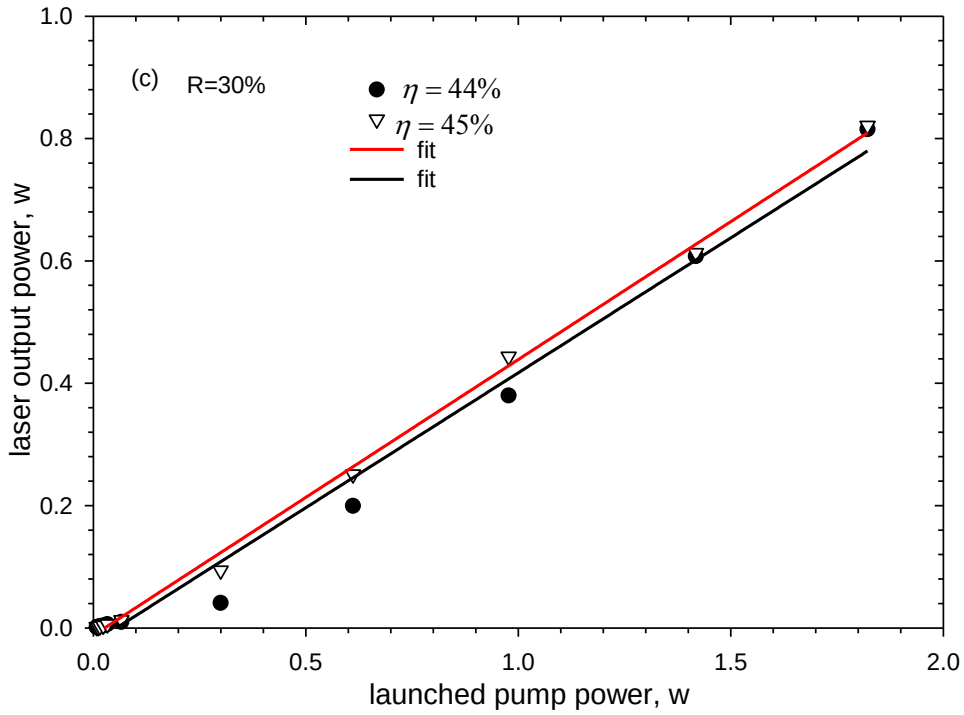

Figure 3.4. Laser output using an output coupler reflectivity of (a) 0% (b) 20% and (c) 30% at 2000 nm.

Here forward direction refers to the increment of input power from zero to maximum value used in this experiment and backward direction refers to the decrement of input power started from forward directions maximum value. The lower triangle denotes the backward direction and the circle represents forward direction of measurement. The fluctuation of output observed for backward direction of measurement shown Figure 3.4 (a) and (c). The cause of fluctuation of power may be due to the heating the fibre ends. It is noted that the fibre tip was not cooled. The cooling fan is used to cool the body of the fibre throughout the experiment to minimise the thermal heating.

The highest efficiency, exhibited by the 20% reflective mirror, is 45% at 1960 nm which is comparable to highest ever reported slope efficiency of 49% reported by M Eichorn [3] for Tm:ZBLAN double clad fibre laser. Further scaling the output is possible by increasing the launch pump power as well as by maintaining proper cooling system to protect from thermal damage of the fibre. As it has been mentioned earlier, a 5.45 m Tm:ZBLAN double clad fibre has been used in this experiment, and the

absorption of pump light was 62%. Therefore, the fibre length was not long enough to absorb the pump power in one pass. To increase further absorption of pump power a second mirror could be placed at the output end with required HR coating at the pump wavelength. Therefore the slope efficiency could be increased further by reflecting the unabsorbed pump power back to the cavity throughout using a mirror coated with HT at 790 nm.

3.1.4 Summary

A Tm:ZBLAN fibre laser operating at 2 μm has successfully been demonstrated using different reflective output coupler mirror. The highest slope efficiency and maximum power achieved were 45% and 1.53 W, respectively, using 20% reflective output coupler. Further output could be scaled but to avoid the damage of fibre ends these experiments were not conducted for further higher output. The lasing wavelength is between 1.95 μm to 1.97 μm depending on the various cavity reflectivities. Moreover laser performance for both forward and backward direction is observed. Fluctuation of output observed for backward direction of measurement due to the heating of fibre ends.

3.1.5 In house Tm:ZBLAN double clad fibre Fabrication and Characterization

This section will describe about the fibre fabrication and characterization of a Tm:ZBLAN double clad fibre. The aim of this in house double clad Tm:ZBLAN fibre fabrication and characterisation is to make a fibre laser at 2.3 μm.

3.1.5.1 Fibre Fabrication

In-house step index ZBLAN fibre has fabricated through extrusion technique (rod-in–tube) [94] as follows (Fabrication by A/Prof. Heike Ebendorff Heidepriem). Cladding glass composition was used as the common ZBLAN glass composition $53ZrF_4$-$20BaF_2$-$4LaF_3$-$3AlF_3$-20NaF. Core index of the glass was increased by replacing the 2 mol% BaF_2 with PbF_2. The billets are creating by melting raw materials (in powder form). When this melts is cast into a mould and cooled down they become billets of about 3x3 cm. The core glass was extruded into a doped 10 mm diameter rod and the cladding glass was extruded into a tube of hexagonal outer and inner circular shape. The next step was the extruded core glass rod was drawn down to a cane of 2 mm size outer diametre. Before fibre drawing, the rod was etched in $ZrOCl_2$/HCl solution to achieve a pristine surface [95]. The cane is therefore inserted into an extruded hexagonal tube. This assembly is then drawn down to fibre, by applying a vacuum over the core cane and cladding tube interface.

3.1.5.2 Numerical Aperture (NA) Measuring Principle

For optical fibres, NA is a very important parameter. It can be used to estimate injection efficiency and coupling loss, and is very important for coupling of fibre to fibre and free space light to fibre. In this case we are interested in measuring the NA as it will allow us to calculate the core refractive index achieved by the addition of the PbF_2. It is noted that, to increase the core refractive index of ZBLAN fibre part of BaF_2 replaced with the PbF_2.

The standard measurement of acceptance angle is the NA, which is the sin of the half acceptance angle, θ_a, for reasonable small angle, as shown in Figure 3.5

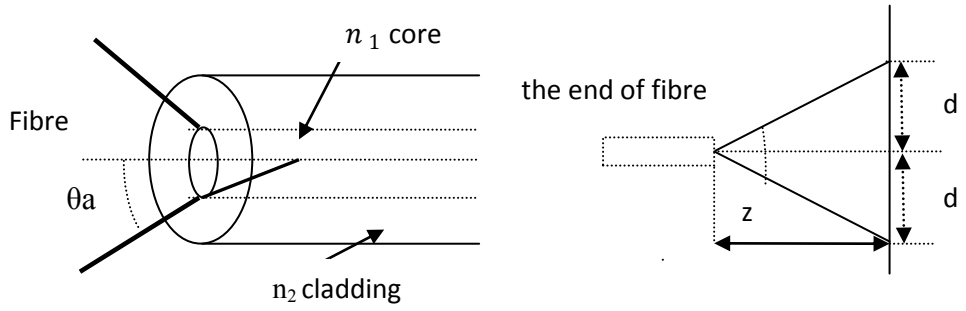

(a) (b)

Figure 3.5. (a) Definition of NA in optical fibre (b) the diagram of measuring principle

Theoretically NA is given by

$$\mathrm{NA} = \sqrt{n_1^2 - n_2^2} = \sin\theta_a \qquad (3.1)$$

Where n_1 is the refractive index of the core and n_2 is the refractive index of the cladding. But the NA can be measured directly by recording the far-field output intensity of the fiber.

The light guiding properties of fibers are symmetrical, so light emerging from a fiber over an angle is equal to its acceptance angle. According to the function of sine, NA is also calculated by formula

$$\mathrm{NA} = \frac{d}{\sqrt{z^2+d^2}} \qquad (3.2)$$

Where, z is the distance between fibre and detector and d is the beam radius.

3.1.5.3 Experimental Measurement

Experimental setup is shown in Figure 3.6. In this experiment a single mode 790 nm diode laser source has been used. In-house hexagonal shaped uncoated fibre was used for characterization. Anamorphic prism to correct the asymmetric beam shape of a laser diode from elliptical to nearly circular in shape, and f= 4.5 mm lens to tightly focus the beam into the fibre core.

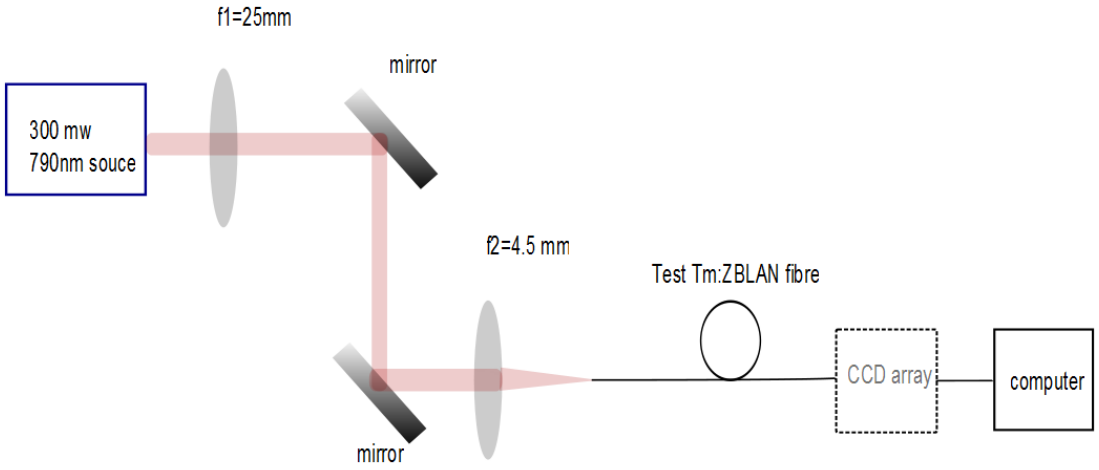

3.6. Experimental setup for a far-field light distribution measurement.

A Spiricon silicon CCD camera (SP5103) was used to capture the output beam of the fibre and it was analyzed by the computer. The beam width was measured by an inbuilt Gaussian fit routine in the software. To eliminate the light propagating in the cladding a high refractive index highly absorbing paint was applied to the fibre („absorptive surface coating").

First the experiment was set up and then aligned properly to ensure the light was effectively coupled into the fibre. A short pice of fibre was taken and then cleaved at both ends. After cleaving the fibre ends it was placed in between the focusing lens and the detector to measure the beam width. By measuring the beam width as well as the distance of the fibre end to the detector we measured the NA of the fibre using equation 3.2.

Three pieces of fibre were chosen to measure the NA. For the first fibre the length was 33 cm and an absorptive surface coating was placed after 18 cm, in the second one the length of the fibre was 27 cm and absorptive surface coating was put after 9 cm and in case of third piece of fibre length was 32 cm and „absorptive surface coating" was placed after 19 cm. The measured value is shown in the table 3.1.

Table 3.1. Data for NA measurement.

Distance Z (mm)	Beam width 2d (mm)	NA	Average NA
8.53	0.48	0.028	0.030
	0.53	0.031	
	0.57	0.033	
8.53	0.68	0.039	0.037
	0.57	0.033	
	0.686	0.040	
8.53	0.717	0.042	0.039
	0.667	0.039	
	0.628	0.036	

This corresponds to a NA of 0.035 ± 0.005. Therefore assuming a refractive index of Tm:ZBLAN glass 1.495 at 790 nm, the core refractive index is 1.4954 ± 0.0001, therefore the Δn, the index difference between core and cladding is 0.0004 ± 0.0001.
The original fibre recipe included 2.2 mol% PbF_2, which was predicted to increase by 0.0015 however measurements indicate only 27% of the predicted Δn was achieved. In the future, we will measure the refractive index of our core and cladding glasses to provide insight into the predicted NA.

The cross-sectional view of the fibre ends was checked under the microscope as shown in Figure 3.7. The aim was to correlate the measured values with the cross viewed image and to check whether an air gap existed. One of challenges is to achieve a defect free interface between the core and cladding glass. It was found that there was no air gap between the core and cladding in the measured fibre end faces and the measured NA‟s were consistent. Cut-back absorption measurement of in-house fabricated fibre will describe in the following section.

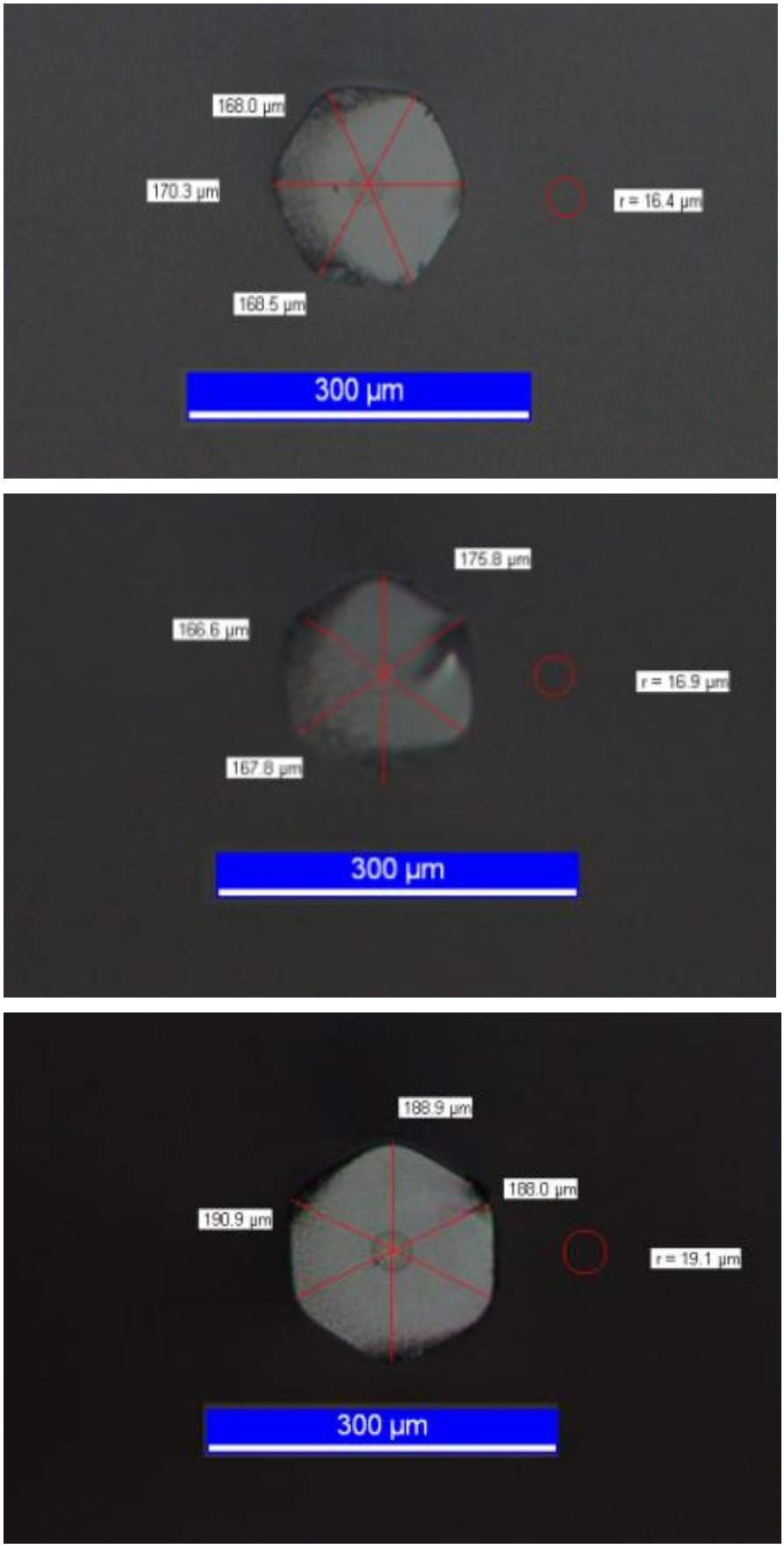

Figure 3.7. Cross view for fibre ends of 3 pieces of fibres

3.1.5.4 Cut-back Measurement

Cut-back experiment is performed along with my co-supervisor David G. Lancaster. To conduct this measurement the 35 W fibre coupled (100µm) 790 nm diode laser was coupled into approximately 1.5 m of the fibre using a 100 µm spot size (pump fibre output was imaged into the test fibre using a pair of f=25 mm aspheric lenses).

The resultant cutback is shown in figure 3.8, with an absorption measured of 10.9 dB/m. The predicted core absorption for this doped fibre was 1.4 dB/m (0.27 wt% Thulium), based on the geometry of the fibre and extrapolated from measured thulium absorptions at 790 nm for higher doped Tm:ZBLAN bulk samples. Therefore the estimated loss of the fibre was 9.5 dB/m. The high loss is likely due to incomplete fusing of the core/cladding interface. From Figure 3.9 it also observed that the core cladding interface of the fibre was not good.

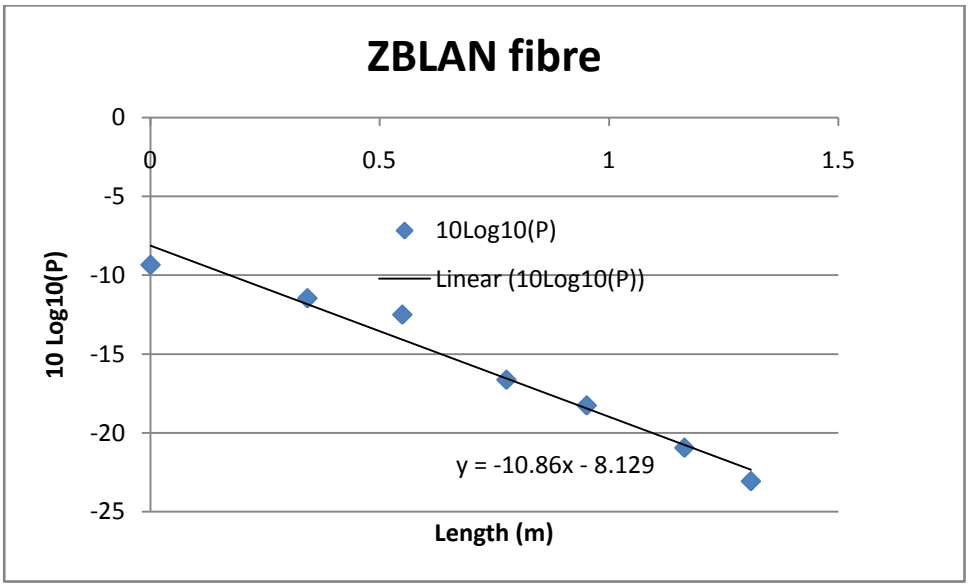

Figure 3.8. Cut-back measurement of the Tm:ZBLAN fibre.

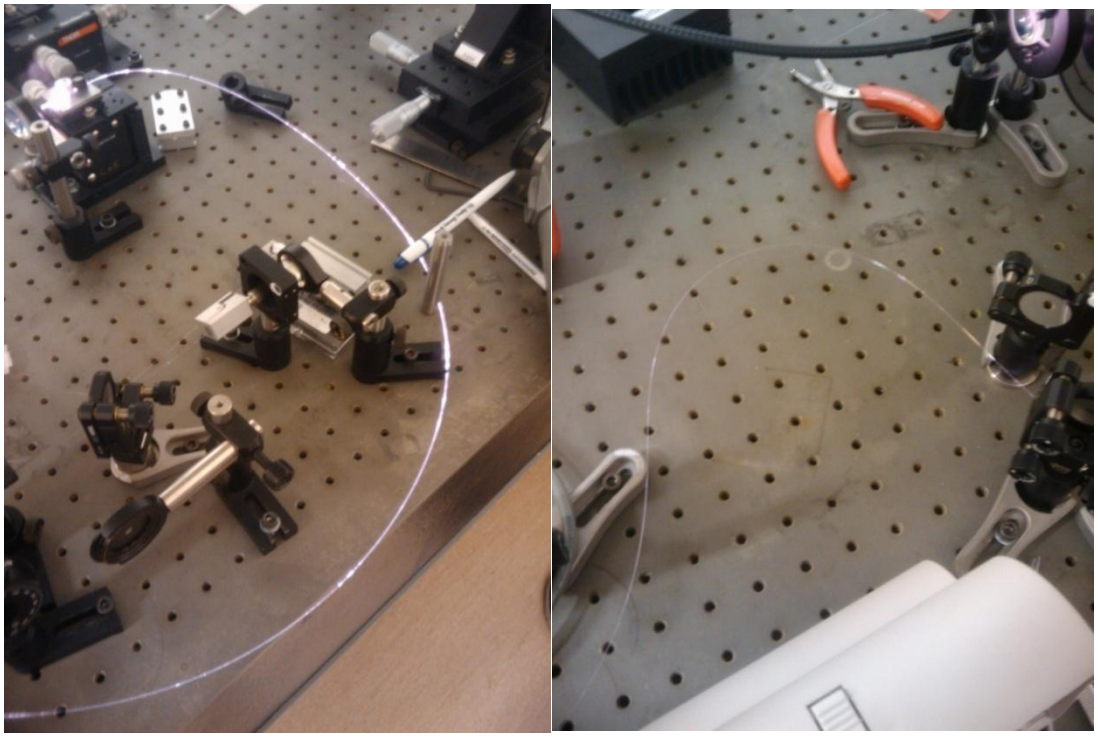

Figure 3.9. Photos of the Tm: ZBLAN fibre guiding 790 nm light in the cladding, highlighting the discrete scattering regions.

3.1.5.5 Summary

The core refractive index was measured to increase by 0.0004 (27% of the predicted value) with the addition of 2.2 mol% of PbF_2. The loss of the fibre was measured by a cut-back method with a result of 9.5 dB/m loss (at 790 nm), which is approximately an order of magnitude too high to consider operating this fibre as a laser especially on the low gain 2.3 μm transition. The higher loss is due to the tiny holes at the interface between the core and cladding region in the fibre (Figure 3.9). To reduce the loss of the fibre the outer and inner surface of the tube should be etched prior to fibre drawing to achieve a pristine surface [97]. A defect free interface between the core and cladding glass is prerequisite to achieve low fibre loss. Therefore future work will focus on further reducing the fibre loss through optimization of fibre drawing conditions and demonstration of lasing at 2.3 μm.

3.2 Development of Er:Yb Fibre Laser at 1570 nm

3.2.1 Introduction and Aim

Fibre lasers operating in the wavelength range of 1.5-1.6 μm have several advantages, such as eye safe nature, good atmospheric transmission and low fibre loss. Such an advantage of ~1.6 μm wavelength makes fibre laser of great importance in many scientific and engineering applications. For example, free space communication, range finding as well as light imaging detection and ranging (LIDAR) [96]. Cladding pumped Er:Yb fibre lasers offer the prospect of high output power at 1.5 μm to 1.6 μm with a high beam quality. Moreover, Er:Yb fibre lasers provide an attractive feature of wavelength flexibility. Cladding pumped erbium fibre lasers have been demonstrated at multi-Watt levels covering the wavelength range of 1.53- 1.62 μm [68]. So the combination of wavelength flexibility, good beam quality, as well as high efficieny makes erbium fibre laser excellent pump source for bulk erbium lasers and thulium fibre lasers. Er:Yb co-doped fibres depend on indirect pumping of the lasing erbium ions through nonradiative energy transfer from Yb ions [70, 71]. This Yb co-doping improves the pump absorption, which is essential to scale the output power through cladding pumping.

Therefore, Er:Yb co-doped fibre has been used in this experiment. The aim of this experiment is to develop watt level output of a 1570 nm source with good beam quality, which will be used as an in-band pump source to develop 2 μm Tm:ZBLAN fibre laser.

3.2.2 Er:Yb Absorption Calculation at 980 nm

It has already mentioned in Chapter 1, section 1.14, that the Er:Yb absorption is more favourable at 975~9080 nm band than 915 nm (see Figure 1.18 in Chapter 1). The SM-EYDF-6/125-HE double clad fibre is supplied by NUFERN. The minimum peak cladding absorption at 915 nm is 0.6 B/m and maximum one is 0.9 dB/m, of this Er:Yb co-doped fibre. However we need to measure the cladding absorption of Er:Yb fibre at 980 nm. As the NUFERN data sheet did not provide any absorption at 980 nm therefore, by using Er:Yb absorption spectra, absorption can be calculated at 980 nm.

From Er:Yb absorption graph (Figure 1.18 in chapter 1) the cladding absorption at 915 nm was calculated to be 1.47dB/m and at 980 nm it is 7dB/m. Therefore the ratio between this two absorption is 7/1.47=4.8. Using this factor the minimum cladding absorption at 980 nm of Er:Yb co-doped fibre becomes 0.6*4.8=2.9 dB/m and maximum is 0.9*4.8= 4.3 dB/m.

Figure 3.10 describes the absorption as a function of fibre length for 4m Er:Yb fibre. It has observed from above graph that the minimum absorption of Er:Yb for 4m is 93.14% and maximum 98.12%.

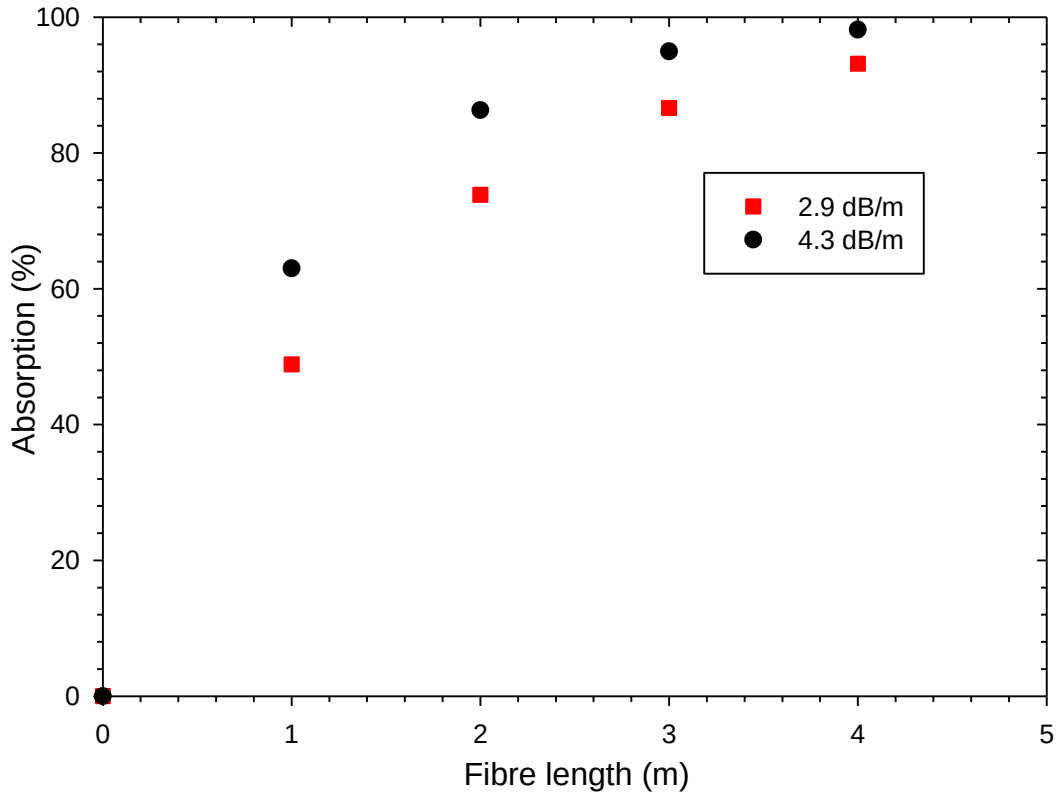

Figure 3.10. Er:Yb absorption calculation for 980 nm pumping.

3.2.3 Fibre Bragg Grating (FBG) Transmission Measurement

Before going to develop 1.57 µm Er:Yb fibre laser source, FBG reflectivity has been verified interms of transmission measurements as follows. Experimental setup to measure the transmission of FBG is shown in figure 3.11. A FBG supplied by TeraXion, Canada was inscribed into the core of passive Germanium doped fibre (GDF) fibre. A supercontinuum white light source has been used to measure the

reflectivity of a FBG. After stripping both ends of the passive fibre, it has been properly cleaned using methanol and been cleaved using YORK cleaver.

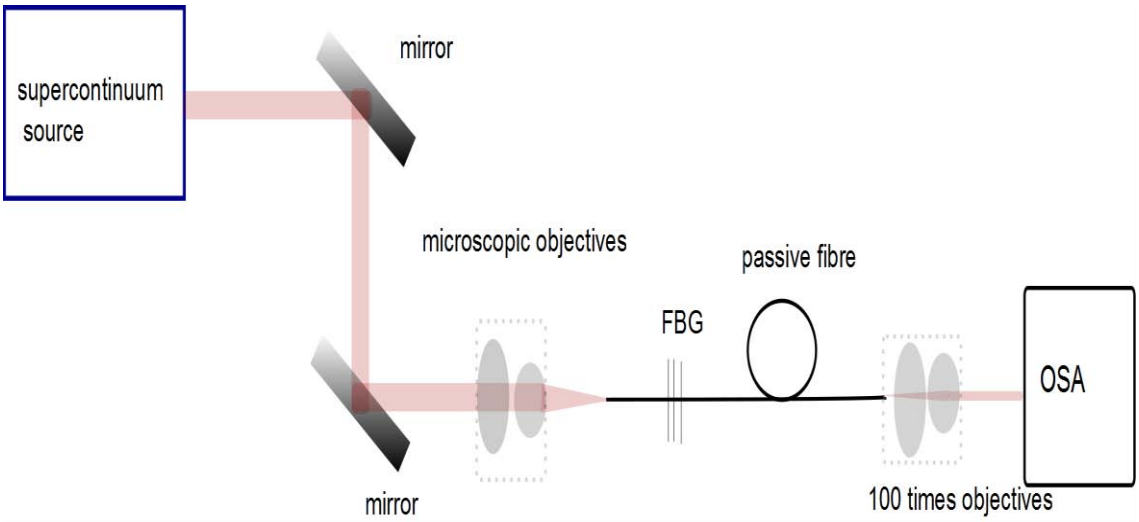

Figure 3.11. FBG transmission measurement set up.

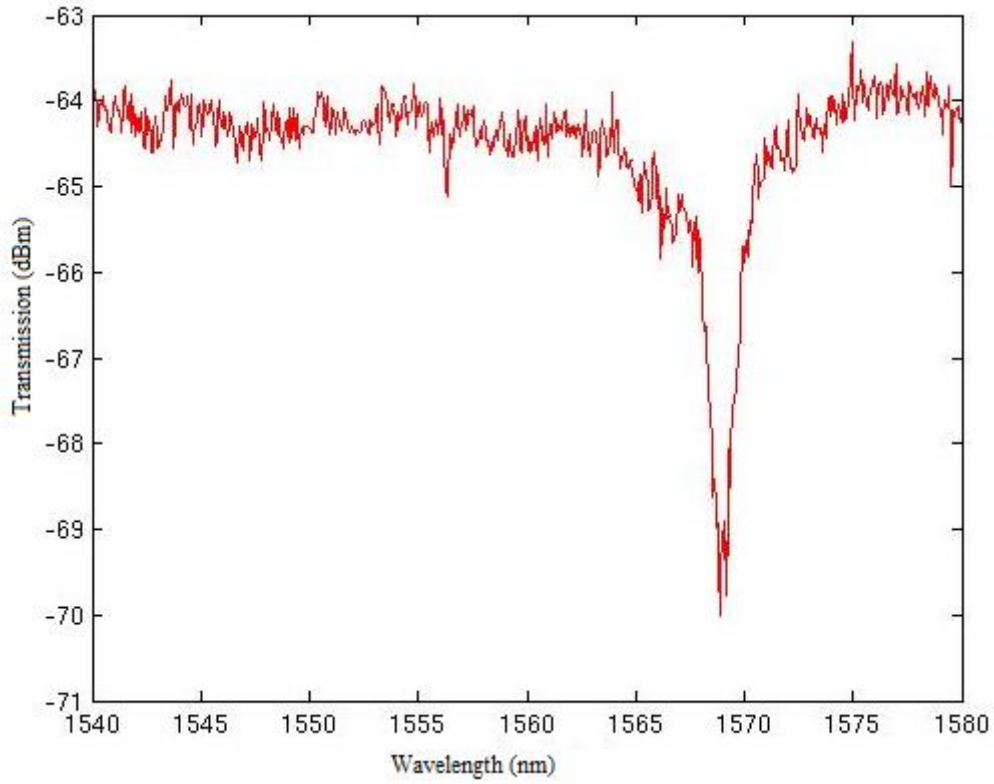

Figure 3.12. A FBG transmission spectrum measured using supercontinuum source

After cleaving the image from the fibre ends was observed using Ericsson splicer. The cleaved ends of the fibre were placed on the V-groove of nanosatges. The white light was coupled to the fibre using microscope objectives and optimised light to the core of a passive fibre. The collimated output was expanded using a 100xs objective. Cladding light was suppressed by using Carbon DAG on both ends. Moreover, an aperture was used to filter the cladding mode and observe the transmission of the FBG using an Optical Spectrum Analyser (OSA) but no transmission appeared. Then paint stripper was put in 20 cm away from the rear ends of the fibre to strip the coating. After stripping, high refractive index paint (absorptive surface coating) was applied on the exposed fibre to totally suppress the cladding mode.

After ensuring that the light was guided in the core an IR camera was placed at the output to optimise the light to the core. The output signal is injected to the OSA to measure the transmission. The output spectrum of passive fibre is shown in Figure 3.12. It has been confirmed from the transmission measurement graph that the reflectivity of FBG is around 1570 nm.

3.2.4 Experimental Setup to Develop 1.57 µm Fibre Laser

Figure 3.13 below gives the experimental set up for the development of 1.57µm Er:Yb fibre laser. Using absorption 4.3dB/m, it has been observed from Figure 3.10, that the maximum absorption at 980 nm is 98.13% for 4 m fibre. Therefore a 4 m long fibre has chosen for the experiment. The ER:Yb double clad fiber supplied by NUFERN having inner clad diameter 125 µm with NA 0.46, and the core diameter 6 µm with NA 0.18. Therefore the V number of Er:Yb fibre is 2.43. Also a passive FUD-3236 1550-GDF fibre has been used in this experiment. A FBG having reflectivity >99% at 1570 nm inscribed to the core of a passive GDF fibre (TERAXION supplied the FBG). The core NA of the passive fibre is 0.12 and mode field diameter (MFD) 11.2 µm and the inner clad diameter 126 µm with NA 0.46. The V number of the passive fibre is 2.7.

After removing the coating from passive GDF end and active Er:Yb fibre it was properly cleaned using methanol. Then the fibre ends were cleaved using YORK cleaver. Thereafter, the passive GDF fibre end and active Er:Yb fibre end were placed on the Ericsson splicer and the cleaving end was observed. The left view angle 0.06, right view angle -0.17 as well as left gap angle 0.27 and right gap angle 0.29 noted.

Therefore, by pressing the fusion button fibre becomes spliced and the splicing loss was observed 0.02 dB in Ericsson splicer. After splicing the passive end with active Er:Yb fibre, the GDF fibre end cleaved at an angle 5.4 degree to avoid the end Fresnel reflection. The cleaved fibre end then placed on v-groove of a nano stage.

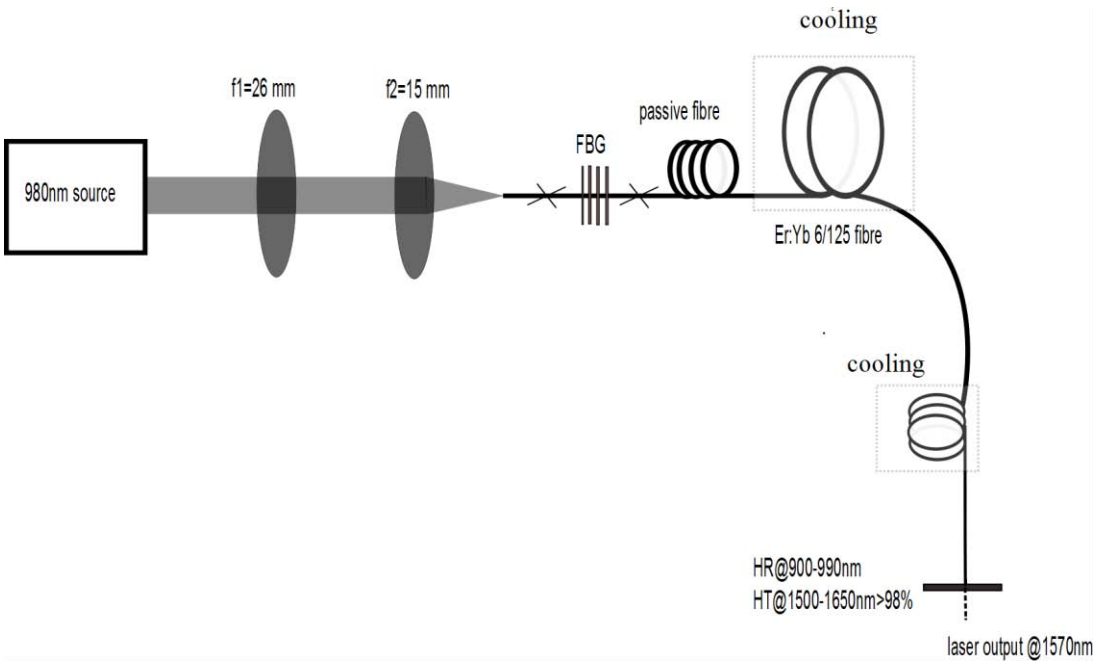

Figure 3.13. Experimental setup for the development of 1570 nm Er:Yb fibre laser.

It is noted that 980 nm 15 W diode has been characterised before started the experiment (see appendix section). A 980 nm light is coupled to the passive GDF fibre using f=26 mm and f=15 mm focal length lenses for collimating and focusing. A FBG which has reflectivity 99.88% acts as an input coupler. The resonator cavity was formed using a high reflective FBG input coupler along with a ~4% Fresnel reflection of rear ends of the fibre. A pump mirror which has HR (900-990 nm) >99.9% and HT (1500-1650 nm) >98% butted to the rear side of the fibre to separate the lasing signal from pump laser wavelength. A cooling fan used to cool the fibre to avoid the thermal damage.

3.2.5 Results and Discussions

Initially fibre laser output was not demonstrated at 1570 nm. Therefore we discuss the procedure required to develop 1570 nm laser. The experiment was conducted in a different way to get 1570 nm output using FBG as a high reflective input coupler.

Firstly, a FBG was spliced with 3 m Er:Yb codoped fibre and then recoated at the splicing region. After recoating the splicing region, it was placed on a microscope slide very carefully and kept for few hours. The Er:Yb fibre wrapped in a 10 cm diameter aluminium cylinder. Both ends of fibre were placed on V-groove of nano stages and light was coupled to the fibre through collimating and focusing lens. The output end of the fibre was butted to the mirror which has HR at 900-990 nm and HT at 1500-1650 nm. Output signal was analysed using a monochromator and the peak wavelength showed at 1545 nm (Figure 3.14). So it was supposed that splicing might be an issue, and re-spliced the FBG but left uncoated and followed the same procedure as stated earlier, but the output signal remain unchanged.

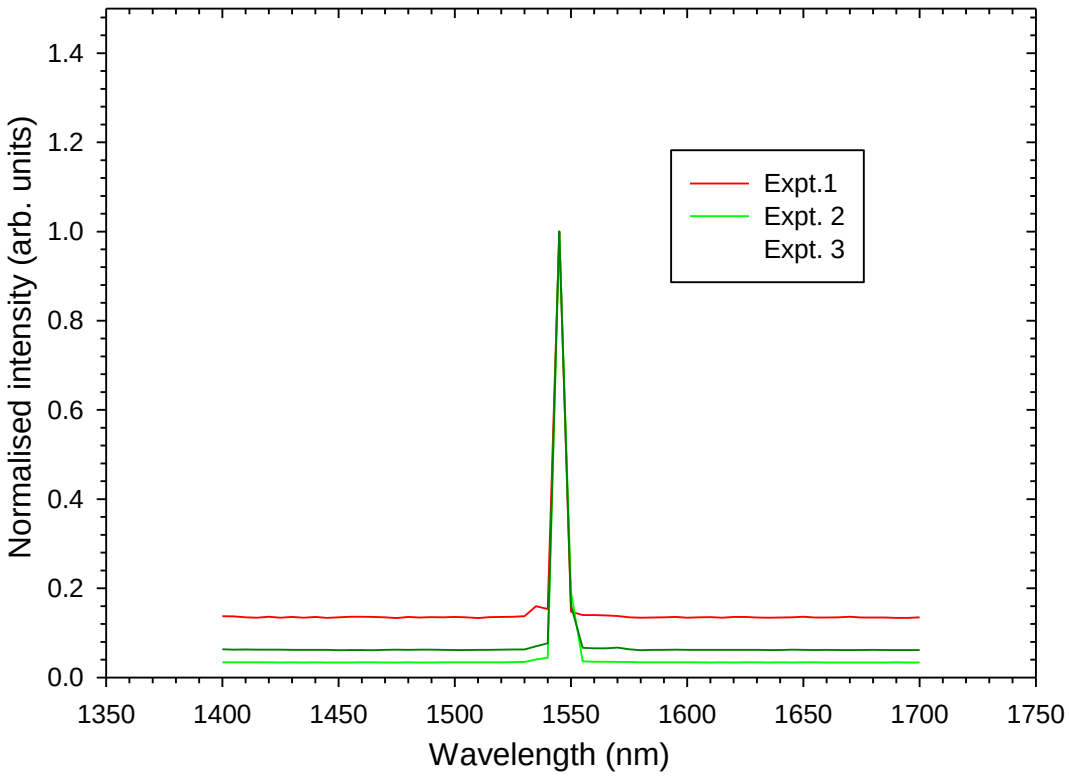

Figure 3.14. Output spectra at 1545 nm.

Therefore, to verify the accuracy of measurement of a monochromator it was calibrated for 2nd order wavelength using HeNe source but the calibration of monochromator was alright.

Thereafter, fibre was spliced again and we kept the grating straight and also kept the splicing part on microscope slide and got same results i.e. peak at 1545 nm. Then, again spliced FBG and kept on microscope slide in such a way so that the splicing region left untouchable. Here longer length (4 m) of Er:Yb fibre used to test whether the wavelength shift or not but the result remains unchanged as shown in figure 3.14. As the FBG is not working properly therefore it has been anticipated that it is necessary to measure reflectivity of FBG. The measured reflectivity in terms of transmission of FBG showed in Figure 3.12. It is noted that the transmission experiment were performed to verify the reflectivity of FBG is at 1570 nm and discussed detailed in section 3.2.3.

After confirmation of FBG reflection spectra at 1570 nm, AR coating of input coupler lenses was checked using OSA. Therefore, 980 nm source was realigned properly. In order to suppress the Fresnel reflection the input end of passive fibre was angle cleaved using YORK cleaver and the angle was 5.5degree. The light was therefore coupled to fibre and observed the output spectrum using monochromator. The output shows the same as at 1545 nm. It was observed then that the mode of passive GDF fibre and active Er:Yb fibre is mismatched. The mode field diameter of passive fibre is 11.2 μm while the mode field diameter of active fibre is 6μm. The calculated V number of passive fibre is 2.7 and active fibre is 2.43. To suppress the higher order modes the FBG kept straight and about 20 cm GDF passive fibre wrapped on 1 inch chuck and the output signal checked using monochromators and it observed that the output is at 1545 nm (Figure 3.14).

The next step was wrapping the active Er:Yb fibre also in 1 inch chucks around 20 cm in order strip the higher order modes. The output signal observed at the monochromators and the spectrum found at 1570 nm as given in Figure 3.15 (length of the fibre was 3.85 m). Therefore, output was recorded using power metre. It is noted that initially active Er:Yb fibre was not cooled. It has been observed that the slope efficiency with respect to the pump power is 17.2% Figure 3.16 (a). The slope efficiency increased much higher when the cooling fan is used to cool the fibre (Figure 3.16 (b). The maximum efficiency of the fibre with respect to the pump power is 28.2%. Efficiency could be improved further, if the fibre was not miss mode matched.

Due to the mode mismatched a significant amount of light lost because of stripping the higher order modes.

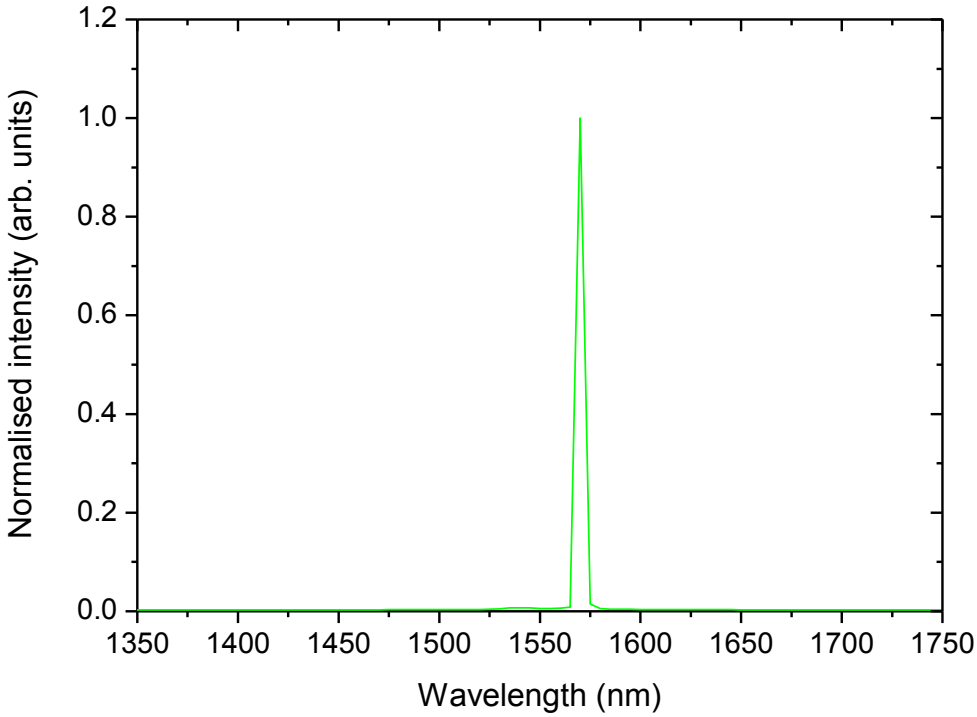

Figure 3.15. The output spectrum of a Er:Yb fibre laser at 1570 nm.

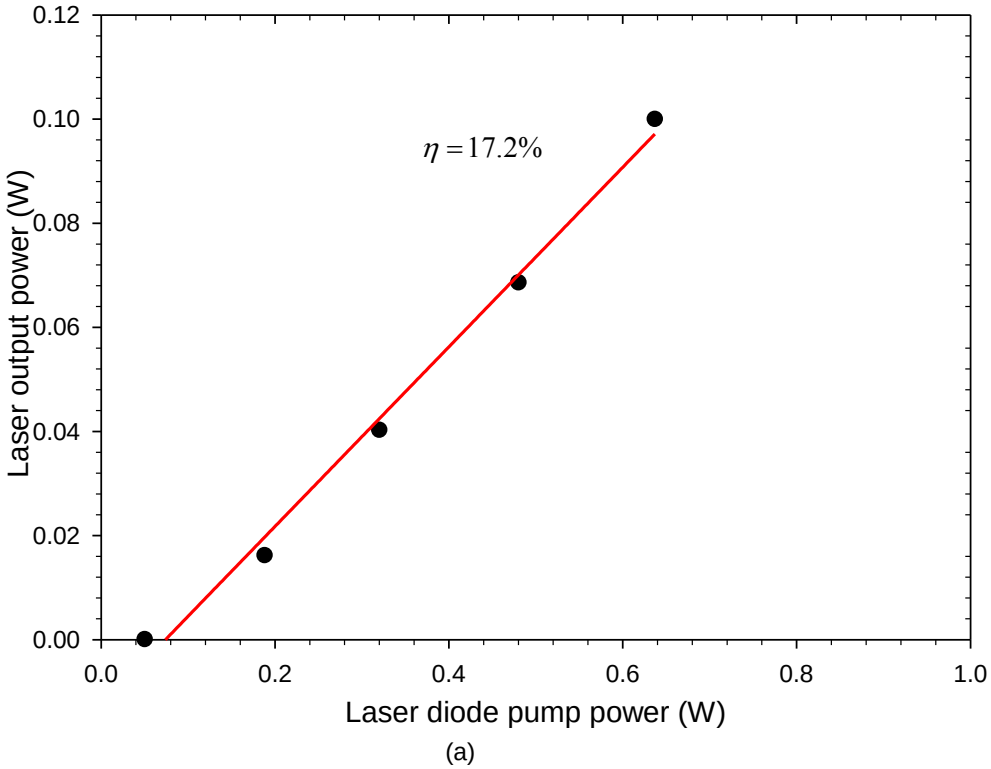

(a)

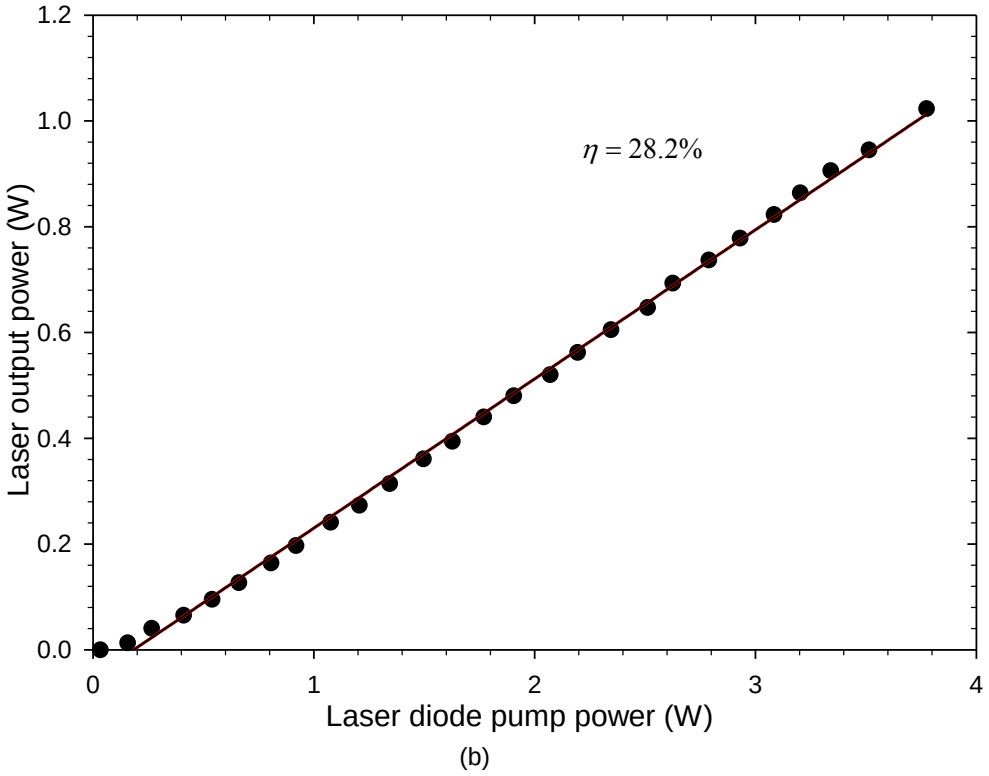

Figure 3.16. Laser output at 1570 nm for Er:Yb double clad fibre (a) without cooling (b) with cooling

3.2.6 Beam Quality Measurement

Measurement and analysis of laser beam characteristics is essential for laser based application such as welding, cutting, cleaning etc. Generally beam characterisation involves measurement of the beam spatial energy density distribution, which is referred to as the beam profile. Beam profile analysis provides an insight of the beam spatial characteristics such as size, shape, position, propagation mode structure properties and beam quality (M^2). The parameter M^2 can be calculated using the following equation [97].

$$M^2 = {}^{\pi \mathcal{W}_0 \theta_o}/_{\lambda} \qquad (3.3)$$

where, $\mathcal{W}_0$ is the beam waist or spot size and θ_0 is the cone half angle as shown in Figure 3.17 (a). It is noted that for M^2 =1 the beam becomes perfect Gaussian beam. The higher M^2 value causes the poor beam quality, as in this respect the beam

propagates far from Gaussian shape. Therefore a beam quality gives a description of how well the light beam is focussed.

An experimental setup for M^2 measurements is shown in Figure 3.17 (b). After collimating the light it has been focused using a longer focal length i.e. 100 mm focal length lens, to avoid overfilling CCD camera. A neutral density filter used in between collimating and focusing lens, and on camera head to suppress the power shown in Figure 3.17 (b). First the location of focusing position ensured by moving the position of camera around the actual focusing position. After locating the waist position a ruler has placed horizontally to measure the distance for every measurement.

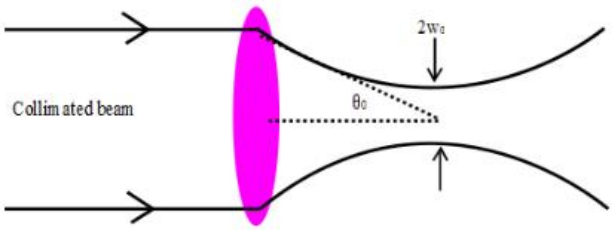

(a)

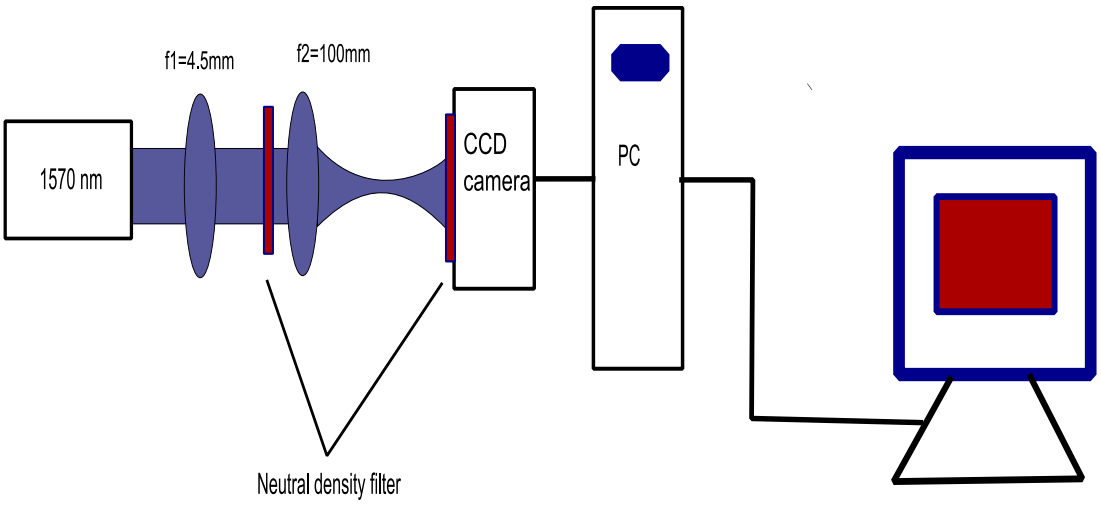

(b)

Figure 3.17. (a) Concept of M^2 used to characterise laser beam quality (b) Experimental set up for beam quality measurement.

Therefore, the CCD camera has moved horizontally 5 mm at every step and recorded the data for Gaussian beam diameter for x direction as well as y direction. The

Gaussian beam width has recorded for every 5mm distance. The data has recorded until beam width is reached to minimum and further moved way to cross Rayleigh range. With the help of beam diameter versus distance a graph fitted by LabVIEW software to measure the beam quality. It is observed from Figure 3.18 that the estimated beam quality of a Gaussian beam along the x direction and y direction is 1.29 and 1.24.

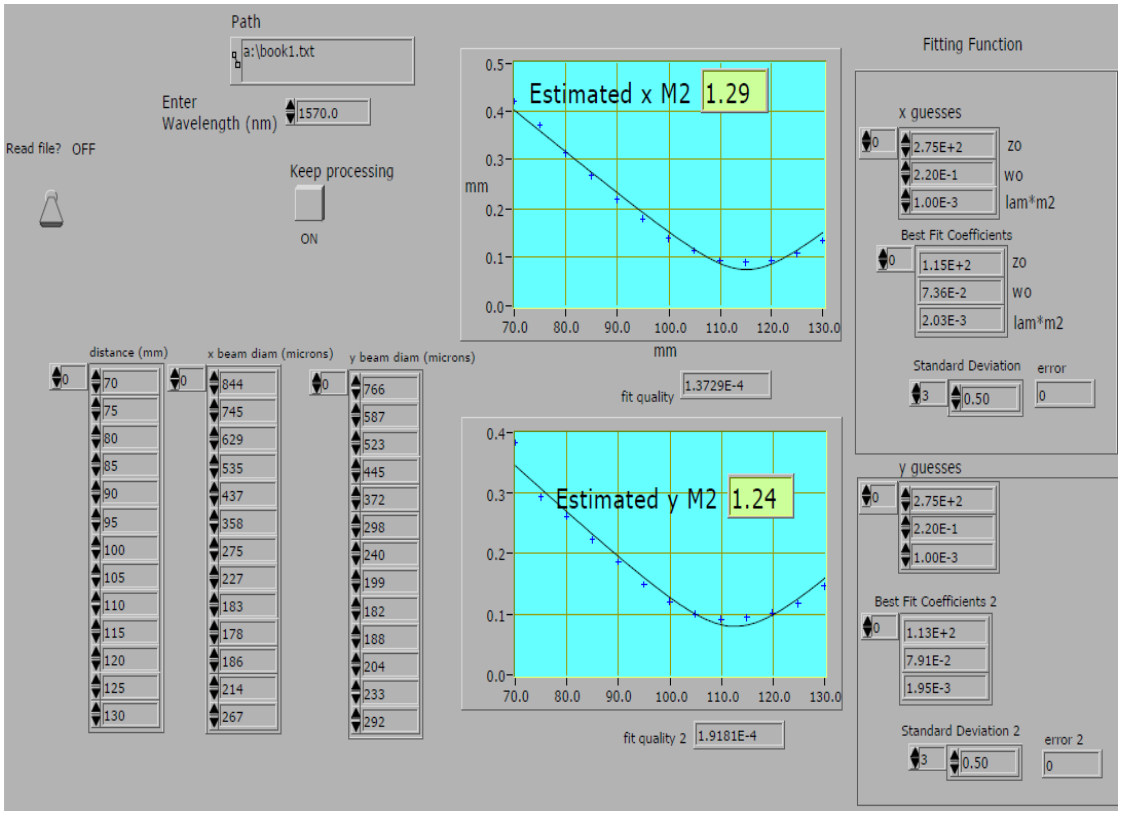

Figure 3.18. Beam quality of 1570 nm output.

3.2.7 Summary

A 1570 nm source has been demonstrated using a 99.8% reflectivity FBG as an input coupler and a 4% Fresnel reflection as an output coupler. The demonstrated output was 1W with slope efficiency 28.2% with respect to pump power. The slope efficiency was improved by air cooling the fibre. The beam quality of 1570 nm output is 1.3. The good beam quality is an essential factor to couple the pump light into the core of a double clad fibre. Initially the output was observed at 1545 nm due to the fact that the maximum gain of Er:Yb fibre at 1550 nm as well as mode mismatched between passive fibre and active Er:Yb co-doped fibre. However, this issue has been tackled through

higher order mode filtering by wrapping the fibre in a 1 inch chuck. The output power can go further, but to avoid the thermal damage of splicing the output is kept at 1 W. Moreover, the slope efficiency could be improved if the passive fibre was mode matched. Because of mode mismatching a significant amount of light lost because of stripping the higher order modes.

3.3 Development of 2 µm Tm:ZBLAN Fibre Laser Using 1.57 µm In-band Pumping

3.3.1 Introduction

In band pumping is to pump the laser light directly into the emitting laser level. Thulium doped fibre laser development at 2 µm using in-band pump source at ~1.6 µm offers advantages of high Stokes‟ limits up to 84%. The lower phonon energy and lower background losses of Tm:ZBLAN leads to the lower lasing threshold at ~2 µm. Moreover, a higher total internal conversion efficiency and higher slope efficiency of Tm:ZBALN fibre are the consequences of the above mentioned advantages. Taking the advantages of Tm:ZBLAN fibre as well as in-band pumping is a great opportunity to develop an efficient Tm:ZBLAN fibre laser using 1570 nm pump source.

A 415 W single mode CW Tm:Silica fibre laser at ~2 µm have reported with a slope efficiency of 60% using an in-band pump source at 1.567 µm [2]. A multimode 2 µm Tm-Silica fibre laser has also been reported with slope efficiency 42% using a 1.61 in-band pump source [67]. Thulium fluoride fibre laser at around 2 µm have also been reported by using a colour centre laser at 1.57 µm [41], 1.58 µm [4] as well as 1.63 µm [42]. The maximum slop efficiency of these fibre lasers is 84%, but the output is limited to only 53 mW. This limitation was might be the unavailability of pump source at around 1.6 µm with sufficient power and good beam quality. But nowadays it is possible to develop around 1.6 µm source with very good beam quality and sufficient output power, to make a Tm:ZBLAN fibre laser at around 2 µm efficiently.

Therefore, in-band pumping approach has been used towards the development of ~2 µm Tm:ZBLAN fibre laser. The aim is to demonstrate the efficient operation of around 2 µm laser using in-band 1570 nm pumping.

3.3.2 Absorption Calculation at 1570 nm

In order to develop a 2 µm laser pump using a 1570 nm source, first the absorption is calculated at 1570 nm from absorption spectra of a Tm doped ZBLAN glass, chapter 1 Fig. 1.11. As the graph was given absorption (cm^{-1}) as a function wavelength, so the

absorption (cm-^{1}) at 1570 nm was calculated by deducing the value from base line to 1570 nm. Therefore, the absorption coefficient at 1570 nm becomes 0.03 cm^{-1} and the corresponding absorption is 0.13 dB/cm. It is noted that the absorption is calculated at 1570 nm using Beer Lamberts law $I=I_0 \exp(-\alpha x)$. Where, $I_{0\ is}$ initial intensity, α is the absorption coefficient and x is distance. Figure 3.19 plotted the calculated absorption as a function of fibre length.

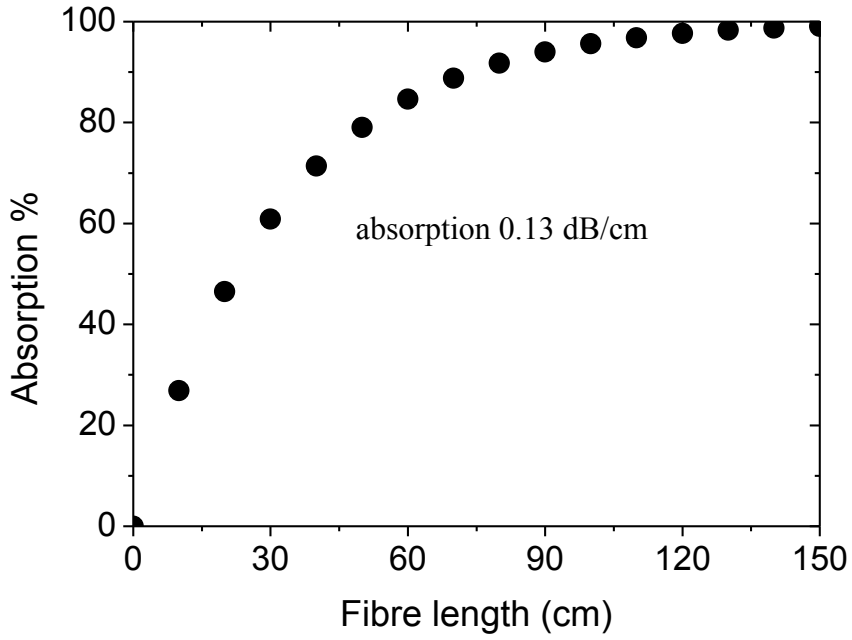

Figure 3.19. Absorption calculation of Tm:ZBLAN at 1570 nm

3.3.3 Experimental Setup

Experimental diagram of In-band pumping Tm:ZBLAN fibre laser development shown in Figure 3.20. Following the development of in-band 1570 nm source, it is then used as a pump source for this experiment. The laser output is delivered through a 6 μm core having NA 0.18. Initially 1570 nm light is collimated and focused using 18.4 mm and 15.29 mm aspheric lenses to coupled the light to the core of a Tm:ZBLAN fibre . As the light was not coupled to the core therefore 4.5 and 4.51 mm aspheric lenses used to collimate and focus the light to the core of a Tm:ZBLAN fibre. Tm:ZBLAN fibre

supplied by FiberLabs, Japan having the core diameter 8 µm with NA 0.15, and the cladding diameter 125 µm with NA 0.48 have been used to perform the experiment. The length of fibre 30cm chosen and the absorption at 1570 nm is 60.84% as evident from figure 3.19.

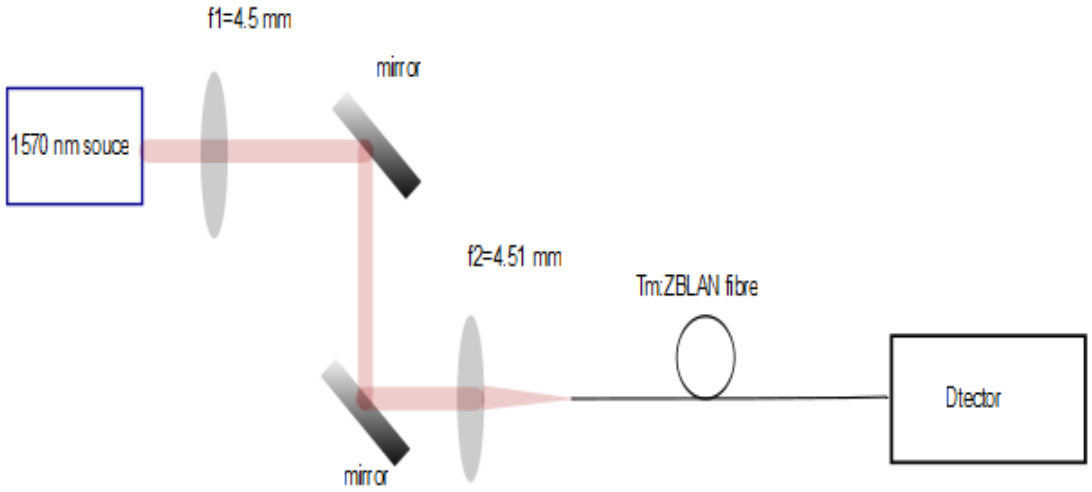

Figure 3.20. Experimental setup towards the development of 2 µm laser using 1570 nm pump source.

3.3.4 Discussion

A 1570 nm source developed in house with a beam quality (M^2) 1.3. The beam quality is important parameter for tightly focusing; specifically it is important for core pumping method. The 1570 nm output coming out from Er:Yb 6 µm core have been collimated and focused and we tried to couple the light into the 8 µm core of Tm:ZBLAN double clad fibre. Initially it has been observed that the light is not guided in the core. Then it was checked alignment of collimated beam and refocused, but light was not coupled to the core. It is noted that the Er:Yb output offers very good beam quality, which is suitable for core pumping and consequently shorter length of fibre needed for fibre laser experiment. Therefore, we chose core pumping approach although the fibre is double clad. The diameter of the collimated beam is also measured and found the value is 6.11 µm, which is comparable to 6 µm core of 1570 nm light. After measuring the collimated beam spot size, therefore the next step was to measure the beam spot size of the focusing beam using knife edge method as follows.

3.3.4.1 Knife-edge Spot Size Measurements

A knife edge technique is a technique to measure the spot size through slicing the beam and recording the corresponding transmitted power. Figure 3.21 describes the schematic diagram for knife measurement.

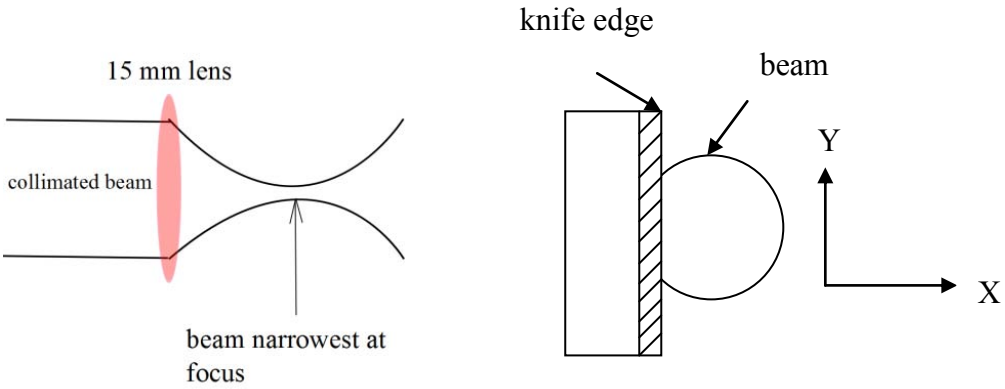

Figure 3.21. Schematic diagram for knife edge measurement

Initially, power of a collimated beam was recorded using power metre which was 108 mW and a 15.29 mm focal length lens was placed in front of collimating light to focus the light. A sharp knife was set on the translational stage. Therefore, the knife edge is moved toward the focal point, and the focal point was ascertained. After locating the focal point the knife edge was placed close to the focal point. At this point the beam cut into micron distance along the x direction as shown in figure 3.21 and power is measured. This procedure is repeated from just above 90% transmitted power to below 10% transmitted power of the beam. The translation stage is moved 100 micron distance along the direction of the beam around the focal point and the above mentioned procedure is repeated until the minimum spot found. After recorded the data the graph is plotted as a function of power versus distance as shown in Figure 3.22 (a), (b), (c), (d). The difference between 90% and 10% power gives the measure of spot size. It is noted that the knife edge measurement of output power plotted in graph 3.22 is ranging from just above 90% to below 10%. Figure 3.22 (a), (b), (c) and (d) plotted power as a function distance of knife edge technique. While Figure 3.22 (e) represents the spot size as a function of distance.

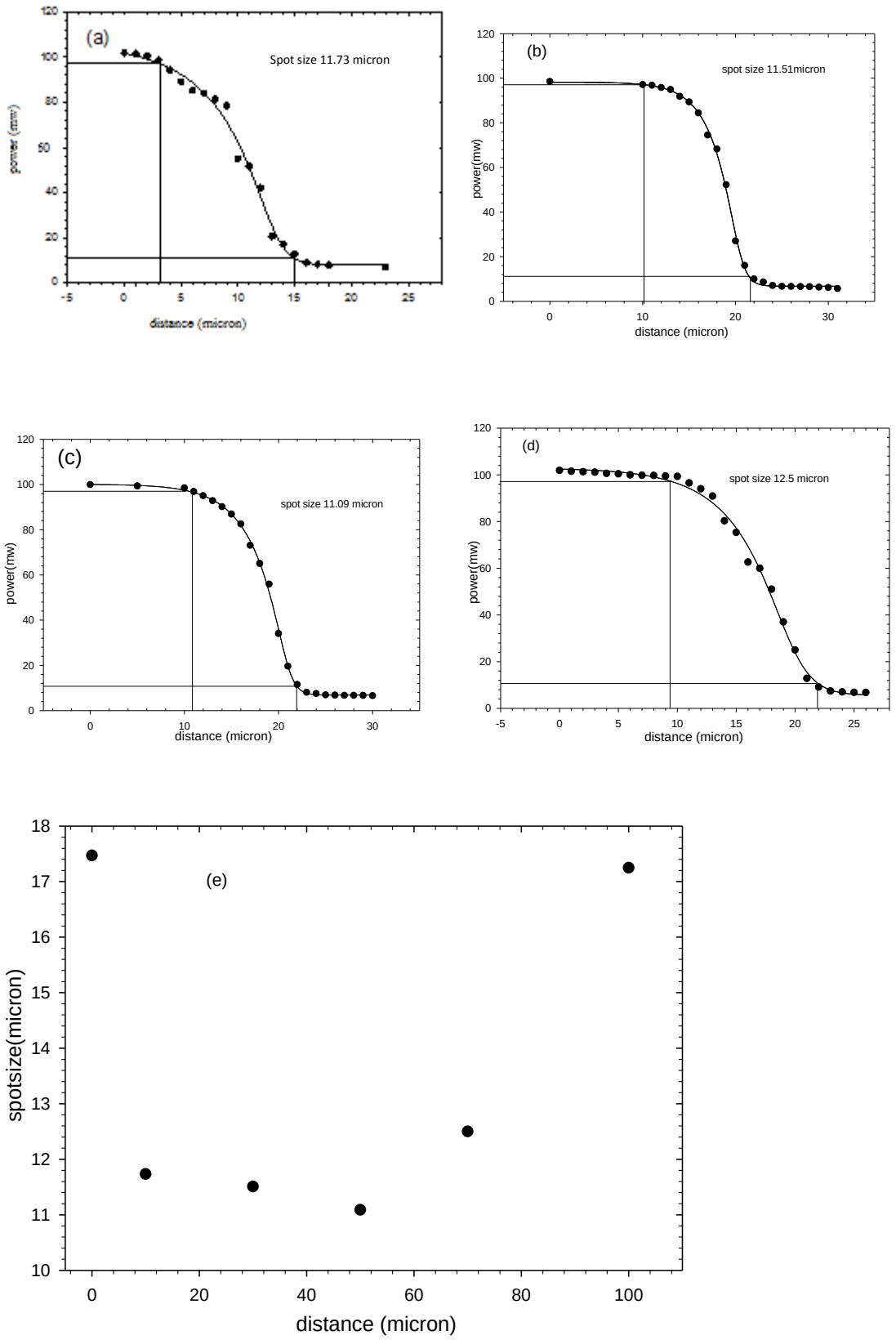

Figure 3.22. Spot size measurement performed using knife edge technique.

A minimum spot size found from the graph is 11.09 μm. This due to the fact that the overfilling the collimated beam when it was passed through the lens as evident in table 3.2. The table below provides the relative picture of beam diameter for different lenses used to collimate and focus 1570 nm light. The diameter of a beam is calculated using the relation, Beam diameter=2*E.F.L*NA, where, E.F.L is the effective focal length of a lens and NA is the numerical aperture of the source

Table 3.2. Calculation of beam diameter of a beam coming out from 6 μm core having NA 0.18 of Er:Yb fibre

Focal length (mm)	NA of lens	Acceptance angle(deg)	Diametre of a lens(mm)	Beam diameter(mm)
4.50	0.42	24.83	3.70	1.62
4.51	0.54	32.68	4.95	1.62
15.29	0.16	18.41	5.0	5.50
18.4	0.15	17.25	5.5	6.62

It is clear from above calculation that the beam is overfilling for longer focal length lens. Therefore the next step was to use shorter aspherics to collimate and focus the light into the core and to measure the core absorption using cut-back method. It is noted that due to the shortage of time knife edge spot size measurement for shorter aspherics did not performed.

3.3.4.2 Cut-back Measurement and Discussion

For cut-back measurement a 1570 nm output has been used as a pump source. A 4.51 mm and a 4.50 mm aspherics having NA 0.54 and 0.52 were used to collimate and focussed the light, so that light be guided into the core of a Tm:ZBLAN fibre.

A 56 cm fibre has chosen for cut-back measurement and 1570 nm light was coupled to the core of a Tm:ZBLAN fibre and optimised. When the light was optimised to the core of a Tm:ZBLAN fibre, it has been tried to remove the light from cladding using high refractive index paints (absorptive surface coating) in the fibre. However, it has been observed that the light was not removed from cladding. Thereby, it has been tried to remove the polymer coating from the middle of the fibre to use absorptive surface

coating in the uncoated region. However, as the Tm:ZBLAN fibre is very fragile, it was not possible to remove the coating from the middle of a fibre. Therefore, to measure the core absorption of pump light, initially output power was recorded when light was not coupled to the core. Then, light into the core has been ascertained through optimisation and by observing the fluorescence through IR viewer. After observing the light coupled into the core, it has been optimised and input end of the fibre kept unchanged. A power metre head was fixed in position and the transmitted output was recorded for every cut-back measurement.

As the transmitted output is composed of core and cladding light, therefore the core absorption for every cutback is considered here as the difference between the output power when pump light coupled only to the cladding and when coupled both to the core and cladding. Symbolically one can write core absorption = $P_{\text{inner cladding}} - P_{\text{core and inner cladding}}$. Where, $P_{\text{inner cladding}}$ is the output power for pump light passing through cladding and $P_{\text{core and inner cladding}}$ is the output power passing through both the core and inner cladding. There might be some contribution of cladding light absorption but that is very negligible for such a short piece of fibre in comparison to the core absorption.

Figure 3.23 shows cut-back core absorption measurement of Tm:ZBLAN double clad fibre. From Figure 3.23 the output extrapolated to zero length is 10log10(P)=17.68, i.e. 58.6 mW and the input power was 185 mW. Therefore, it is assumed that the coupling efficiency to the core of a fibre was estimated at 31.6%.

From cut-back measurement as shown in figure 3.23, it has been observed that the pump absorption at 1570 nm is 0.05 dB/cm, which shows some discrepancy with calculated absorption 0.13 dB/cm (from absorption spectra Figure 1.10) . Therefore the next step is to calculate the absorption cross section from cut back absorption and to compare with literature as follows.

Absorption cross section is calculated by using $\sigma = \alpha/N$, where $\alpha = 0.013$ cm^{-1} is the absorption coefficient (calculated from absorption 0.05 dB/cm), N is the ion density calculated using $N = \frac{M \times \delta \times NA}{MW \times \text{total batch weight}}$, where, M = 20000 ppm =20 gm/litre is the mass of dopants, δ = 4.33 g/cm^3 is the ZBLAN glass density, NA = 6.023×10^{23} is the Avogadro"s number, MW = 225.93 is the TmF_3 molecular weight and total batch weight is the weight for glass sample. Therefore, using the above parameters the absorption cross-section becomes 0.54×10^{-22} cm^2. While the calculated absorption

the absorption cross section 1.35×10^{-22} cm^2 [56]. It is observed that the measured absorption is 2.5 times less than calculated value from literature.

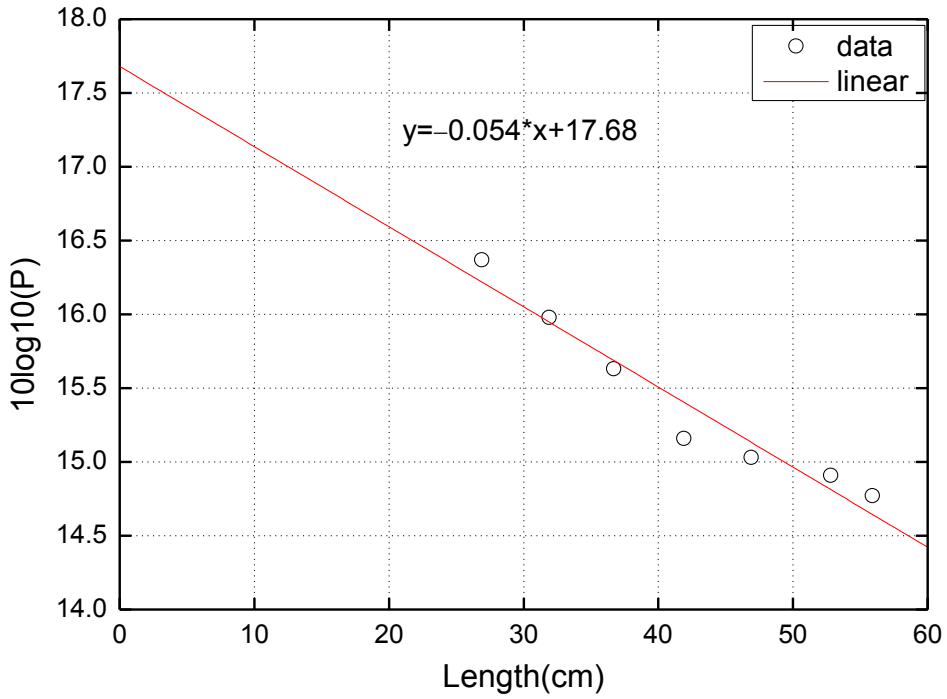

Figure 3.23. Core absorption measurement of a Tm:ZBLAN double clad fibre using cut-back method.

Moreover, pump absorption at 1570 nm of Tm:ZBLAN fibre having 8 µm core and 125 µm inner cladding has been calculated from data sheet supplied by FiberLabs, Japan as follows. It has found from data sheet that the absorption at 1570 nm is 0.19 dB/m and the core absorption becomes

$$\left(\pi r_{\text{innerclad}}^2 \ / \pi r_{\text{core}}^2\right) * 0.19\text{dB/m} = (125^2/8^2) * \frac{0.19\text{dB}}{\text{m}} = 46.3\text{dB/m}$$

As a result core absorption at 1570 nm is 46.3 dB/m and the corresponding absorption coefficient is 0.1 cm^{-1}. Considering this calculated absorption values, 95% of pump light should absorb to the core of a 30 cm fibre.

Therefore for accurate measurement of cut-back absorption shorter fibre length should be used, as according to Tm:ZBLAN fibre data sheet, most of the pump light should absorb at around 30 cm fibre length. Therefore, two things are essential to perform meaningful operation of fibre laser at 2 µm using 1570 nm pumping. Firstly, careful adjustment is required to couple the pump light to the core. Secondly to measure the

core absorption efforts are needed to remove the coating from the body of the fibre. Once getting accurate picture of core absorption and careful adjustment of optical elements to couple the light into core it would be possible to develop fibre laser at 2 μm using 1570 nm pumping. Therefore development of 2 μm laser using core pumping method is a subject of future work.

3.3.5 Summary

A 2 μm Tm:ZBLAN fbre laser was tried to develop using 1570 nm in-band pumping approach. According to core pump absorption calculation of a Tm:ZBLAN fibre, it shows that the absorption is only 31.2% for 56 cm fibre. This measurement was the initiative to measure the pump absorption. However considerable effort is needed to remove the coating from the body of the fibre, in order to measure the pump absorption accurately. Initiatives were taken to remove the coating from the body of the fibre but due to the fragile nature of ZBLAN fibre as well as time limit of the thesis it was not possible to finish. Further research is needed to measure the pump absorption accurately. Also coupling efficiency of pump light to the core should be improved considerably for fibre laser operation. Once the appropriate measurement is finish it is possible to go for fibre laser development through the optimization of 1570 nm pump light to the core.

3.4 Conclusion

A 1.53 W Tm:ZBLAN fibre laser at around 2 μm have been developed and demonstrated using 790 nm pumping with a maximum slope efficiency of 45%. Er:Yb co-doped fibre laser at 1570 nm has also been developed with maximum efficiency 28.2% for an in-band pumping. The measured beam quality of 1570 nm was 1.3, which is suitable for core pumping. The core pumping is mainly due to relatively good beam quality offered by Er:Yb sources which allows the use of core pumped fibre configurations. Initiatives were also taken to develop a Tm:ZBLAN fibre laser at ~2 μm using 1.57 μm source in a core pumping method. However from cut back absorption measurement, it has been observed that the absorption efficiency only is 31.2%. The cut-back measured absorption cross section shows some discrepancy with

literature results. It is noticeable that in cut-back measurement it is not been possible to suppress the cladding light, due to some experimental difficulties as stated earlier. This experiment should be conducted in near future to demonstrate efficient operation of fibre laser at ~2 μm using in-band 1570 nm pump source.

Chapter 4

Conclusion and Future Work

The motivation of this thesis was to investigate the Tm:ZBLAN fibre laser of around 2 μm using 790 nm pumping, and 1570 nm in-band pumping. So this thesis is primarily focused on developing a 2 μm Tm:ZBLAN fibre laser, and Er:Yb fibre laser at 1.57μm for in-band pumping.

The lower phonon energy and lower background losses of Tm:ZBLAN leads to the lower lasing threshold at ~2 μm. Moreover, a higher total internal conversion efficiency and higher slope efficiency of Tm:ZBALN fibre are the consequences of low phonon energy and low loss of Tm:ZBLAN fibre. Taking the advantages of Tm:ZBLAN fibre and in-band pumping, it is a great opportunity to develop an efficient Tm:ZBLAN fibre laser at ~2 μm.

The need for Tm:ZBLAN fibre lasers was discussed, including 790 nm pumping as well as in-band pumping in Chapter 1. In in-band pumping laser, active ions are pumped directly to the upper laser level from the ground state resulting a very high Stokes efficiency of around 2 μm for Tm:ZBLAN and Tm:Silica fibre lasers. It is noted that, Tm:Silica fibre lasers at around 2 μm become a mature technology in terms of output power using 790 nm pumping as well as ~1.6 μm in-band pumping. While for Tm:ZBLAN fibre laser the maximum output at 2 μm is 20 W [3] using a 790 nm pumping, and it is only 53 mW [4] for in-band pumping. Therefore, Tm:ZBLAN fibre has potentiality for the development of around 2 μm laser, particularly through in-band pumping.

In this thesis, a 1960 nm Tm:ZBLAN fibre laser was demonstrated with 1.53 W output and maximum slope efficiency of 45%, which is comparable to the highest reported slope efficiency of 49% [3]. The output could be scaled further through proper thermal management. For the experiment, a 5.45 m fibre has been used, and demonstrated that for a laser of 1970 nm the absorption of 790 nm pump light to the fibre is 62%. Therefore, by placing a mirror which is HR at 790 nm at opposite end of the fibre, the residual unabsorbed pump power could be passed through the fibre. Thereby, the gain as well as efficiency can be improved.

Moreover, 1.57 μm Er:Yb fibre laser has been developed using high reflectivity FBG as an input coupler and 4% Fresnel reflection at rear end of the fibre as an output coupler. The Watt level output is measured with slope efficiency of 28.2%, with respect to the diode pump power. As beam quality is an important parameter, especially where tight focusing is necessary, therefore M^2 value is measured which is 1.3 for 1.57 μm laser. It is observed that slope efficiency was increased due to the cooling of the fibre. Slope efficiency of 1.57 μm laser could be improved further if there was no mode mismatch between passive GDF fibre and active Er:Yb co-doped fibre.

One of the main aims of this thesis was to develop 2μm Tm:ZBLAN fibre laser using 1570 nm pumping. As it is already showed that this source offers very good beam quality, it is possible to pump directly to the core of a Tm:ZBLAN fibre. The measured pump light coupling to the core is 31.6% and absorption is only 31.2% for 30 cm fibre. Therefore, to demonstrate an efficient fibre laser at 2 μm, the coupling efficiency of 1570 nm pump light is anticipated to improve. Therefore, this study will help further to develop 2 μm laser using in-band pumping.

As understanding the pump absorption behaviour is necessary for an appropriate design of a double clad fibre laser, pump absorption of a different shape of a double clad fibre has been analysed using MATLAB code. It is represented that the pump absorption increases by breaking the symmetry of a double clad fibre. Moreover, pump absorption can also be increased by offsetting the core. Therefore, pump absorption is favourable when the symmetry of a double clad fibre becomes broken. This is due to the fact that the skew rays never interact to the core of a circular fibre.

Due to the time limit of the thesis, only a development of ~1.9 μm Tm:ZBLAN fibre laser has been completed and a development of 2μm Tm:ZBLAN fibre laser using 1.57 μm pumping will be a subject of future work. A home-made Tm:ZBLAN double clad fibre is under preparation and will be used for the future development of fibre lasers at 2 μm and 2.3 μm.

In summary, this thesis has presented some significant research on different types fibre laser, in particular, Tm:ZBLAN, and revealed some interesting features of fibre lasers. It is anticipated that the outcome of this thesis will have some contributions in many potential applications in the areas of LIDAR, Sensing, Medicine, Defence industry and materials processing.

Appendix

A1. Model Verification

In order to implement the model in an accurate and correct way, firstly the literature results [92] have been reproduced using the same parameters as mentioned in the literature. A 10 m fibre was used in the simulation. The core NA of the fibre is 0.175 and an inner cladding NA 0.48. The diameter of the core is 20 µm surrounded by a circular inner cladding of 600 µm. The doping density is 20000 ppm by volume, container number is 1000 and the launched power is 90W [92]. To calculate the data points from graphs shown in literature, Engauge Digitizer 4.1, a digitize software has been used. After reading the data from literature, it was plotted to compare with the simulation results (see figure A1). Figure A1 shows the pump absorption as a function of fibre length. It is observed from Figure A1 (a), (b) that the pump absorption is increases for increasing the fibre length up to 4 m. Thereafter, increasing the fibre length for circular shape the pump absorption becomes saturated due to the non absorption of skew rays as in Figure A1 (a). It is evident from the graph that the results are comparable with the literature.

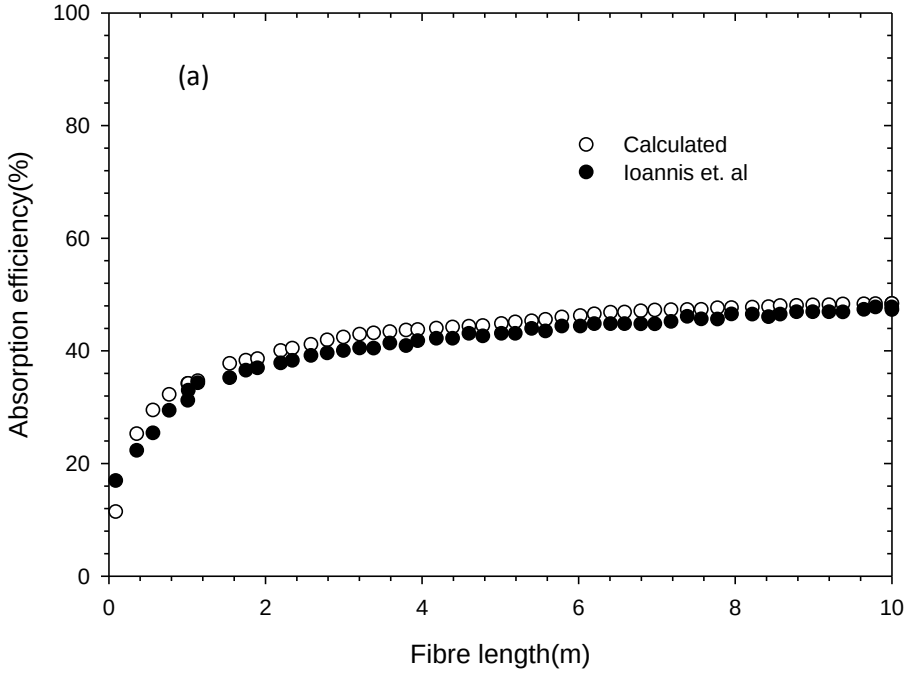

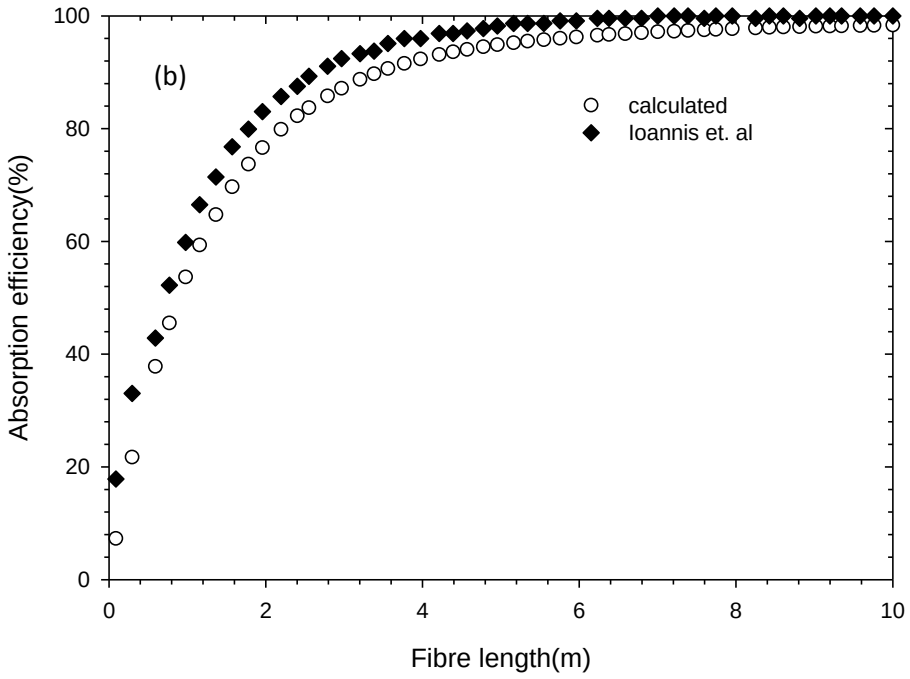

Figure A1. Comparison of absorption efficiency with literature for (a) circular and (b) square shape fibres having the 20 μm core and 600 μm inner cladding.

A2. LIMO Diode Characterisation

A diode characterisation is followed by cut-back experiment. Hence, in the following we discuss the diode characterisation. In diode characterisation, a 35 W 790 nm limo diode has been characterised as follows. First a 100 μm core diameter fibre patch connected to the diode has been placed on a nano stage and collimated using a plano convex lens having the focal length f_1=26.2 mm. After properly aligned and collimated, the light has been focused using plano convex lens with a focal length of f_2=20.0 mm. A Thorlabs power meter (model S314C) has been placed properly to collect and record the 790nm output. It has been observed in Figure A2 that the threshold values for diode power at around 9.8 amperes and the efficiency is 0.9 W/A of Limo diode.

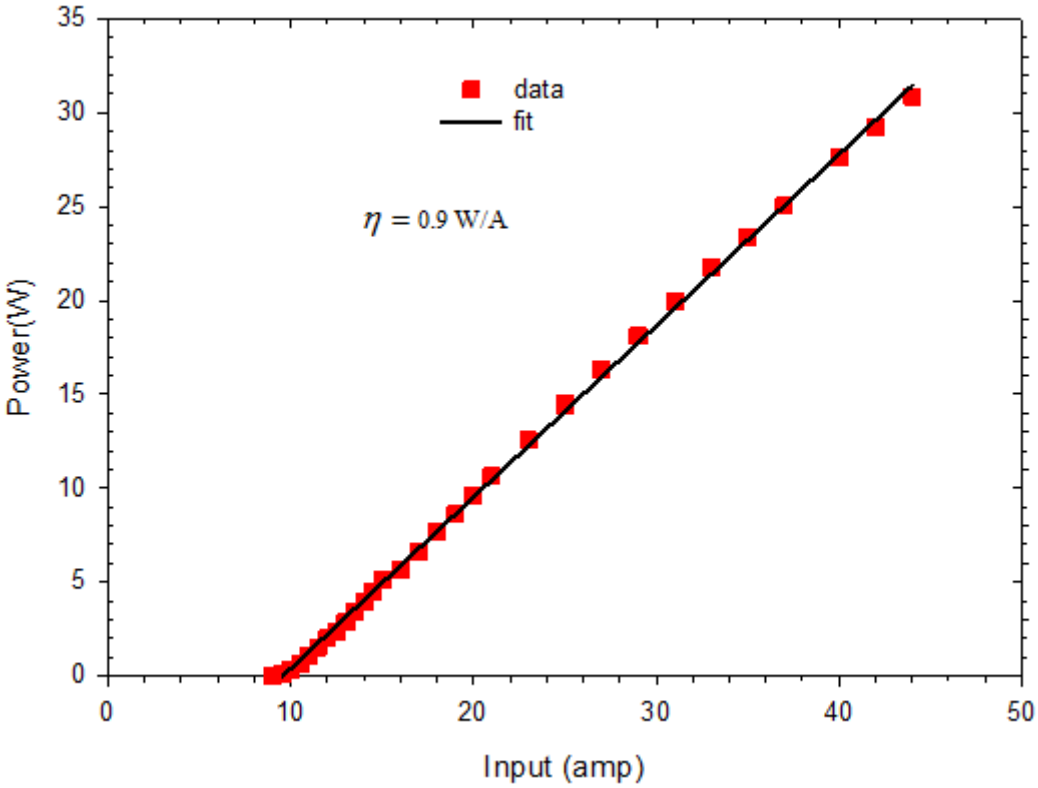

Figure A2. 790 nm diode characterization.

A3. Diode Fluctuation Measurement

This section describes the measurement of diode power fluctuation. As in cut-back experiment, it is necessary to keep power fixed throughout the experiment, i.e. no power fluctuation is desired. Therefore, after diode characterization it has been checked the diode fluctuation for different input power. The power has been recorded in a 5 minute interval. Figure A3 is plotted the diode power as a function of time. It is observed from Figure A3 that for increasing the diode input power, the diode fluctuation decreases. Therefore, a higher input is necessary to set for cut-back measurement to avoid fluctuation of power.

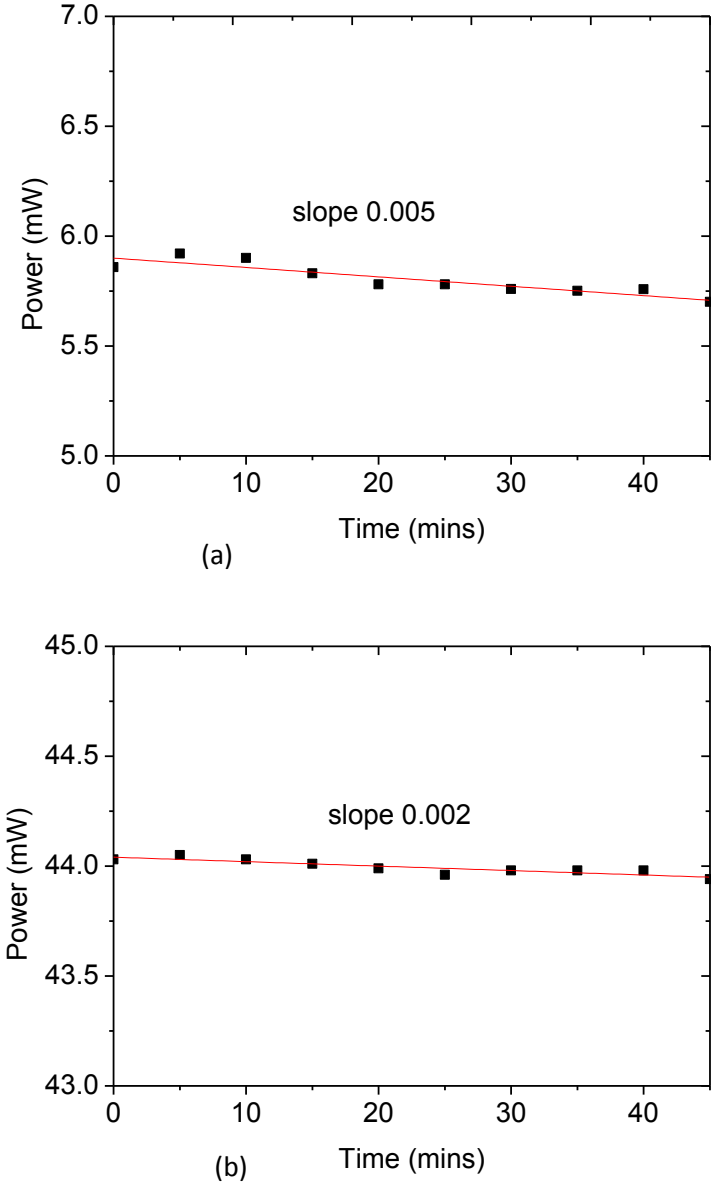

Figure A3. Diode power fluctuation measurements for (a) low power and (b) relatively higher power.

A4. 980 nm Diode Characterisation

A 980 nm 15 W source out of 200 µm patch fibre has been used as a pump source to develop 1570 nm source. Initially diode is fixed for 30 Ampere, though the driver goes upto 50 Ampere. The diode is cooled using CPU fans. The duty cycle is kept fixed 86% throughout the characterisation. After collimating the beam, the diode data was

recorded using Thorlabs power metre head. From the calibration graph A4, it shows the diode efficiency is 0.32 W/A.

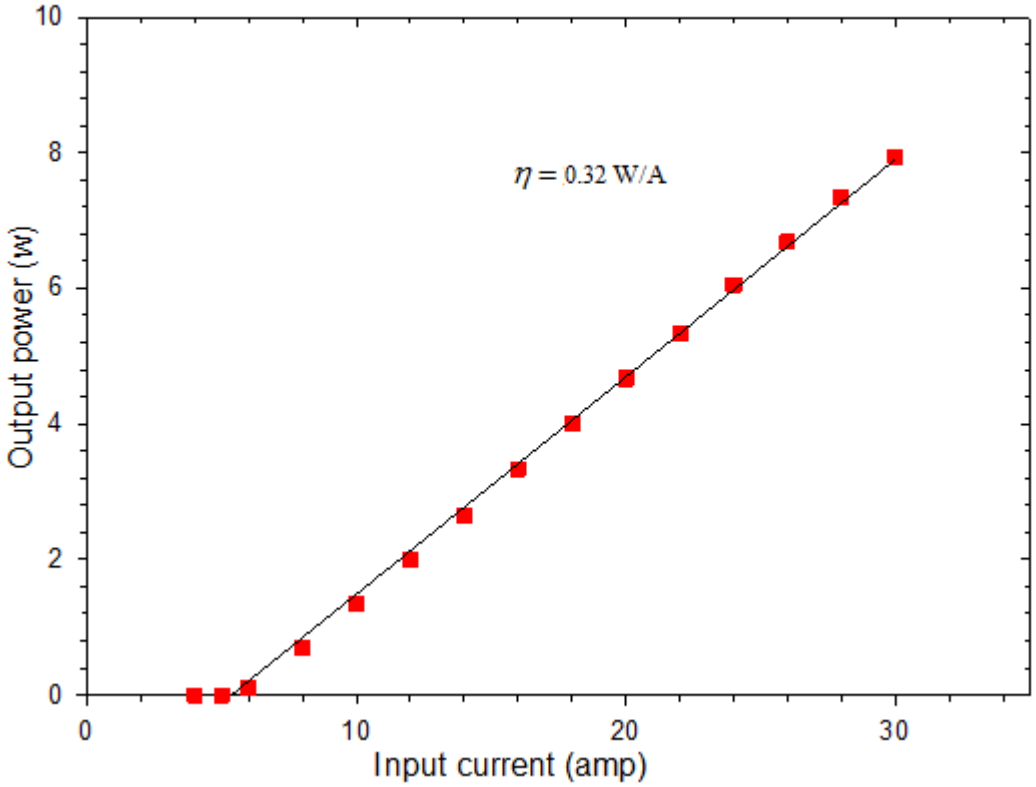

Figure A4. 980 nm diode characterisation.

Bibliography

[1] T. Ehrenreich, R. Leveille, I. Majid, K. Tankala, G. Rines, and P. F. Moulton. 1-kW, all-glass Tm:fiber laser. Fiber Lasers VII: Technology, Systems, and Applications (2010) (Session 16: Late breaking news).

[2] M. Meleshkevich, N. Platonov, D. Gapontsev, A. Drozhzhin. 415W Single-Mode CW Thulium Fiber Laser in all-fiber format. IPG Photonics, 50 Old Webster Rd., Oxford, MA, 01540, USA V.Sergeev, V.Gapontsev. IPGLaser GmbH, Siemenstrasse 7, Burbach, D -57299, Germany.

[3] M. Eichhorn and S. D. Jackson. Comparative study of continuous wave Tm^{3+} doped silica and fluoride fibre laser. Applied Physics B 90, 35-41 (2008).

[4] T. Yamamoto, Y. Miyajima, T. Komukai, and T. Sugawa. 1.9 μm Tm-doped fluoride fibre amplifier and laser pumped at 1.58um. Electronics Letters 29, 986 (1993).

[5] T. H. Maiman. Stimulated optical radiation in ruby masers. Nature 187, 493-494 (1960).

[6] V. P. Gapontsev. High power fibre laser and its application. in Proceedings of the 4th International Symposium on High-Power Fiber Lasers and Their Applications, St. Petersburg, Russia, June 2008.

[7] R.M. Measure. Laser Remote Sensing: Fundamentals and Applications. (Krieger Publishing Company, Malabar Florida) 1992.

[8] G.M. Hale, M.R. Querry. Applied Optics 12, 555 (1973).

[9] K. Scholle, S. Lamrini, P.pp Koopmann and P. Fuhrberg. 2 μm laser sources and their possible applications. Frontiers in Guided wave optics and optoelectronics ISBN 978-953-7619-82-4, February 2010.

[10] IPG, "YLR-HP Series: 1-50kW Ytterbium Fibre Lasers (2009), retrieved August 6, 2009, http://www.ipgphotonics.com/.

[11] S. W. Henderson, P. J. M. Suni, C. P. Hale, S. M. Hannon, J. R. Magee, D. L. Bruns, and E. H. Yuen. Coherent laser radar at 2 μm using solid-state lasers. Geoscience and Remote Sensing. IEEE Transactions on 31, 4-15 (1993).

[12] G. J. Koch, J. Y. Beyon, B. W. Barnes, M. Petros, J. Yu, F. Amzajerdian, M. J. Kavaya, and U. N. Singh. High-energy 2 μm Doppler lidar for wind measurements. Optical Engineering 46, 116201-116214 (2007).

[13] S.-J. Xia, J. Zhuo, X.-W. Sun, B.-M. Han, Y. Shao, and Y.-N. Zhang. Thulium Laser versus Standard Transurethral Resection of the Prostate: A Randomized Prospective Trial. European Urology 53, 382-390 (2008).

[14] W. A. Clarkson, D.Y. Shen, P. J. Jander and J. K. Sahu. Tm doped fiber laser pumped by a cladding-pumped Er,Yb fiber laser, Optoelectronics Research Centre, University of Southampton, 2006.

[15] R. J. Mears, L. Reekie, S. B. Poole, and D. N. Payne. Neodymium-doped silica singlemode fibre lasers. Electronics Letters 21, 738 (1985).

[16] H. Po. E. Snitzer, R, Tumminelli, L. Zenteno, F. Hakimi, N. M. Cho, and T. Haw. Double clad high brightness Nd fibre laser pumped by GaAlAs phased array. Presented at the Optical Fibre Communication, Conference Paper PD07 (1989).

[17] H. Po, J. D. Cao, B. M. Laliberte, R. A. Minns, R.F. Robbinson, B. H. Rockney, R. R. Tricca and Y. H. Zhang. Electronics Letters 29, 1500 (1993).

[18] R. Mauer. Optical waveguide light source. U.S. Patent 3 808 549, Apr. 30, 1974.

[19] CE. Snitzer, H. Po, F. Hakimi, R. Tumminelli, and B. C. McCollum. Double-clad, offset core Nd fibre laser. Optical Fiber Sensors, vol. 2, OSA Technical Digest Series. Washighton, DC: Optical Society of America, 1988.

[20] H. Zellmer, A. T¨unnermann, and H. Welling. Double-clad fibre laser with 30 W output power. in OSA TOPS, vol. 16, Optical Amplifiers and Their Applications. Washington, DC: Optical Society of America, 1997.

[21] D. Mercuse. Bell System Technical Journal 56, 5 (1977).

[22] D. Mercuse. Gaussian approximation of the fundamental modes of graded index fibres. Journal of Optical Society America 68, 103-109 (1978).

[23] M.F.G. Digonnet. C. J. Gaeta, Applied Optics 24, 333 (1985).

[24] A. W. Snyder and J. D. Love. Optical waveguide theory. Chapmann and Hall, 1983.

[25] K. Ohsawa, T. Shibata, K. Nakamura, and S. Yoshida. Fluorozirconate glasses for infrared transmitting optical fibers. Proceedings of the 7th European Conference on Optical Communication (ECOC), pp. 1.1-1–1.1-4, Copenhagen, Danmark, September 1981.

[26] J. Lucas, M. Chanthanasinh, M. Poulain, M. Poulain, P. Brun, and M. J. Weber. Preparation and optical properties of neodymium fluorozirconate glasses. Journal of Non-Crystalline Solids 27, 273–283 (1978).

[27] M. Poulain, and J. Lucas. Verres fluores au tetrafluorure de zirconium proprietes optiques d'un verre dope au Nd^{3+} Materials Research Bulletin 10, 243–246 (1975).

[28] Xiushan Zhu and N. Peyghambarian. High-Power ZBLAN Glass Fiber Lasers: Review and Prospect. Advances in Optoelectronics, Volume 2010 (2010), Article ID 501956, doi:10.1155/2010/501956.

[29] P. France, M. G. Drexhage, J.M. Parker, M. W. Moore, S. F. Carter, and J. V.Wright. Fluoride Glass Optical Fibres, Blackie and Son, London, UK, 1990.

[30] G T. Kanamori and S. Sakaguchi. Preparation of elevated NA fluoride optical fibres. Japanese Journal of Applied Physics, vol. 25, no. 6, pp. L468–L470, 1986.

[31] L. F. Johnson, G. D. Boyd, and K. Nassau. Proceedings of IRE (1962).

[32] L. F. Johnson, J. E. Geusic, and L. G. Van Uitert. Coherent Oscillations from Tm^{3+}, Ho^{3+}, Yb^{3+} and Er^{3+} Ions in Yttrium Aluminium Garnet. Applied Physics Letters **7**, 127-129 (1965).

[33] L. F. Johnson, L. G. Van Uitert, J. J. Rubin, and R. A. Thomas. Energy Transfer from Er3+ to Tm3+ and Ho3+ Ions in Crystals. Physical Review 133, A494 (1964).

[34] B. H. Soffer and R. H. Hoskins. Energy Transfer and CW Laser Action in Tm^{3+}:Er2O3, Applied Physics Letters 6, 200-201 (1965).

[35] D. C. Hanna, I. M. Jauncey, R. M. Percival, I. R. Perry, R. G. Smart, P. J. Suni, J. E. Townsend, and A. C. Tropper. Continuous-wave oscillation of a monomode thulium doped fibre laser. Electronics Letters 24, 1222-1223 (1988).

[36] B. M. Walsh and N. P. Barnes. Comparison of Tm:ZBLAN and Tm: silica fiber lasers; Spectroscopy and tunable pulsed laser operation around 1.9 μm. Applied Physics B 78, 325-333 (2004).

[37] D. C. Hanna, R. M. Percival, R. G. Smart, and A. C. Tropper. Efficient and tunable operation of a Tm-doped fibre laser. Optics Communications 75, 283-286 (1990).

[38] J. N. Carter, R.G. Smart, D.C. Hanna, and A.C. Tropper. CW diode-pumped operation of 1.97 μm thulium doped fluozirconate fibre laser. Electronics Letters 26, 599-601 (1990).

[39] R. G. Smart, J. N. Carter, A. C. Tropper, and D. C. Hanna. Continuous-wave oscillation of Tm3+ -doped fluorozirconate fibre lasers at around 1.47 μm, 1.9 μm

and 2.3 μm when pumped at 790 nm. Optics Communications 82, 563-570 (1991).

[40] R. M. Percival, D. Szebesta, C.P. Seltzer, S.D. Perrin, S.T. Davey and M. Louka. 1.6 μm semiconductor diode pumped thulium doped fluoride fibre laser and amplifier of very high efficiency. Electronics Letters 29 21210 (1993)

[41] R. M. Percival, D. Szebesta, C. P. Seltzer, S.D. Perrin, S.T. Davey, and M. Louka. A 1.6-μm pumped 1.9 μm thulium-doped fluoride fibre laser and amplifier of very high efficiency. IEEE Jounal of Quantum Electronics 31, 489-493 (1995).

[42] D. C. Hanna, I. R. Perry, J. R. Lincoln, and J. E. Townsend, "A 1-Watt thulium-doped cw fibre laser operating at 2 μm," Optics Communications 80, 52-56 (1990).

[43] S. D. Jackson and T. King. High-power diode-cladding-pumped Tm-doped silica fiber laser. Optics Letters 23, 1462-1464 (1998).

[44] T. Becker, R. Clausen, G. Huber, E. W. Duczynski, and P. Mitzscherich. Spectroscopic and laser properties of thulium doped YAG at 2 μm. Optical Society of America 150-153 (1989).

[45] R. A. Hayward, W. A. Clarkson, P. W. Turner, J. Nilsson, A. B. Grudinin, and D. C. Hanna. Efficient cladding-pumped Tm-doped silica fibre laser with high power single mode output at 2μm. Electronics Letters 36, 711-712 (2000).

[46] S. D. Jackson. Cross relaxation and energy transfer up conversion processes relevant to the functioning of 2 μm Tm3+-doped silica fibre lasers. Optics Communications 230, 197-203 (2004).

[47] S. D. Jackson and S. Mossman. Efficiency dependence on the Tm and Al concentrations for Tm-doped silica double-clad fibre lasers. Applied Optics 42, (2003).

[48] P. F. Moulton, G. A. Rines, E. V. Slobodtchikov, K. F. Wall, G. Frith, B. Samson, and A. L. G. Carter. Tm-Doped Fibre Lasers: Fundamentals and Power Scaling. IEEE Journal of Selected Topics in Quantum Electronics 15, 85-92 (2009).

[49] M. Eichhorn. High-peak-power Tm-doped double-clad fluoride fibre amplifier. Optics Letters 24 3329 (2005).

[50] Y. Tang and J. Xu. High Power Tunable Tm3+-fiber Lasers and Its Application in Pumping Cr2+:ZnSe Lasers. Frontiers in Guided wave optics and optoelectronics ISBN 978-953-7619-82-4, February 2010.

[51] N. P. Barnes, W. J. Rodriguez, B.M. Walsh. Journal of Optical Society America B, 13, 2872 (1996).

[52] B.M. Walsh. Review of Tm and Ho materials; spectroscopy and lasers. NASA Langley research centre, Hampton, VA 23681.

[53] G. Armagan, B. M. Walsh, N. P. Barnes, E. A. Modlin, A. M. Buoncristiani. Proceedings on Advanced Solid State Lasers, 20, 141(1994).

[54] A. M. Tkachuk, M. F. Joubert, R. Moncorge, D. I. Mironov, A. A. Nikitichev. Optics & Spectroscopy 85, 885 (1998).

[55] J.L. Doualan, S. Girard, H. Haquin, J.L. Adam, J. Montagne. Spectroscopic properties and laser emission of Tm doped ZBLAN glass at 1.8 μm. Optical Materials 24 563-574(2003).

[56] S. Agger, J.H. Povlsen and P. Varming. Single-frequency thulium-doped distributed feedback fibre laser. Optics Letters 29, 1503-1505 (2004).

[57] R.G. Smart, J.N. Carter, A.C. Tropper and D.C. Hanna. Continuous-wave oscillation of Tm-doped fluorozirconate fibre laser at around 1.47m, 1.9 and 2.3 when pumped at 790nm. Optics Communication 82, 563-570 (1991).

[58] J. Geng, J. Wu, and S. Jiang. Efficient operation of diode-pumped single-frequency thulium-doped fibre lasers near 2 μm. Optics Letters 32, 355-357 (2007).

[59] N. Y. Voo, J. K. Sahu, and M. Ibsen. 345-mW 1836-nm Single-Frequency DFB Fibre Laser MOPA. IEEE Photonics Technology Letters 17, 2550 (2005).

[60] J. Xu, M. Prabhu, J. Lu, K. Ueda, and Da Xing. Efficient double-clad thulium-doped fibre laser with a ring cavity. Applied Optics 40, 1983-1988 (2001).

[61] R. Reisfeld, C.K. Jorgensen. Hand book on the Physics and Chemistry of Rare Earths, K.A. Gschneidner, Jr., L. Eyrinh (Elsevier Sci. Publishers 1987) Chapter 58.

[62] R. M. Percival, D. Szebesta, C.P. Seltzer, S.D. Perrin, S.T. Davey. Highly efficient CW cascade operation of 1.47 and 1.82 um transition in Tm-doped fluoride fibre laser. Electronics Letters 28, 1866-1867 (1992).

[63] E. Snitzer, H. Po, F. Hakimi, R.Tumminelli and B.C. McCollum. Erbium fibre laser amplifier at 1.55 um with pump and Yb sensitized Er oscillator. Proc. Conf. Optical Fibre Communication, New Orleans, LA, Paper PD2, 1988

[64] Y. H. Tsang, A.F. El-Sherif and T.A. King. Broadband amplified spontaneous emission fibre source near 2um using resonant in-band pumping. Journal of Modern Optics 52, 109 (2005).

[65] R. M. Percival, D. Szebesta, and S.T. Davey. Highly efficient and tunable operation of a two color Tm-doped fluoride fibre laser. Electronics Letters 28, 671-672 (1992).

[66] D. Y. Shen, J. K. Sahu, and W. A. Clarkson. High-power widely tunable Tm:fibre lasers pumped by an Er,Yb co-doped fibre laser at 1.6μm. Optics Express 14, 6084–6090 (2006).

[67] Y. H. Tsang and T.A. King. Multi-mode 2μm Tm-silica fibre lasers with 1.61μm in-band pumping. Journal of Modern Optics 54, 1659-1667 (2007).

[68] M. Laroche, P. Jander, W.A. Clarkson, J.k. Sahu, J. Nilson and Y. Jeong. High power cladding-pumped tunable Er,Yb-fibre laser. Electronics Letters 40, 855-856 (2004).

[69] P. Blixt, J. Nilsson, T. Carlnäs, and B. Jaskorzynska, "Concentration-dependent upconversion in Er^{3+} doped fiber amplifiers: Experiments and modelling. IEEE Photonics Technology Letters 3(11), 996–998 (1991).

[70] J. D. Minelly, W. L. Barnes, R.I. Laming, P.R. Morkel, J.E. Townsend, S.G. Grubb, and D.N, Payne. Diode array pumping of Er3+/Yb3+ co-doped fibre laser and amplifiers," IEEE Photonics Technology Letters 5, 301 (1993).

[71] G.G. Vienne, J.E. CAplen, L. Dong, J.D. Minelly, J. Nilsson, and D.N. Payne. Fabrication and characterization of Yb3+:E3+ phosposilicate fibre for lasers. Journal of Lightwave Technology 16 1990 (1998).

[72] K. Tankala, B. Samson, A. Carter, J. Farroni, D. Machewirth, N. Jacobson, U. Manyam, A. Sanchez, M.-Y.Cheng, A. Galvanauskas, W. Torruellas, and Y. Chen. New developments in high power eye-safe LMA fibers. Proc. SPIE 6102, 610206 (2006).

[73] Y. Jeong, S. Yoo, C. A. Codemard, J. Nilsson, J. K. Sahu, D. N. Payne, . Horley, P. W. Turner, L. M. B. Hickey, A. Harker, M. Lovelady, and A. Piper. Erbium:ytterbium codoped large-core fibre laser with 297 W continuous-wave output power. IEEE Journal of Selected Topics in Quantum Electronics 13, 573–579 (2007).

[74] A. Yusim, J. Barsalou, D. Gapontsev, N. S. Platonov, O.Shkurikhin, V. P. Gapontsev, Y. A. Barannikov, and F. V. Shcherbina. 100 watt single-mode CW

linearly polarized all-fiber format 1.56 μm laser with suppression of parasitic lasing effects. Proc. SPIE 5709, 69–77 (2005).

[75] D. Y. Shen, J. K. Sahu, and W. A. Clarkson. Highly efficient Er,Yb-doped fibre laser with 188 W free-running and >100 W tunable output power. Optics Express 13, 4916–4921 (2005).

[76] L. Zenteno. „High-power double-clad fiber lasers. Journal of Lightwave Technology 11, 1435 (1993).

[77] A. Bertoni, G.C. Reali. A model for optimisation of double clad fibre laser operation. Applied Physics B 66, 547-554 (1998).

[78] D. Inissis, D.J. DiGiovanni, T.A. Strasser, A. Hale, C. Headley, A.J. Stentz, R. Pedrazzani, D. Tipton, S.G. Kosinsky, D.L. Brownlow, K.W. Quoi, K.S. Kranz, R.G. Huff, R. Espindola, J.D. LeGrange, G. Jacobovtz-Veselka, D. Boggavarapu, X. He, D. Caffey, S. Gupta, S. Srinivasan, K. McEuen, R. Patel. CLEO "97 Post-deadline papers, CPD31-2 (1997).

[79] H. Zellmer, U. Willamowsky, A. Tunnermann, H. Welling, S. Unger, V. Reichel, H.R. Muller, J. Kirchhof, P. Albers. „High-power CW neodyminum-doped fibre laser operating at 9.2 W with high beam quality. Optics Letters 20, 578–580 (1995).

[80] T. Weber, W. Luthy, H. P. Weber, V. Neuman, H. Berthou, G. Kotrotsios, J. P. Dan, and H. E. Hintermann. Cladding-pumped fibre laser. IEEE Journal of Quantum Electronics 31, 326–329 (1995).

[81] J. Xu, M. Prabhu, J. Lu, K. Ueda, and D. Xing. Efficient double-clad thulium-doped fibre laser with a ring cavity. Applied Optics 40, 1983–1988 (2001).

[82] A. Liu and K. Ueda. Propagation losses of pump light in rectangular double-clad fibers. Optical Engineering 35, 3130–3134 (1996).

[83] M. P. Goorjian, A. Tafloye, M.R. Joseph and C. S. Hagness. Computational modeling of femtosecond optical solitons from Maxwell"s equations. IEEE Journal of Quantum Electronics 28, 2416-22 (1992).

[84] C.S. Hagness, D. Rafizadeh, T.S. Ho, & A. Tafloye. FDTD microcavity simulations: design & experimental realization of waveguide-coupled single mode ring and whispering gallery mode disk resonators. IEEE Journal of Lightwave Technology 15, 2154-65 (1997).

[85] Y. Tsuji, & M, Koshiba. Adaptive mesh generation for full vectorial guided-mode and beam propagation solutions. IEEE Journal of Selelected Topics in Quantum Electronics 6, 163-9 (2000).

[86] D. Kouznetsov & J. Moloney. Efficiency of pump absorption in double clad fibre amplifiers. II. Broken circular symmetry. Journal of Optical Society America B 19, 1259-63 (2002).

[87] P. Leproux S. Fevrier. V. Doya, P. Roy and D. Pagnoux. Modeling & optimisation of double clad fibre amplifiers using chaotic propagation of the pump. Optical Fibre Technolology 7, 324-339 (2001).

[88] A. Liu & K. Ueda. The absorption characteristics of circular, offset & rectangular double clad fibres. Optics Communication 132, 511-518 (1996).

[89] D. Kouznetsov & J. Moloney. Efficiency of pump absorption in double clad fibre amplifiers. I. Fibres with circular symmetry. Journal of Optical Society America B 18, 743-9 (2001).

[90] D. Kznetsov & J. Moloney Efficiency of pump absorption in double clad fibre amplifiers. III. Calculation of modes. Journal of Optical Society America B 19, 1304-9 (2002).

[91] N. A. Mortensen. Air-clad fibres: pump absorption assisted by chaotic wave dynamics. Optics Express 15, 8988 (2007).

[92] I Dritsas, T Sun & K T V Grattan. Numerical simulation based optimisation of the absorption efficiency in double-clad fibres. Journal of Optics A: Pure and Applied Optics 8, 49-61(2006).

[93] D. Marcuse. Principles of Optical Fibre Measurement. Academic Press, New York, 1981.

[94] H. Ebendorff-Heidepriem and T. M. Monro. Extrusion of complex preforms for microstructured optical fibres. Optics Express, 15, 15086 (2007).

[95] H. Ebendorff-Heidepriem, D.G. Lancaster, K. Kuan, R.C. Moore, M.S.I. Sarker, T.M. Monro, Extruded fluoride fibre for 2.3 μm laser application, CLEO, 2011.

[96] V. Philippov, C. Codemard, Y. Jeong, C. Alegria, J.K. Sahu, J. Nilsson, and G.N. Pearson. High energy in-fibre pulse amplification for coherent lidar applications. Optics Letters 29, 2590 (2004).

[97] R. Corte, R. Villagomez, V Coello and R. Lopez. Laser beam quality factor (M^2) measured by distorted Fresnel zone plate. Revista Maxicana Defisica 54, 279 (2008).